Doctoral Dissertation

CPG-based Rhythmic Manipulation for a Multi-Fingered Hand from Human Observation

Yuichi Kurita

December 20, 2004

Department of Information Systems
Graduate School of Information Science
Nara Institute of Science and Technology

A Doctoral Dissertation
submitted to Graduate School of Information Science,
Nara Institute of Science and Technology
in partial fulfillment of the requirements for the degree of
Doctor of ENGINEERING

Yuichi Kurita

Thesis Committee:
  Professor   Tsukasa Ogasawara   (Supervisor)
  Professor   Shin Ishii   (Co-supervisor)
  Associate Professor   Yoshio Matsumoto   (Member)

CPG-based Rhythmic Manipulation for a Multi-Fingered Hand from Human Observation *

Yuichi Kurita

Abstract

In this thesis, a CPG-based control based on human manipulations is proposed for rhythmic manipulations by a multi-fingered hand. Humans can dextrously manipulate various objects using their fingers cooperatively. Adaptive motions in animals and insects can also be observed according to a variety of environments. Neurophysiological studies have revealed that rhythmic motor patterns such as locomotion are coordinated by central pattern generators (CPG) and take an important role in the adaptive motions. In a rotating manipulation of an object, rhythmic finger motions can be observed. The CPG-based control of the fingers has possibilities to achieve dextrous capabilities like humans. In this study, Human's rhythmic manipulations is investigated. Based on the analysis, the CPG-based control for dextrous manipulations is proposed.

Human's force programming is investigated in the chapter 3 by the experiments where subjects grasp various weighted objects. Anticipatory calculation of the fingertip force before the grasp takes an important role in human's sophisticated grasp. In the experiments, the applied grip/load force and the electromyography (EMG) of intrinsic muscles are simultaneously measured. The effects of the rhythmic motions and the force programming on the grasping motions are analyzed based on the experiments.

Human's rhythmic motions are investigated in the chapter 4 by measuring contact condition during a rotating manipulation of a cylindrical object. Typical

---

contact patterns are detected by the measured contact information that can apparently represent the rhythmic movements during the manipulation. The rhythmic motions of the fingers during the rotating manipulations are investigated by the typical contact pattern.

A CPG model is constructed based on the measured typical contact patterns in the chapter 5. The CPG issues the motion-triggers to the robot fingers in order that the robot fingers can move cooperatively and synchronously. The experimental results in the dynamic simulation show that the CPG-based control of the fingers can perform the rotating manipulation using the generated contact pattern.

A control method of the switching cycle of the grasping fingers by the joint margin feedback is presented in the chapter 6. The property of the oscillatory output can adaptively change. by the appropriate feedback to the neurons that constitute the CPG. Manipulations using the fingers require the relocation of the grasping fingers. The appropriate switching cycle of the fingers changes depending on the object size. A smooth change of the velocity of the grasped object can also be achieved by correlating the neural output with the desired velocity of the object. A four-fingered hand demonstrates the rhythmic manipulations based on the proposed method.

The results suggest the importance of the rhythmic motions during human's manipulations and the effectiveness of the CPG-based control. In addition, these results provide efficient guidelines to achieve dextrous manipulations like humans using a multi-fingered hand.

Keywords:

Manipulation, Central Pattern Generator(CPG), Rhythmic motions, Contact pattern, Multi-fingered hand

Acknowledgements

Contents

List of Figures

List of Tables

Chapter 1

Introduction

1.1. Background

Robots have been developed in the 1970-80's as industrial machines and sophisticated in the 1990's, which play soccer, walk like a dog, and feel and talk like human beings. Researches in many areas of robotics have made it possible to produce such varieties of robots.

However, the ability of robots to grasp and manipulate objects still remains a fascination for many researchers. Although a significant progress has been made in the development of dextrous robot end effectors in the last fifteen years, these robot hands were only variants of the parallel jaw gripper. Some specialized single degree of freedom grippers have been successfully developed. However, they are largely limited to the case where the grasped objects are in a small, well-known set, and are not truly dextrous in the general sense. Robots have come to take an active role not only in industrial factories, but also in home, hospital, farm, space, and deep sea. Robot hands that can stably grasp and dextrously manipulate objects like humans are required in these environments.

In recent years, multi-fingered robot hands have been attracting robotics researchers. Multi-fingered hands can take various grasping configurations according to the objects and achieve dextrous manipulations by relocating fingers. However, many traditional methods for multi-fingered manipulations have been based on a model of the grasped object. In order to exploit the robot hand in the real environment, it is not practical to make the precise models of all the object and

store all the modeling data in the system.

It is known that motions of animals that can adapt to a variety of environments are controlled by a nervous system covering all the body. Neurophysiological studies have revealed that rhythmic motor patterns such as locomotion in animals and insects are coordinated by neural circuits referred to as central pattern generators (CPG). The rhythmic patterns generated by the CPG take an important role in rhythmic activities, such as breathing, fluttering and walking. In the locomotion of animals, a musculo-skeletal system is driven by rhythmic patterns generated by a rhythm generator in vertebra and a reflex system based on the sensations from peripheral nerves. Based on these findings in biology and neurophysiology, a number of adaptive walking control methods for multi-legged robots have been proposed.

However, few approaches based on the analysis of human's rhythmic motions have been proposed for multi-fingered manipulations. Humans can dextrously and cooperatively manipulate various objects using their fingers. Several findings in paleoanthropology show that the mechanical dexterity of the human's hand has been a major factor in allowing Homo sapiens to develop a superior brain. Although artificial hands have been built that are stronger and faster than the human's hand, the performance of the manipulation is not satisfactory when a sufficiently broad scope of manipulation tasks is considered. To achieve dextrous capabilities like humans by a robot hand, it is important to measure human's skills and apply the findings to the robot hand manipulations.

1.2. Research aim and approach

Looking at previous researches of robot hands from the viewpoint of practical applications, there are some problems, for example, the requirement of a precise object model.

To relax the restriction, researchers have proposed various measuring methods of the grasped object. However, because sensors are consistently affected by noises in the real environment, it is very difficult to even build a precise model of one object, much less all the objects in the environments.

In the studies of the walking control for multi-legged robots, a CPG-based

adaptive control has been proposed biologically inspired by analyzing animals' walking patterns. The effectiveness of the CPG-based adaptive walking in real environments has also been confirmed. However, few approaches based on the analysis of human's rhythmic motions have been proposed for multi-fingered manipulations because the dexterity and the complexity of the manipulations using multiple fingers have been emphasized more strongly than the complexity of the locomotion. Recently, human's rhythmic motions of the fingers in a rotating manipulation have been observed by measuring the trajectories of fingers. This fact suggests that finger motions make the transition from the feedback control based on peripheral sensations into the feedforward control based on the central nervous system as humans attain proficiency.

In order to exploit the CPG-based control to a rhythmic manipulation, manipulation patterns are required. However, the pattern models generated by the CPG have not been investigated because few researches have been focused on the feedforward control and rhythmic patterns of the fingers during the manipulations. This thesis proposes the CPG-based rhythmic manipulation for a multi-fingered hand based on the human observation.

In the first half part of this thesis, the investigation of human's feedforward control and rhythmic motions using multiple fingers is conducted. The force programming based on the object properties is considered important in human's sophisticated grasp. In the previous studies of the force programming, the grasping force has been measured for the analysis. In order to eliminate the contribution of the tactile sensations, the time delay of the tactile feedback has been exploited. However, the available time period is so short that the difference was hard to be detected due to the noise problem. In this study, the force programming is investigated by measuring electromyography (EMG) before the tactile feedback affects. Next, a motion pattern during a rotating manipulation is measured. A typical contact pattern during the manipulation involving the relocation of the fingers is presented by analyzing the measured contact information.

In the last part, a CPG-based control for multi-fingered manipulations is proposed and demonstrated. A CPG steadily generates oscillatory output unless external input is given to the neurons. The CPG can also generate various patterns affected by the external input, such as sensory feedback. A Joint angle

3

feedback to the neurons that constitute the CPG controls the switching cycle of the grasping fingers according to the object size. The effectiveness of the proposed method is demonstrated by performing rotating manipulations of several sized objects using a four-fingered hand system.

The contributions of this thesis are:

- Investigation of the effects of the rhythmic motions and the force programming during the grasping motions.

- Representation of rhythmic patterns during rotating manipulations by showing typical contact patterns.

- Proposal of a CPG model that generates a similar contact pattern to that of human.

- Experiment of the CPG-based rotating manipulations by a simulation.

- Demonstration of the rotating manipulation using a multi-fingered hand by the proposed CPG-based control.

1.3. Thesis outline

This thesis proceeds as follows:

Chapter 1: Introduction

   has presented the background, aim, approach, and contributions of this thesis.

Chapter 2: Literature review

   introduces the relevant literature in robotics and physiology. This chapter considers other robotic approaches to achieve dextrous manipulations using multi-fingered hand systems. This chapter also addresses the mechanism of human's grasping motions and the control system in animals that generates rhythmic patterns.

Chapter 3: Investigation of feedforward control in human's grasping motions

examines the effects of the rhythmic motions and the feedforward control in the human's grasping motions. The grip/load force and electromyography (EMG) are simultaneously measured during the motions. The EMG activities that are not affected by the tactile feedback are investigated. Subjects grasp various weighted objects in the two experimental conditions: the rhythm condition and the free condition. The rhythmic motion and the force programming are investigated by the experiments.

Chapter 4: Rhythmic motion patterns in human's manipulations
investigates rhythmic patterns during rotating manipulations. When subjects attain proficiency in the rotating manipulation, rhythmic motions of the fingers can be observed. The motion patterns are formalized by measuring the contact condition between the fingers and the object using force sensing resistors (FSRs). A typical contact pattern is detected by the measured contact information. The rhythmic rotating motions are investigated based on the typical contact pattern.

Chapter 5: CPG-based manipulation
demonstrates that a CPG model can generate a similar contact pattern to the human's typical pattern measured in the previous chapter. This chapter also proposes a control method of the fingers based on the rhythmic pattern generated by the constructed CPG. Experimental results show that rotating manipulations can be performed by the proposed CPG-based control.

Chapter 6: Rhythmic manipulations using a multi-fingered hand by the CPG-based control
demonstrates the rhythmic manipulations by exploiting the CPG-based control. The property of the oscillatory output of the CPG can be changed depending on the external input to the neurons. Joint margin feedback to the neurons can change the switching cycle of the fingers according to the object size. Experimental results show that the proposed method can rhythmically manipulate various sized objects whose models are not given.

Chapter 7: Conclusion

concludes this thesis, and gives suggestions for future work. Following that are a number of appendixes.

Chapter 2

Related work

2.1. Introduction

This chapter reviews the relevant literature in robotics and physiology. This chapter considers other robotic approaches to achieve dextrous manipulations using multi-fingered hand systems. The mechanism of human's grasping motions from a viewpoint of control systems is also introduced. The control system in animals that generates rhythmic patterns is described. A biologically inspired CPG-based control is also addressed.

2.2. Exploiting a multi-fingered hand

Robotic hands have been developed with the aim of matching the human hand in terms of dexterity and adaptation capabilities to equip either a dextrous manipulator or human beings as a prosthetic device. In many years, some specialized single degree of freedom grippers and variants of parallel grippers have been exploited in industrial factories as end effectors of manipulators. However, manipulative capabilities of these simple hands are largely limited because of the specialization. As robots come to take an active role in substitute for humans, stability and dexterity of grasping and manipulations are required. In order to achieve these capabilities, robotic hands require the following abilities:

- Can form various grasping shapes according to object shapes and the ob-

jective of each task.

- Can relocate the fingers and accomplish the task by itself.

- Can control the force on the object's according to the object properties, such as weight and material.

Multi-fingered hands have multiple degrees of freedom and redundancy in their joints. These characteristics attract researches of artificial multi-fingered hands; there have been many activities in design, analysis, and control in recent years.

Some pioneer three-fingered hands, such as the Okada hand[1] began the trend of the development of more sophisticated end effectors. Numerous multi-fingered hands have been built and successfully demonstrated, notably the Salisbury hand[2], the Utah/MIT hand[3], the Waseda series of hands[4], the Belgrade/USC hand[5], the Bologna hand[6], and the DLR hand[7]. A wide range of design strategy has been followed in the production of these hands[8, 9]. A number of different arrangements of the fingers have been adopted, although the most popular arrangement mimics that of the human hand, with a "thumb" opposing two or more "fingers". Some hands are tendon-driven[3, 6, 9], and some powered by actuators in the hand unit itself[8, 10].

2.3. Control of grasping and manipulations

2.3.1 Dextrous manipulations by a multi-fingered hand

How to configure the fingers of multi-fingered hands is the first natural question when the hand grasps an object. This is the problem of grasp synthesis, or grasp planning. Many researchers have concentrated on this grasp synthesis[11, 12] and planning[13, 14]. Additional works have focused on grasp analysis[15, 16]. In order to evaluate different possible grasp choices, various grasp quality measures have been proposed[17, 18].

Given a grasp analysis/plan, there have been extensive works in the area of the grasp control. Real-time control of robot hands is difficult due to the complexity of the dynamic models, and the difficulty of extracting good sensory information.

A good approach that has been used by a number of researchers is impedance control[19], or stiffness control[9, 20].

In order to maintain the grasp of an object under external disturbances, a lot of works have concentrated on grasp stability. The issue of how many fingers or contacts is required to constrain a given object under various contact condition (frictionless point contact, etc.) is the key question. Significant works in this area have established bounds on the number and type of contacts[21, 22]. The definition of "Force Closure" and "Form Closure" grasps have emerged from these works[23, 24]. Form Closure is generally defined as the ability of a grasp to prevent motions of the object, relying on only unilateral, frictionless contact constraints[25]. Force Closure, on the other hand, is defined in [25] as the situation where motions of the object are constrained by suitably large contact force of the grasp (usually considering friction). An example is shown in Fig.2.1. The figure shows a three-fingered grasp of a planar circle. The grasp is not Form Closure in the sense above since a moment at the center of the circle can not be resisted by the fingers (with frictionless contact). However, the grasp is Force Closure under friction, since in this case the fingers can squeeze suitably to invoke sufficient tangential frictional force at the contact points to resist the moment at the center.

From the above example, we can see that friction takes an important role in reducing the number of fingers theoretically necessary for grasp. Humans perform dextrous grasp with as few as two fingers. This reduction in the number of required fingers is largely due to the friction at the fingertips. For robotics applications, a fine control of frictional force requires the sensation of effects such as a slip[26]. In recent years, various sensors have been developed that can sense a state of stress in the fingertip[27, 28] and slips on the contact surface[29, 30, 31]. A force control based on the slip sensing has also been proposed[28, 30, 32].

Many of above works have concentrated on the specified grasp in that the finger positions remain fixed to the same points on the grasped object during the analysis. There has been a number of works on regrasp from one distinct grasp configuration to another[33, 34]. For the case of regrasp by successive fingers discretely changing position on a grasped object, this regrasping is known as finger gaiting[25].

9
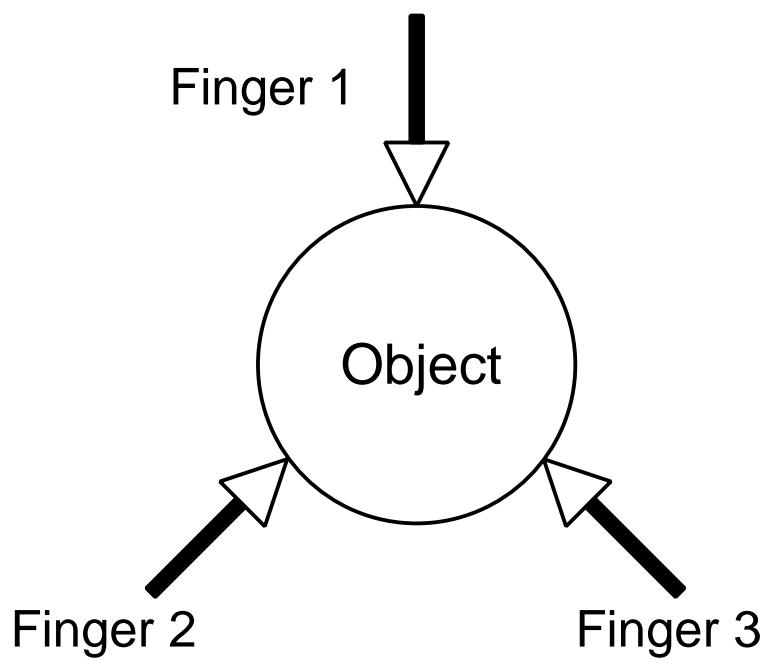
Figure 2.1. A force closure but not a form closure grasp
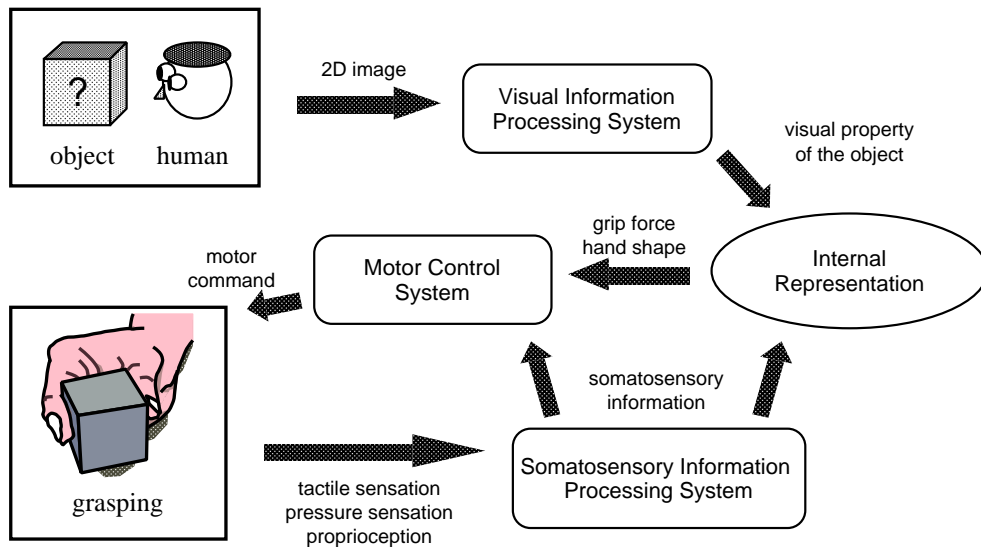
Figure 2.2. Control flow of grasping motions

2.3.2 Control mechanism of human's finger motions

Neurophysiologists and occupational therapists have concentrated on the control mechanism of human's finger motions. The control system can be generally classified into feedforward and feedback control systems. In the feedforward control, motor commands are programmed in advance and the motions do not change depending on sensory stimulations. In the feedback control, on the other hand, the motions are largely affected by the sensory stimulations.

The control flow of grasping motions is briefly shown in Fig.2.2. When a person grasps an object, the object is recognized by visual perception in advance of the motion. The visual information about the object is processed in the visual processing system and stored in the brain as internal representations. The grasping force and the hand shape are calculated by the internal representations. The resultant information is processed in the motor control system and the motor commands are given to muscles. Consequently, the grasping motions are performed.

Somatosensory information such as tactile, pressure, and kinesthetic sensations can be given by the grasping motions. The information directly affects the

motor control system and revises the internal representations via the somatosensory information processing system. Johansson et al. have revealed that the grip force is controlled according to the material of the object surface, and the grip force decreases when cutaneous sensations are denervated by the experiments where a subject pinches a small object with two fingers (thumb and index fingers)[35, 36, 37]. These results suggest that the tactile information is essential to stably grasp an object without slippage. Therefore, several force control strategy based on the slip sensing has also been proposed[28, 30, 32].

Many researchers have also focused on the feedforward control of human motions. They have revealed that the applied grip force by the fingertips increases according to the object size[38, 39, 40, 41], which is caused by "size-weight illusion"[42]. The motions are also affected by visual illusions[43, 44, 45]. These results suggest that the feedforward control based on the visual information is taking an important role on the grasp. Although the size and the motions of the object can be recognized by vision, the object properties such as weight and friction coefficient can not be obtained without the tactile sensations. The feedforward control is affected by the accumulated tactile information that revises the internal representation of the object. Flanagan et al. have revealed that humans program the grasping force in advance of the motion[46, 47, 48]. They have also argued that the force programming is affected by the object properties.

2.4. Rhythmic motions and CPG-based control

2.4.1 Control mechanism of biologic rhythmic motions

Rhythm patterns in the locomotive motions of animals, such as locomotion of quadruped animals, fluttering of birds, and swimming of fish, are generated in some central neural units. Basically, any sensor signal is unnecessary to produce these rhythm patterns. Biological systems are characterized by their behavioral patterns with complexity of large degrees of freedom that will be stably and flexibly generated depending on the state of the environment.

The information flow in voluntary movements is shown in Fig.2.3. The higher level that includes association area, premotor cortex, and supplementary motor

area programs motions. The lower level that includes motor area, brainstem, spinal cord, and musculo-skeletal system controls the motions. The voluntary control system of walking speed and stride is in the higher-level that programs the motion.

2.4.2 Central Pattern Generator

Neurophysiological studies have revealed that a hierarchical structure is present in the locomotor systems. Shik et al. have demonstrated that decerebrate cats can walk on a treadmill by steady electrical stimulation to the midbrain region[49]. Moreover, animals adopt different gaits depending on the stimulation strength and the speed of the treadmill. This fact shows that a complex type of behavior can be controlled by a simple type of top-down signal, while it is not determined uniquely by the signal but is influenced by functional and environmental constraints.

Rhythmic motor patterns are coordinated by neural circuits referred as the central pattern generator (CPG)[50]. Although isolated CPGs can generate rhythmic activities without sensory or descending signals, the interaction between the CPG and the sensory input may be indispensable for locomotion in a natural environment. Centrally generated rhythm is entrained by the sensory signals that are induced by the rhythmic movement of the motor apparatus in animals. This fact strongly suggests that the motor output is an emergent property of a dynamic interaction between the neural system, the musculo-skeletal system, and the environment[51].

Although various models have been proposed to demonstrate neural rhythms, the essential feature common in all models is the mutual inhibition between the neurons. The most simple mutual inhibition network that a generates rhythmic pattern is shown Fig.2.4. This model oscillates when the following condition is satisfied:

- Both neurons N_1 and N_2 suppress each other.

- Impulse rate of the neural output is reduced gradually.

- Constant impulse is input to neurons N_1 and N_2.

13
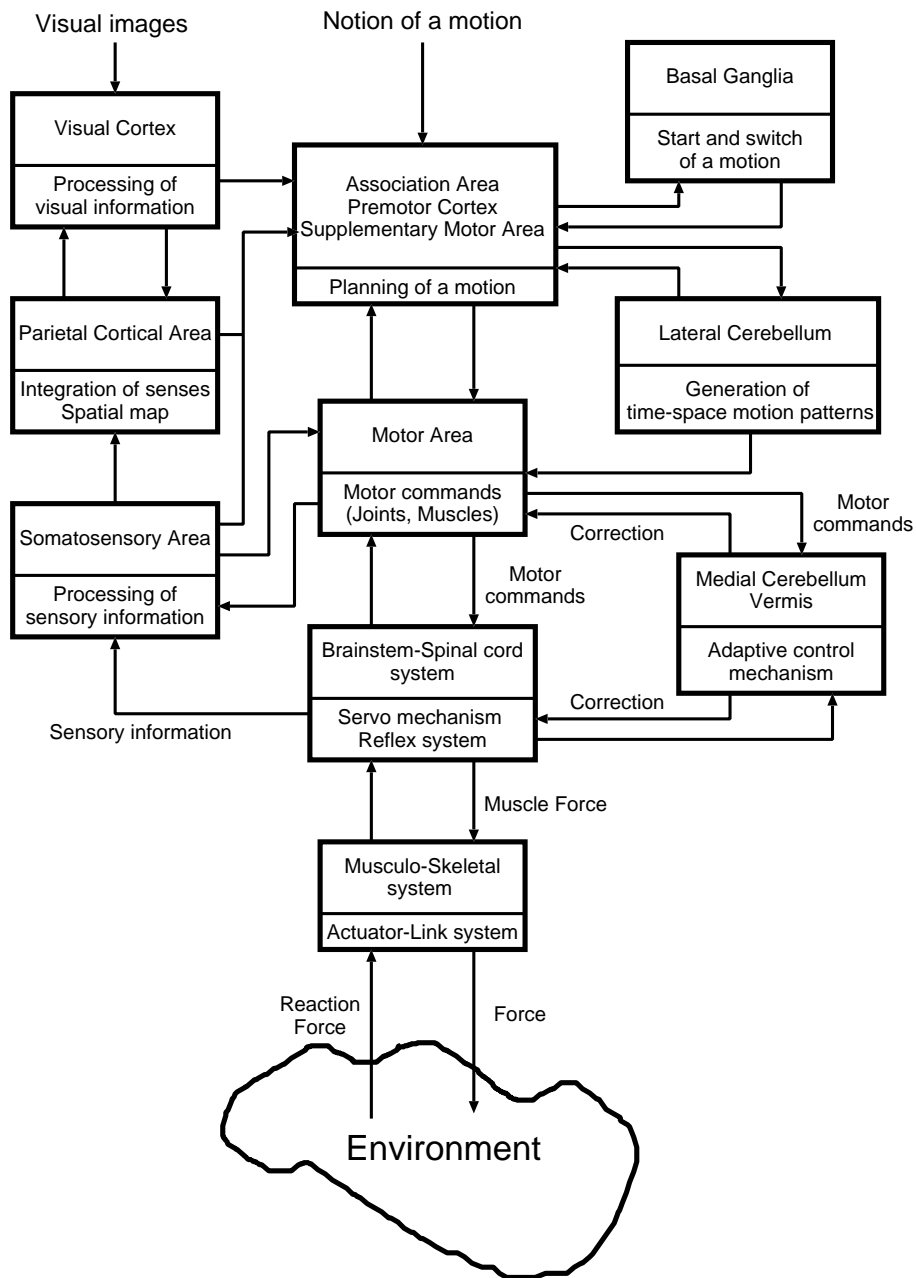
Figure 2.3. Information flow of voluntary movement control
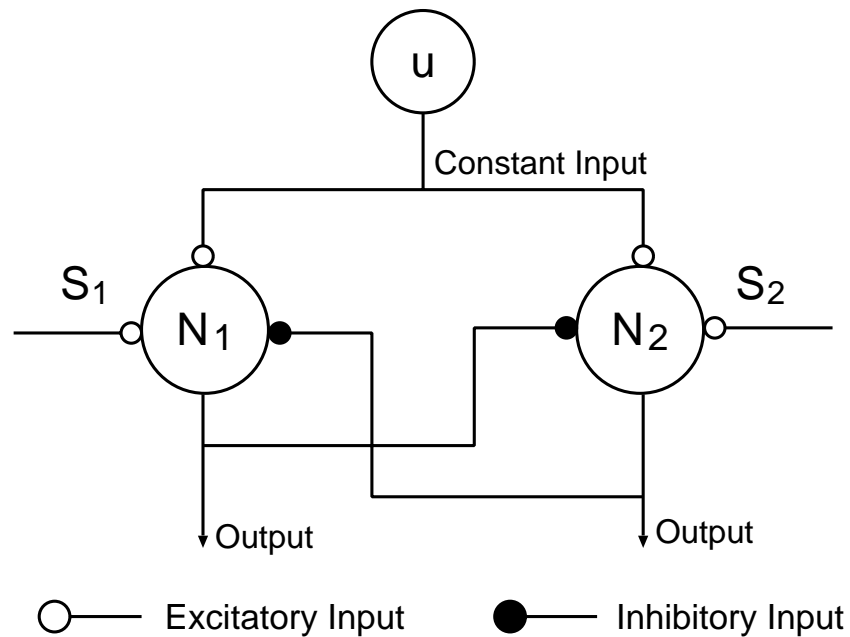
Figure 2.4. Most simple mutual inhibition network

This network is a kind of relaxation oscillator; only one neuron can fire at a time due to the mutual inhibition, and the alternation of the firing neuron is caused by the adaptation in the firing neuron and the recovery of the activity in the resting neuron[52]. This network can be considered a basic model of fluttering of bird wings, chewing and other simple rhythms.

2.4.3 Rhythmic motions of fingers

Although humans are not the only creatures capable of manipulations, the manipulation is essentially a human activity. The large fraction of the human motor cortex devoted to manipulations and the number and sensitivity of mechanoreceptors in our palms and fingertips are indications of the importance of manipulations in humans. Physiologists have investigated human dextrous manipulations through years[53, 54, 55, 56].

Researchers in robotics have classified human's grasping and manipulation with eyes to provide a knowledge-based approach for grasp configuration of robot

hands[57, 58]. Occupational therapists have also proposed various classifications of human manipulations. For example, Exner has classified in-hand manipulations into the following three categories to evaluate human manipulation skills[59]:

Translation: Movements of an object from a palm to finger surface and the vise versa.

Shift: Manipulations by alternating movements of fingers.

Rotation: Manipulations using fingertips to move an object around its axis.

In the shift and the rotation, relocation of fingers is involved, for example, regrasp of a pen and rotation of a cap.

Rhythmic motions can be observed in these relocating motions of the fingers. In rotating motions, because humans can rotate an object only about $\pi/2$ to π [rad] at once, the relocating and rhythmic motions are consequently observed. Taguchi et al. have measured the trajectories of human's finger motions during the rotating manipulation of a cylindrical object by a motion capturing system. They have observed rhythmic finger motions and argued that the finger motions may be controlled by the feedforward control when the subjects attain proficiency[60]. This result suggests that the CPG-based control is suitable for the shifting and the rotating manipulations in that the relocating motions are involved.

2.5. Conclusion

This chapter has situated the work in this thesis in the relevant literature. A brief review of the state of the art in robot hand hardware and the characteristics of a multi-fingered hand have been provided. Significant grasping and manipulation strategies have been introduced and the approaches that exploit a multi-fingered hand for dextrous manipulations have been presented. This chapter has also introduced the rhythmic motions and the control system in animals and humans. A CPG that can generate a rhythmic pattern has been shown and the capability of the CPG-based control on manipulations has been addressed.

Chapter 3

Investigation of the feedforward control in human's grasping motions

3.1. Introduction

Human's rhythmic motions of the fingers have not been studied because the dexterity and the complexity of manipulations using multiple fingers have been emphasized strongly. However, rhythmic motions can be observed in the relocating motions of the fingers. Human naturally learns rhythmic motions when he attains proficiency. Moreover, human can efficiently and robustly grasp various objects. Force programming based on the information about the object properties, such as the weight and friction coefficient of the grasped object, takes an important role in human sophisticated grasp. This chapter focuses on the rhythmic motions of humans and the feedforward control in grasping motions.

This chapter begins by developing a simultaneous measurement system of force and electromyography (EMG). A force measurement device can measure applied grip and load force on the object by a built-in force sensor. The measured force is utilized for detecting the contact between the fingers and the object surface. A surface EMG measurement system is exploited and the measured EMG is utilized for the investigation of the effects by the force programming before the fingers contact on the object. Adductor Pollicis (AdP) and Abductor Pollicis

Brevis (AbPB) muscles are measured by the developed system. Since intrinsic muscles are not significantly affected by motions of the arm, these muscles are adequate for the measurement.

A pilot experiment is conducted for the determination of the time range in that the force programming affects the measured EMG. Based on the pilot experiment, six subjects perform grasping motions, and the grip/load force and EMG are measured.

In the experiment, two conditions are set up. One is the "rhythm condition" where a subject performs a task keeping the timing with the bell that rings at the interval of 1.5[sec]. The other is the "free condition" where a subject can determine the timing to perform the task. The object weight changes from 300[g] to 900[g]. By comparing the results, effects of the rhythmic motion and the force programming can be investigated.

3.2. Anticipatory force programming

Fukuda et al. have proposed a computational scheme to investigate human grasping motions by a computational approach and discussed the relation between the object cognition and the hand shape[61]. They have argued that at least five computational problems, mentioned below, have to be solved to perform grasping motions suitably:

1. **Determination of the combined force**
   Computing the external force applied to an object so that the desired condition of the object can be achieved.

2. **Determination of the grasping points**
   Computing the grasping points on the object surface.

3. **Force distribution**
   Computing the force applied to each grasping point.

4. **Formation of the hand configuration**
   Computing the hand configuration to grasp the object.

5. **Hand control**

Generating the motor command to perform the grasping motion.

These computational problems can be applied on a precision grip (a pinch grip with the thumb and the index fingertips). When a person holds an object with the precision grip, only thumb and index fingers contact on the object surface. Supposing the object is symmetry and the center of mass exists at the center of the object, the hand configuration for stable grasp is limited. This fact simplifies the second (determination of the grasping points) and the fourth (formation of hand configuration) problems. Moreover, the thumb and the index finger have to apply the same force and torque on the object in order to grasp without rotation. This fact also simplifies the third (force distribution) problem. Therefore, the dominant problem in the precision grip among these four problems through the problem of the hand control is the first problem (determination of combined force). This fact indicates that a problem of the force programming is very important for the grasping motions.

Several studies have concentrated on the force programming based on the measurement of the grip and load force [38, 48, 41]. The grip and load force have been measured only after the fingers contact on the object because the force is measured by a built-in force sensor. In these studies, the time delay of tactile feedback is exploited for the investigation in order to eliminate the effect of the tactile sensation from the measured grip/load force. The fastest monosynaptic reflex such as the stretch reflex even takes $30 \sim 50$[msec] to affect the motor control. Based on this fact, the measured grip/load force for $30 \sim 50$[msec] just after the contact can be assumed as the force that is not corrected by the tactile sensations[62]. However, in this method, the available time period is so short that the difference was hard to be detected due to the noise problem.

In this study, the force programming is investigated by measuring electromyography (EMG) before the tactile feedback does not affect. The EMG is the signal that is generated by the contraction of muscles and can be measured not only after but also before the contact on the object. Moreover, the grip/load force are simultaneously measured to detect the contact.
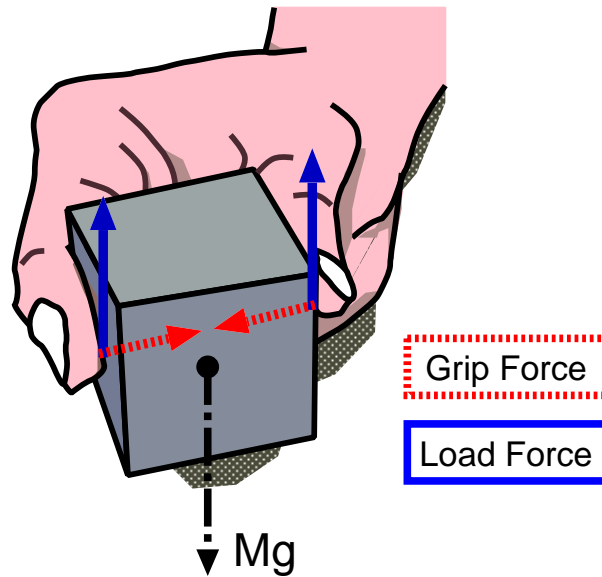
Figure 3.1. Grip and load force

3.3. Development of a simultaneous measurement system of the grip/load force and the finger EMG

3.3.1 Grip and load force

When an object is grasped, grip and load force are applied on the object. Human efficiently controls the grasping force depending on the weight and the friction coefficient of the object. The grip force is vertical force along the contact surface (a dash line in Fig.3.1) and gives pressure on the object to grasp. Load force is horizontal force along the surface (a solid line in Fig.3.1). The load force gives force in the opposite direction to the gravity force and is generated by the friction between the fingertip and the object. When an object is grasped by a pinch grip, grip force f_g, load force f_l, the object weight m, and the gravity acceleration g

satisfy Eq.(3.1):

$$f_l = \frac{mg}{2} \tag{3.1}$$

In order to grasp an object stably without a slip, the grip and load force should satisfy the following equation:

$$\frac{\mu f_g}{f_l} > 1 \tag{3.2}$$

where μ is the friction coefficient between the fingertip and the object surface.

Johansson et al. have investigated the relation between the grip and the load force when human grasps objects that have various friction condition and revealed that human generates about 1.4-fold grip force of the theoretical minimum force to grasp the object[35]. Moreover, they have argued that the force is controlled by perceiving a partial slip on the contact surface (incipient slip)[36]. Tada et al. have revealed that a stick margin on the contact surface has about the same profile if the object weight and friction coefficient are widely varied. They have also demonstrated that the grasping force can be appropriately controlled by keeping the stick margin constant[32]. These works indicate that the grip and load force are controlled by perceiving the slippage on the contact surface.

3.3.2 Measurement device of the grip/load force

Figure 3.2 shows the measurement device that can measure grip and load force. A 6-axis force-torque sensor (nano-sensor: BL-Autotec) is attached in the device to measure the force. The specification of the sensor is shown in Table 3.1.

The size of the device is 70[mm] (top width) ×50[mm] (length) ×110[mm] (height). The two gripping surfaces are covered with cotton (static friction coefficient is 0.7). The weight of the device is changeable at intervals of 300[g] (300[g], 600[g], and 900[g]) by putting leaden blocks in load containers. It is enough to measure the applied force only on the one side since the device is approximately symmetric so that the force on both sides should be the same in the precision grip.
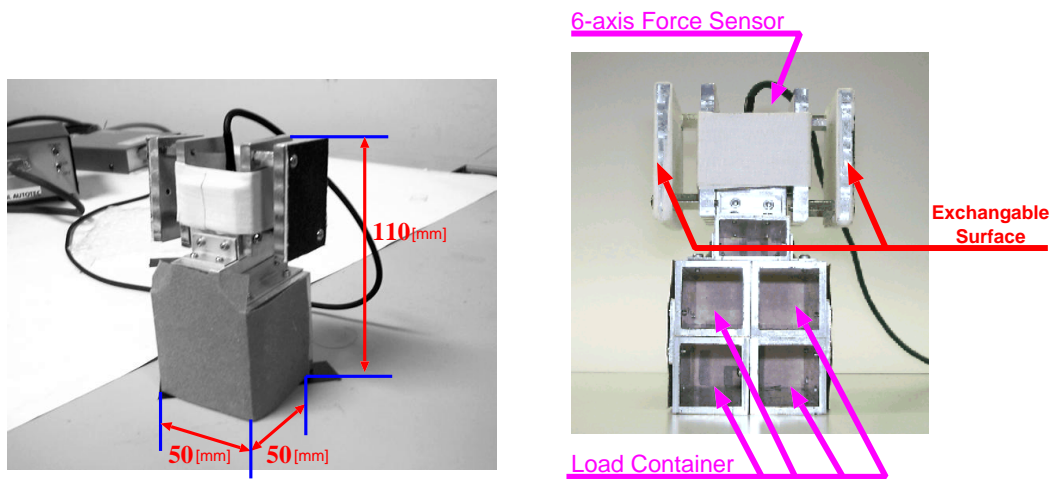
Figure 3.2. Measurement device of the grip/load force

Table 3.1. Specification of the 6-axis force-torque sensor

Load rating	Force	49.0[N]
	Torque	0.392[N·m]
Resolution	Fx, Fy	0.0323[N]
	Fz	0.098[N]
	Tx, Ty	0.000196[N·m]
	Tz	0.000265[N·m]
Size		$\phi 17 \times 22$[mm]
Weight		35[g]

3.3.3 Measurement of the finger EMG

The precision grip has a complexity and redundancy since at least 15 muscles have a direct or an indirect contribution in exerting force[62]. Because it is difficult to measure all the muscles related with grasping motions, the easy-to-measure muscles that intensively act during the motions are selected. The EMG is measured by a surface EMG measurement method.

Target muscles

The static equilibrium of force is required in a pinch grip using the thumb and the index fingers. According to biomechanical constraints, the extrinsic muscles with tendons spanning all links are best suited for providing continuous output force, whereas the intrinsic muscles can adjust and modulate the grip force by stabilizing the metacarpal/phalangeal joints and counteracting rotational moments. In a tip-to-tip pinch grasp, the adductor pollicis (AdP) muscle directly provides the compression force and the abductor pollicis brevis (AbPB) muscle is the antagonist of the AdP muscle[62].

Based on these analyses, the AdP and the AbPB muscles that control the adductive and the abductive motions of the thumb respectively are measured. Fig.3.3(a) shows the position of the AdP muscle and Fig.3.3(b) shows the position of the AbPB muscle. Since these intrinsic muscles are not significantly affected by the motions of the arm, measuring these muscles is adequate to estimate the motions of the thumb.

Simultaneous measurement system of the grip/load force and the finger surface EMG

The surface EMG of AdP and AbPB are measured by an operational bioinstrumentation system (GE Medical Systems SYNA ACT MT-11). The system is comprised of a receiver, a transmitter, and a head amplifier. The surface EMG is measured by two electrodes attached on the skin surface around the target muscles (see Fig.3.4). Since the surface EMG method measures the activities of the muscles around the attached surface, it is not suitable to measure a specific muscle. However, the surface EMG measurement is not invasive and easier to
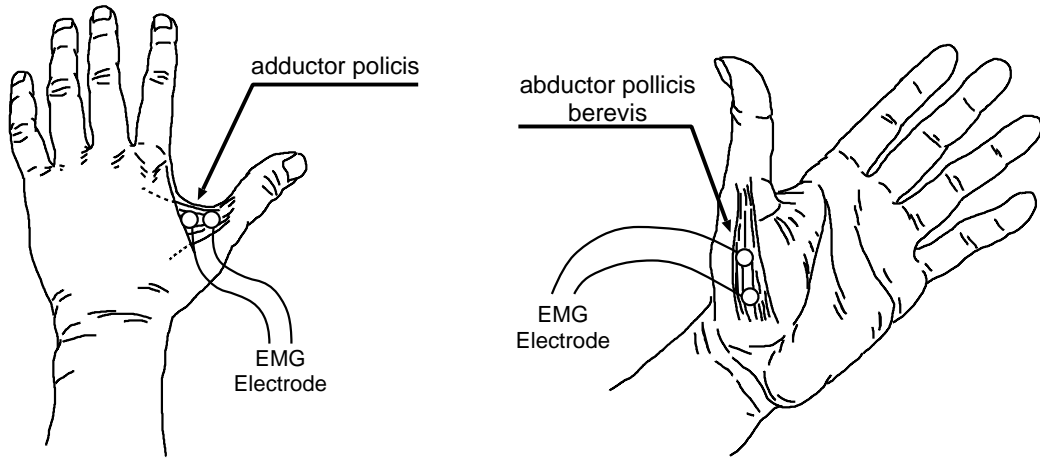
(a) adductor pollicis (AdP) muscle   (b) abductor pollicis brevis (AbPB) muscle

Figure 3.3. Target muscles
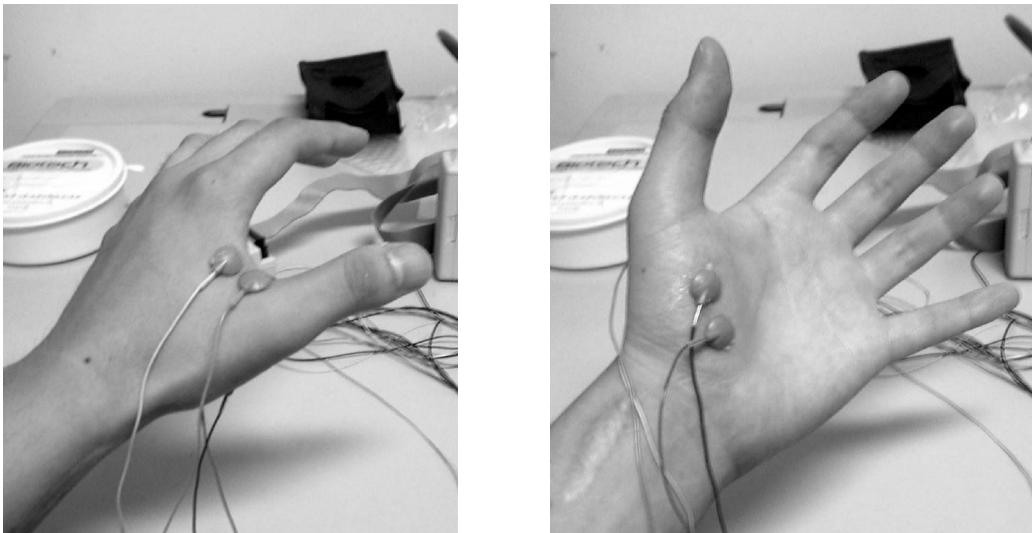
(a) adductor pollicis (AdP) muscle   (b) abductor pollicis brevis (AbPB) muscle

Figure 3.4. Measurement scene of the surface EMG
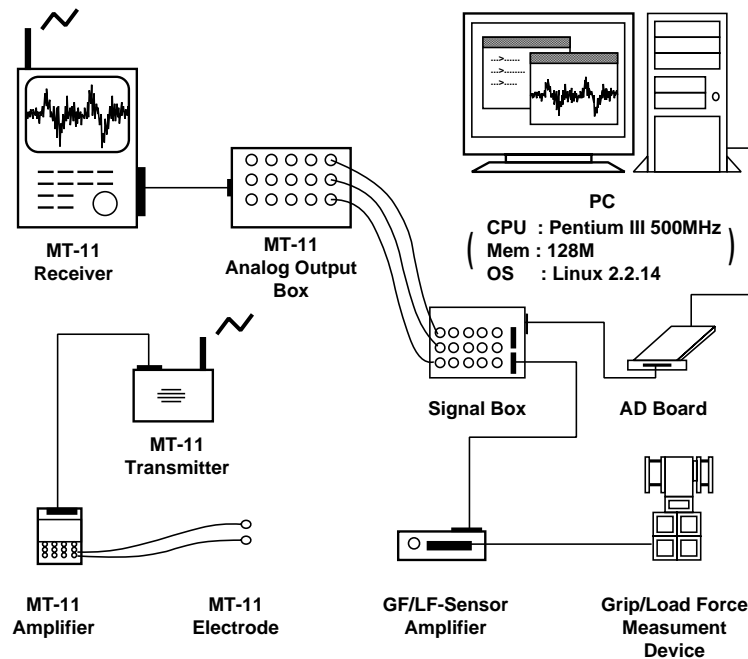
Figure 3.5. System configuration

measure than using needle electrodes.

A simultaneous measurement system of the grip/load force and the finger EMG is developed that is comprised of the force measurement device and the surface EMG measurement system. The system configuration and the system overview are shown in Fig.3.5 and Fig.3.6 respectively.

Analysis method of the surface EMG

A pilot experiment is conducted to determine the analysis method of the measured surface EMG. A subject puts a rubber glove on his hand, and the AdP/AbPB muscles are measured. In the experiment, the object weight is set 900[g].

The grasping motions in the experiment are shown in Fig.3.7. The subject approaches the object ((b) and (c) in the figure) from the initial position (c). After grasping the object (d), he lifts up it to about 300[mm] height ((e),(f),(g)) and lifts down it to the table ((h),(i)). Finally, he releases fingers from the object
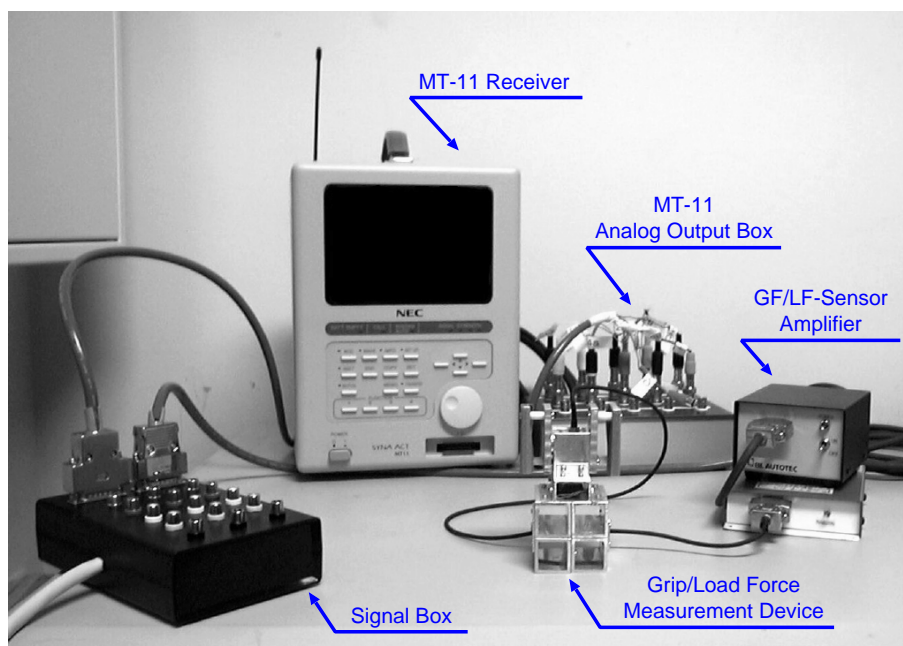
Figure 3.6. System overview
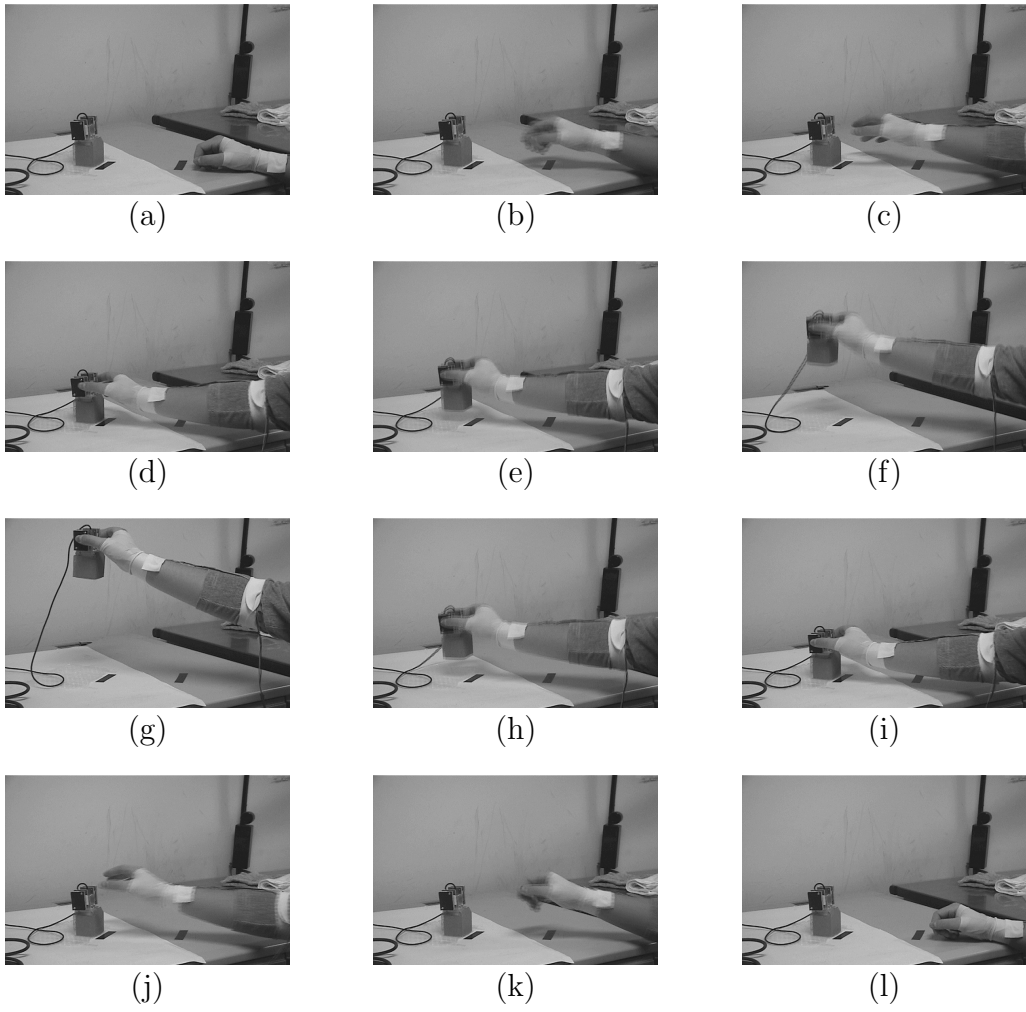
Figure 3.7. Experimental scenes during the grasping motion
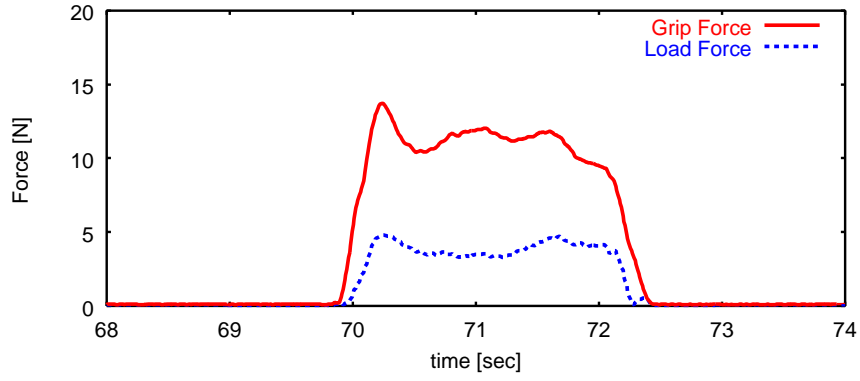
(a) Grip and load force
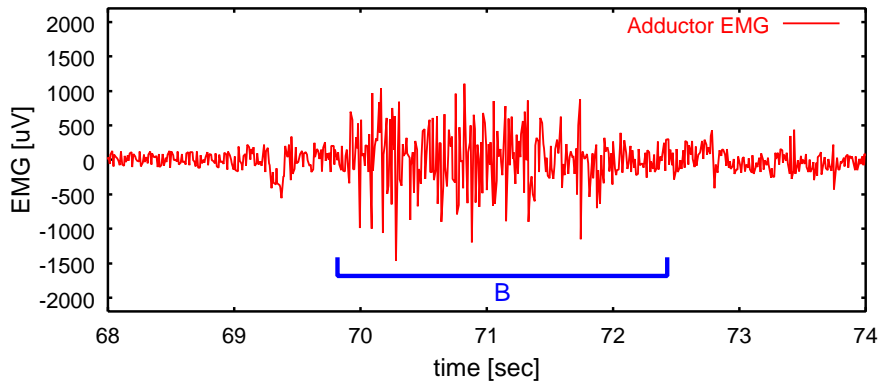
(b) AdP EMG activity
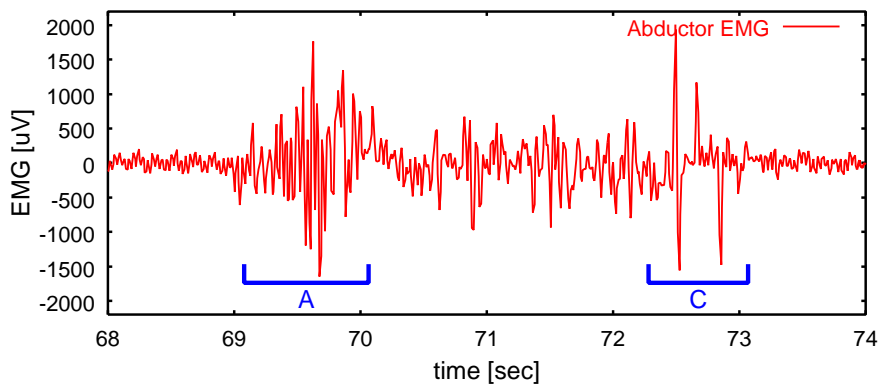
(c) AbPB EMG activity

Figure 3.8. Grip/load force and EMG of AbPB and AdP (pilot exp.)
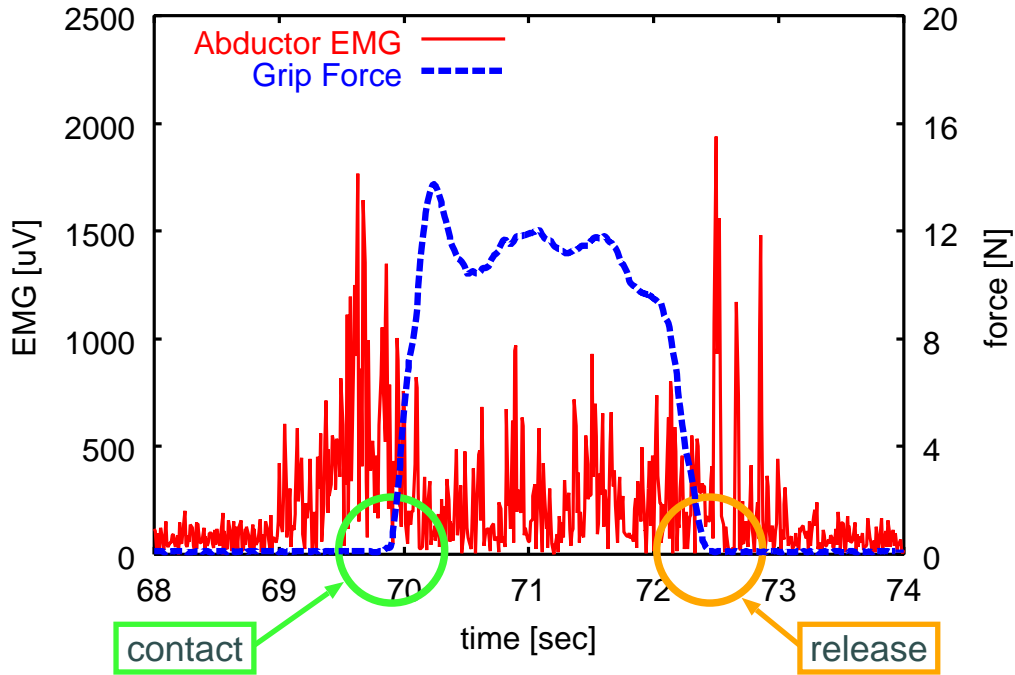
Figure 3.9. Grip force and AbPB EMG (pilot exp.)

and moves back to the initial position ((j), (k), (l)).

The measured EMG signals of the AdP and the AbPB muscles are shown in Fig.3.8. The measured signals are sampled at 100[Hz], digitally low-pass filtered at 30[Hz], and rectified. The measured grip and load force are the applied force on the thumbs side of the object. From the AdP and the AbPB EMG that are shown in Fig.3.8(b) and (c), the antagonistic activities can be observed. The intensive activities of the AbPB EMG can be observed at first (**A** in the figure). Next, the AdP activity can be observed (**B**) and the AbPB activity arises again (**C**).

The grip force and the AbPB EMG in Fig.3.8 are superimposed and shown in Fig.3.9. The force is measure after the fingers contact on the object surface. Therefore, the fingers contacted on the object at the rising of the grip force and the fingers released from the object at the trailing of the grip force. From the figure, the intensive activity can be observed before the contact. The AbPB

29
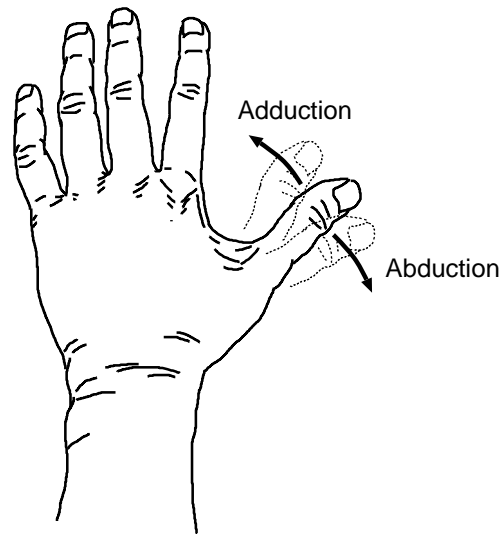
Figure 3.10. Adduction and abduction of the thumb

muscle controls the abduction motions of the thumb (the abductive direction in Fig.3.10) and the AdP muscle controls the adduction motions (the adductive direction in Fig.3.10). When the thumb stretches in order to grasp an object, the thumb moves in the abductive direction and the AbPB muscles acts (**A** in Fig.3.8). When the fingers give pressures on the object, the thumb moves in the adductive direction and the AdP muscles acts (**B**). Finally, when the fingers are released from the object, the thumb moves in the abductive direction again and the AbPB muscles acts (**C**).

Let us consider the implications of the AbPB EMG activities. Since the AbPB muscle controls the abductive movements of the thumb, the activities correspond to the stretch movements of the thumb. However, the thumb moves in the adductive direction before the contact. Now, it is supposed the AbPB activities are caused by the increase of the thumb's stiffness. Fig.3.11 shows the AbPB EMG activities when the thumb's stiffness increases. It can be observed that the AbPB activity increases when the thumb's stiffness increases.

Johansson et al. have revealed that grip and load force apply on the object cooperatively [35]. In order to achieve such a sophisticated grasping motion, it is important to program the applied force on the object anticipatively based on the
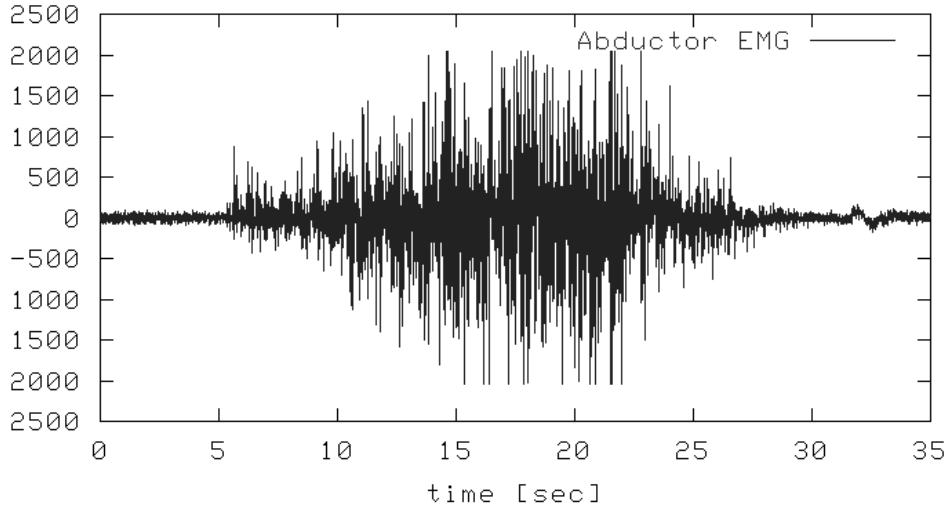
Figure 3.11. Measured EMG signals of the thumb

information of the weight and the friction coefficient of the grasped object[61]. Smooth lifting motions can be performed by applying the force just after the contact.

The grip force and the AbPB EMG activity around the contact are shown in Fig.3.12 when a subject grasps the object whose weight is 300[g], 600[g], and 900[g]. The intensive activities can be observed before the contact (meshed area in Fig. 3.12). Despite the fingers have not contacted on the object surface in this area, the EMG activities seem to be affected by the object weight. Now the range of 0.4[sec] before the contact is defined as "pre-contact period" where the intensive activities can be observed. In the pre-contact period, the tactile sensations about object properties have not been obtained. This fact indicates that the weight-correlated activities in the AbPB EMG seem to correlate with the force programming. Based on the analysis, the AbPB EMG activity in the pre-contact period is focused and investigated in the following section.
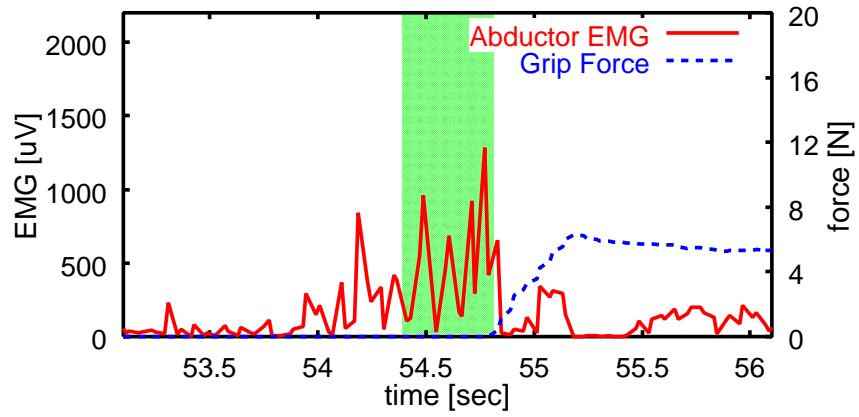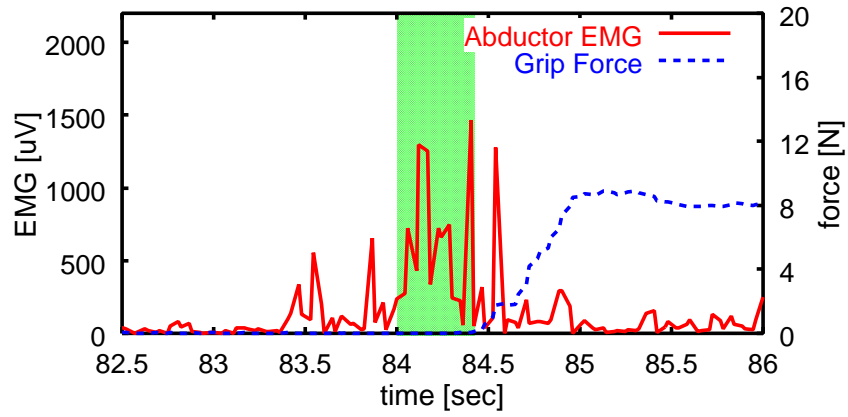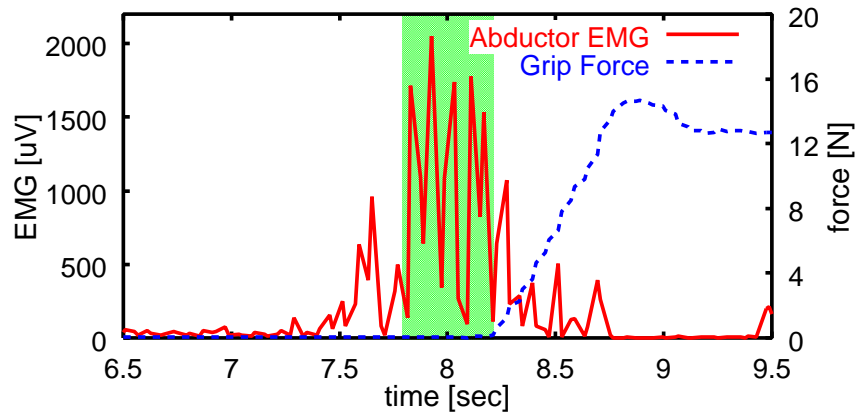
Figure 3.12. Grip force and AbPB EMG in the pre-contact phase (pilot exp.)

3.4. Simultaneous measurement of the grip/load force and the finger EMG during grasping motions

3.4.1 Experimental condition

Experiments are conducted using the simultaneous measurement system described in Section 3.3. Subjects grasp the measurement device whose weight is 300[g], 600[g], or 900[g]. The subjects have practiced the grasping tasks until they have got used to the object weight.

Six healthy right-handed male subjects in the age group of $23 \sim 31$ years old volunteered for the experiments (Subject A, B, C, D, E, and F). Subjects have not been given the information about the objective of the experiment.

Rhythm condition

A subject was seated on a chair with his arm placed on a table in order to lift up the object naturally. The subject was required to perform the task keeping the timing with the bell that rang at intervals of 1.5[sec]. Fig.3.13 shows the procedure of the task in the experiment. In one trial of the task, the subject performed the following motions:

1. At the first bell, the subject starts an approach motion.

2. At the second bell, the object is grasped and lifted up at the height of 300[mm] with a precision grip.

3. At the third bell, the object is lifted down and placed on the table slowly.

4. At the forth bell, subject's fingers are released from the object and his hand is placed at the initial position.

The experimental scenes are shown in Fig.3.14. At first, a subject puts his fingers on the table ((a) in the figure). The subject approaches the measurement device ((b), (c)) and lifts up the object at the 300[mm] height ((d), (e)). Then,
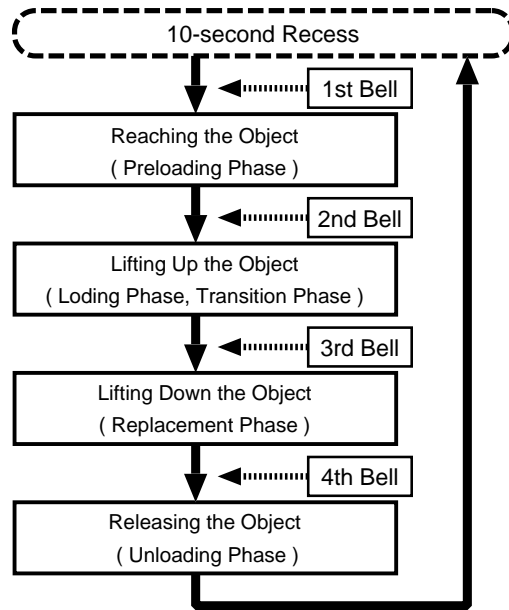
Figure 3.13. Procedure of the grasping motion

he lifts down to the table ((f), (g)), releases from the object (h), and moves his hand to the initial position (l).

The experiment consisted of six sets of the trials in that a subject lifts up and down the object. Each set consists of 10 trials with the same object weight. Subjects were required to perform the trials for two sets in each weight (300[g], 600[g], and 900[g]). The total time for each trial was 6[sec]. Intermissions (3[min]) were given between the sets.

Free condition

Although the experimental setup is almost the same as the rhythm condition, the subjects are not required the rhythmical actions.

The experiment consisted of six sets of the trials in that a subject lifts up and down the object and each set consists of 10 trials with the same object weight. Subjects were required to perform the trials for two sets in each weight (300[g], 600[g], and 900[g]). The total time for each trial was 6[sec]. Intermissions (3[min]) were given between the sets.
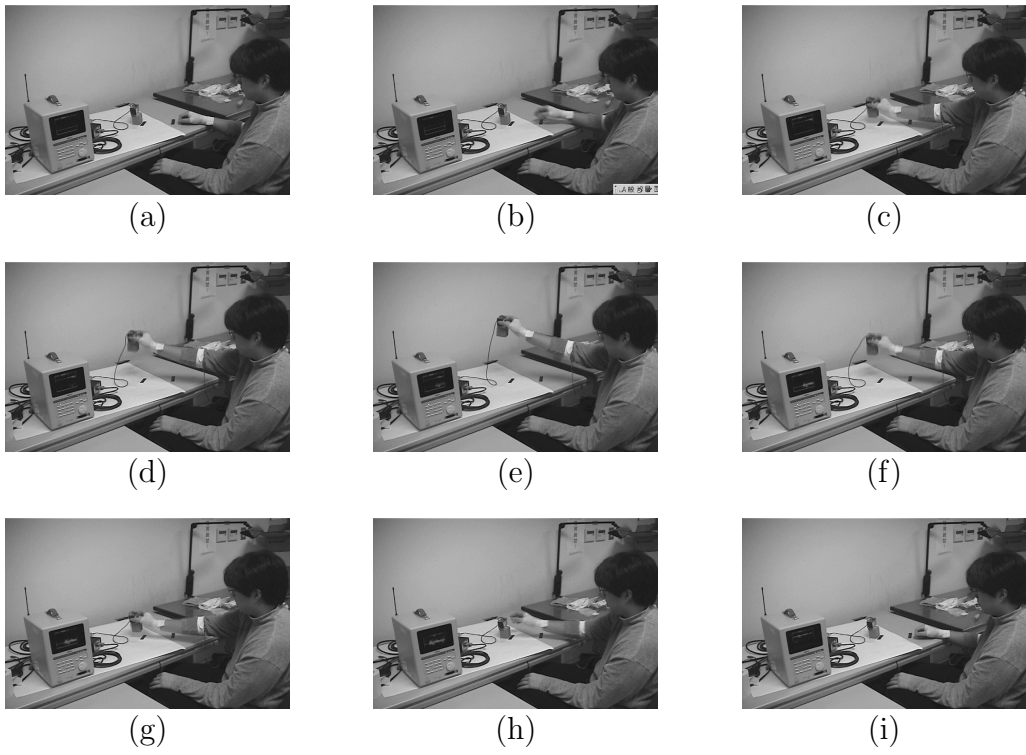
Figure 3.14. Experimental scenes
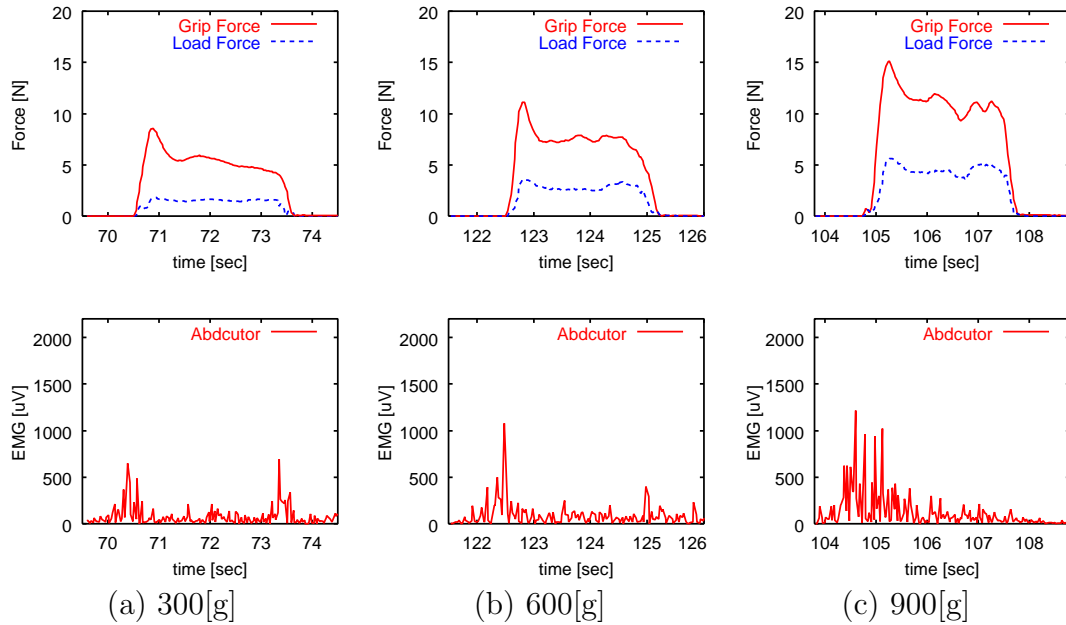
Figure 3.15. Experimental results (rhythm condition, subject A)

3.4.2 Experimental results

Rhythm condition

Fig.3.15 shows the experimental results for the subject A in the rhythm condition. The upper figures show the grip/load force and the lower figures show the AbPB EMG activities.

The grip force and the AbPB EMG of the subject A around the contact are shown in Fig.3.16. The EMG activities before the contact seem to change depending on the object weight. In order to quantitatively evaluate the difference of the EMG activities among the object weights, the average of the EMG activities for 0.4[sec] in the pre-contact period and the mean of the averages are calculated. Fig.3.17 shows the result (error bars indicate the standard deviation). For the subject A, the EMG activities of 300[g] and 600[g] are similar, but larger activity can be observed when the weights is 900[g]. For other subjects, the EMG activities seem to increase as the weight increases.
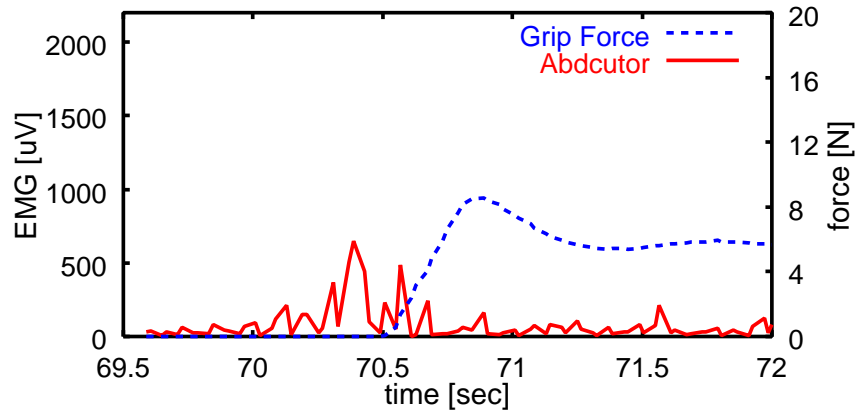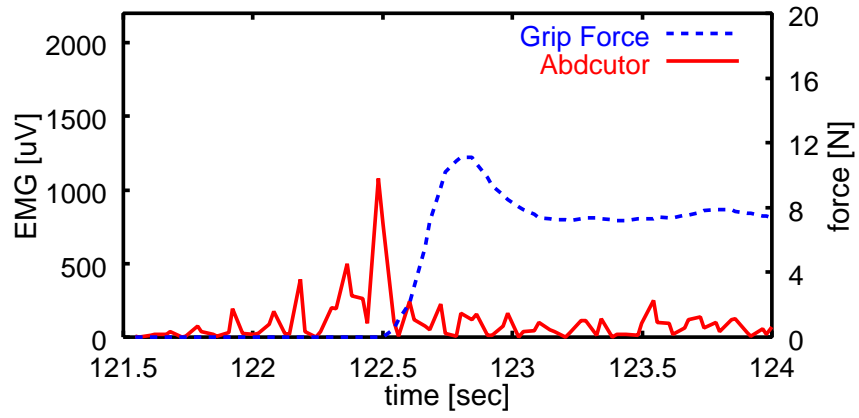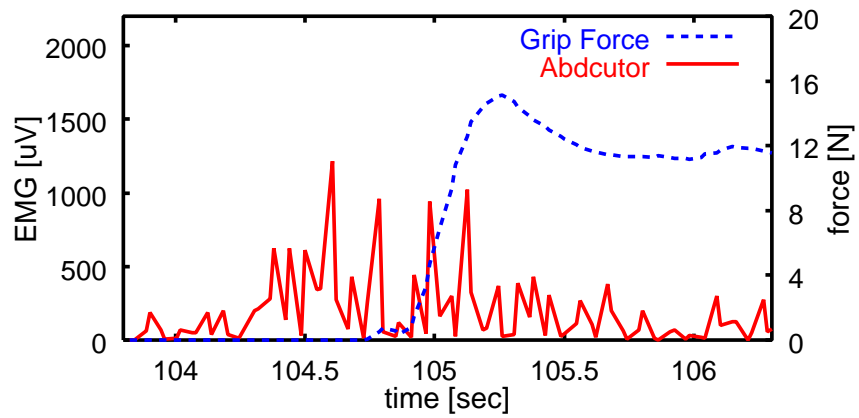
Figure 3.16. Grip force and AbPB EMG (rhythm condition, subject A)
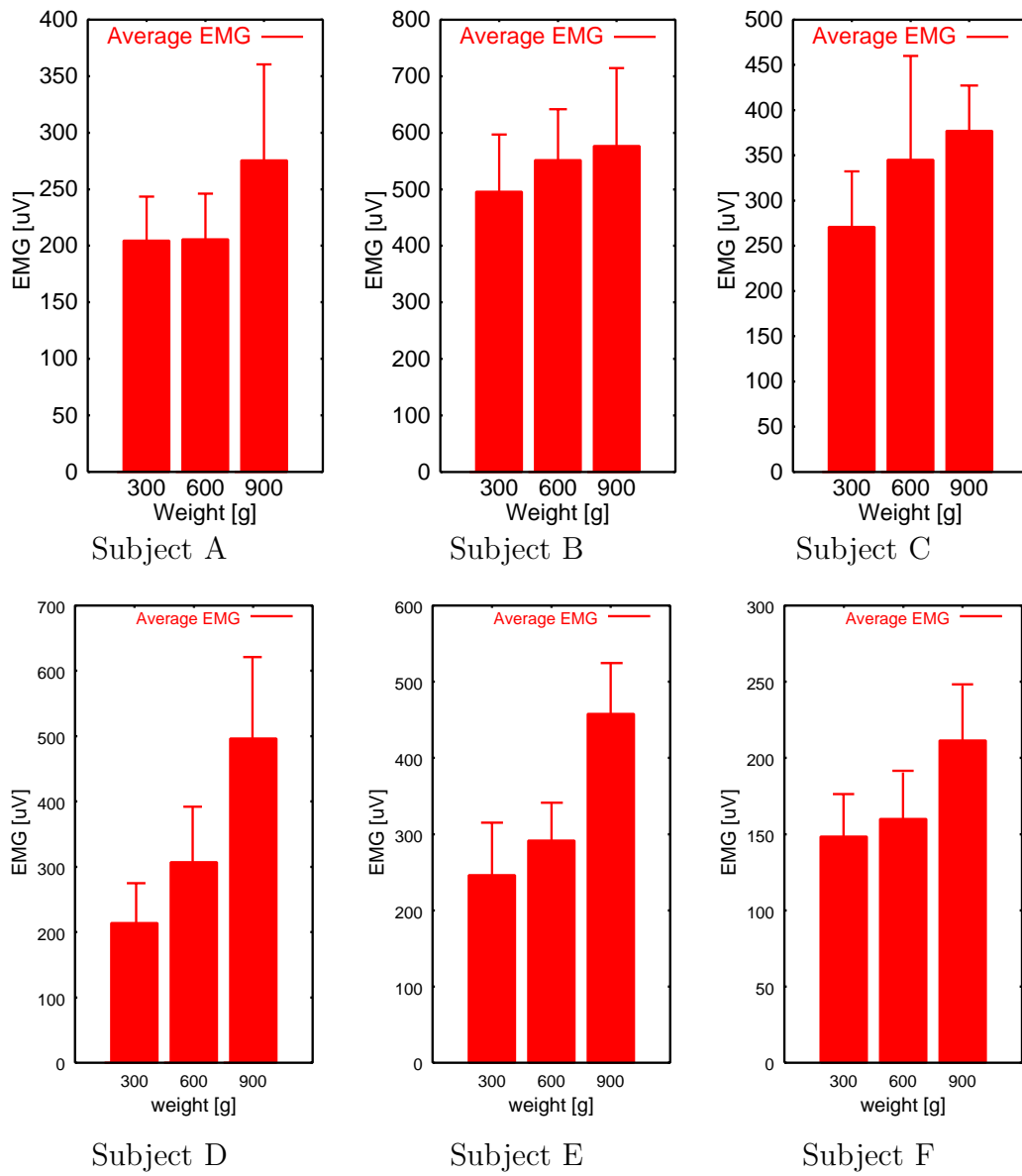
Figure 3.17. Mean of the average EMG in the pre-contact period (rhythm condition)

Table 3.2. Results of Bonferroni's significance test (rhythm condition)

	Sub. A	Sub. B	Sub. C	Sub. D	Sub. E	Sub. F
300-600	NS	NS	$\star\star$	$\star\star$	$\star$	NS
600-900	$\star\star$	NS	NS	$\star\star$	$\star\star$	$\star\star$
300-900	$\star\star$	$\star$	$\star\star$	$\star\star$	$\star\star$	$\star\star$

$\star\star : p < 0.01, \quad \star : 0.01 < p < 0.05, \quad NS : p > 0.05$

The difference of the EMG activities between the object weights is statistically analyzed by the Bonferroni's significance test. The calculation method of the Bonferroni's test is shown in the appendix A. The results are shown in Table 3.2. In the table, 300-600 indicates the result of the test between the activity when the weight is 300[g] and the activity when the weight is 600[g].

Since the EMG activities vary widely, as we can observe from the standard deviation in Fig.3.17, the difference can not be detected in some condition. However, the difference in the 300-900 condition can be detected for all the subjects. This result suggests that the object weight affects the AbPB EMG activities in the pre-contact phase. Although several works have revealed that the peak of the grip force during grasping motions is affected by the force programming[48, 63], the weight-related activities in the AbPB EMG have not been reported yet. The AbPB activity seems to correlate with thumb's stiffness. It is very interesting that the experimental results suggest that human controls the stiffness of the fingers by the feedforward control depending on the object weight.

Free condition

Fig.3.18 shows the experimental results for the subject A in the free condition. The upper figures show the grip/load force and the lower figures show the AbPB EMG. In order to quantitatively evaluate the difference of the EMG activities among the object weights, the average of the EMG activities for 0.4[sec] in the pre-contact period and the mean of the averages are calculated. Fig.3.19 shows the result (error bars indicate the standard deviation).
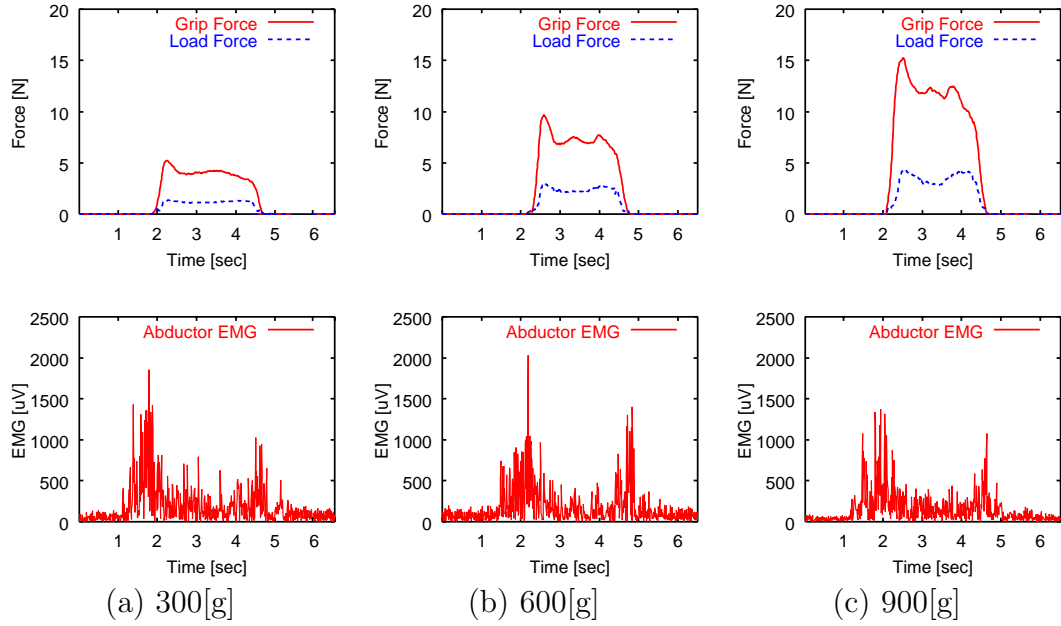
Figure 3.18. Experimental results (free condition, subject A)

In the free condition, the EMG activities do not increase depending on the weight. These results are apparently different from the results in the rhythm condition. This suggests that the rhythmic motion based on the bell sounds affects the grasping motion.

3.5. Conclusion

This chapter has investigated the rhythmic effects and the feedforward control of grasping motions by measuring the grip/load force and the finger surface EMG of AbPB/AdP muscles simultaneously.

The simultaneous measurement system has developed that consists of a measurement device of the applied force and a surface EMG measurement system. Since the grip and load force can be measured after the contact between the object and the fingertips, the measured force is used for the detection of the contact.

Adductor Pollicis (AdP) and Abductor Pollicis Brevis (AbPB) muscles have
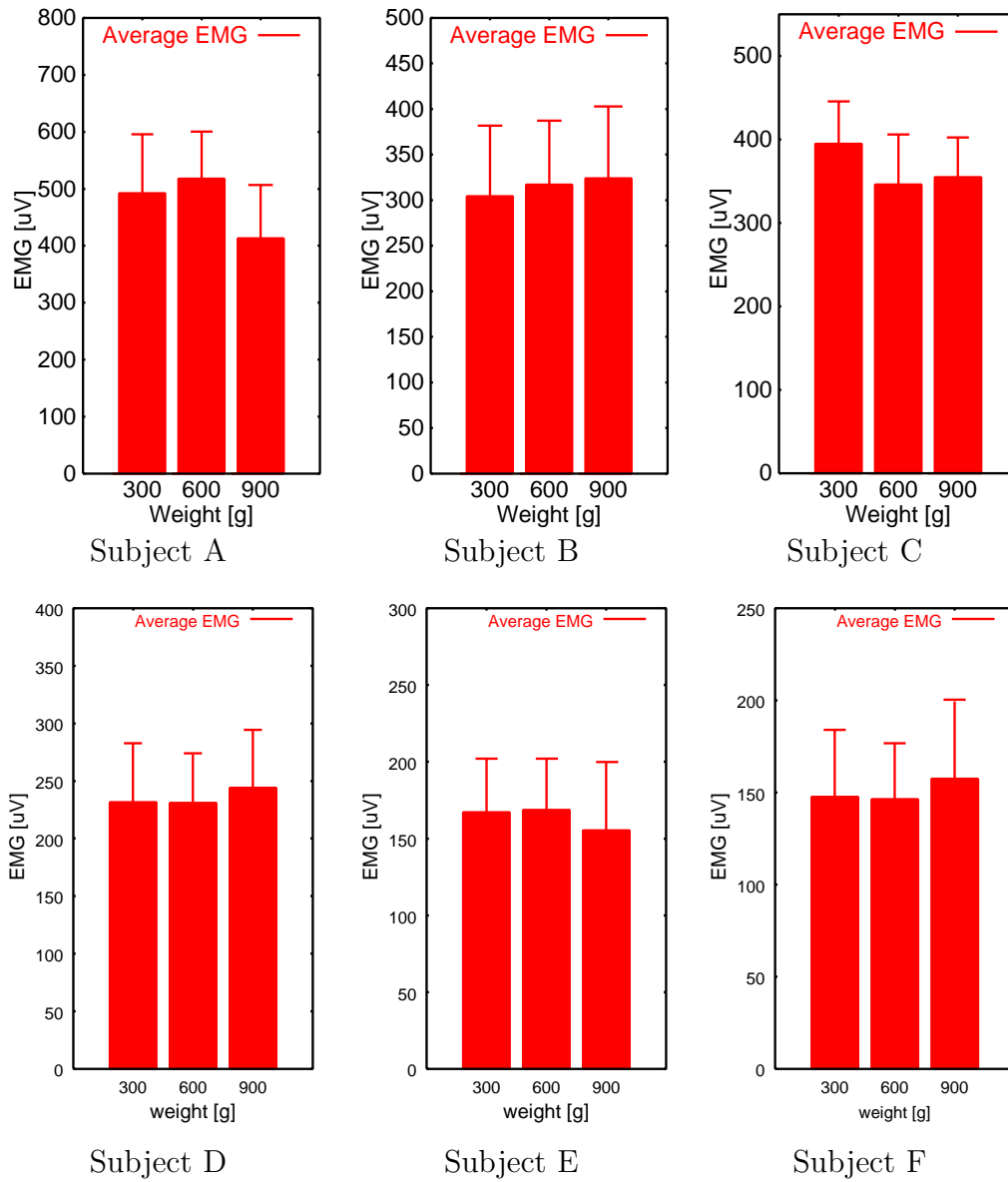
Figure 3.19. Mean of average EMG in the pre-contact period (free condition)

been measured by the EMG measurement system. The AdP muscle controls the adduction motions of the thumb and the AbPB muscle controls the abduction motions. Since these intrinsic muscles are easy to measure by a surface EMG measurement method and not significantly affected by the motions of the arm, these muscles are suitable for the measurement. The measured EMG activities have been exploited for analyzing the force programming before the correction by the tactile sensations.

A pilot experiment has been conducted to determine the analysis method for the measured surface EMG. The intensive activities of the AbPB muscle have been measured in the range of 0.4[sec] before the contact. The range has been defined as "pre-contact period".

The experiments have been conducted using the simultaneous measurement system. Six subjects have grasped the measurement device whose weight is 300[g], 600[g], or 900[g]. In the experiment, two conditions are set up. In the rhythm condition, the subjects have been required to perform the tasks rhythmically keeping the timing with the bell. In the free condition, they have not been required the rhythmical actions. The difference of the measured EMG activities in the pre-contact period have been statistically analyzed by the Bonferroni's significance test. The experimental results suggest that the object weight affects the AbPB EMG activity. The weight-related activities in the AbPB EMG have not been reported yet. These analyses indicate the importance of the feedforward control in the grasping motions and the rhythmic motions in the human's manipulations.

Chapter 4

Rhythmic motion patterns in human's manipulations

4.1. Introduction

Taguchi et al. have reported that fingers during human's rotating manipulations are controlled according to rhythmic patterns when humans attain proficiency[60]. Motion patterns of legs in walking of animals have been formalized based on the observation of the contact and release on the ground from the sequential photographs[64, 65]. Supposing human's fingers as a multiple manipulator system, the same formalization method of the motion patterns can be applied to the finger motions.

A number of applications for human-machine interfaces have been proposed based on the measurement of the hand shape and the joint angles of the fingers using cameras, motion capturing systems, and sensor gloves[66, 67, 68]. During rhythmic motions, the fingers move iteratively along similar trajectories. In order to achieve such rhythmic motions using a robot hand, it is not important to imitate the trajectories and the hand shape of human precisely. The significant questions are "Which finger does move?" and "When the finger does move?". This information can be measured by the contact condition between the fingers and the object.

Firstly, this chapter describes a measurement system of the contact patterns between fingers and an object during rotating manipulations. A subject manipu-

lates a cylindrical object using four fingers and the contact condition is measured by the developed measurement system. Next, typical contact patterns are detected based on the measured contact information that can apparently represent the rhythmic movements during the manipulation. The rhythmic motions of fingers during the rotating manipulations are investigated based on the typical contact pattern.

4.2. Investigation of rhythmic manipulations based on the contact condition

4.2.1 Measurement system

In order to grasp an object using a robot hand, two elastic fingers or three rigid fingers are necessary for the static stability. If the robot hand has an additional one finger, it is enough to relocate fingers keeping the static stability during the manipulation. Therefore, a number of dextrous robot hands that have four fingers have been developed[3, 7]. Considering that a four-fingered robot hand is exploited for a manipulation, human's rotating manipulations using four fingers are measured in this study.

The contact condition during the rotating manipulation is measured using force sensing resistors (FSRs) that are shown in Fig.4.1(a). The specification of the FSR is shown in Table 4.1. In the experiment, a subject puts rubber fingercaps in that the FSRs are attached on the fingertips (thumb, index, middle, and ring fingers) and rotates a cylindrical object whose diameter is 65[mm] and weight is 20[g]. The system overview is shown in Fig.4.1(b). The sampling frequency of the FSRs is 50[Hz].

4.2.2 Experimental condition

The experimental scene is shown in Fig.4.2. Five subjects (Subject A, B, C, D, and E) performed the experimental tasks after they had practiced the manipulation sufficiently. The subjects have not been given information about the objective of the experiment.

Table 4.1. Specification of FSRs

Active area diameter	5.0[mm]
Thickness	0.3[mm]
Active range	$9.8 \sim 980$[kPa]
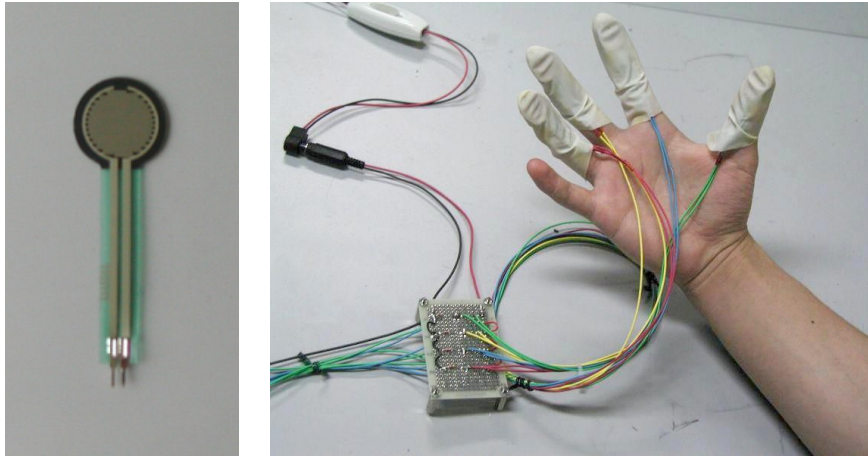
(a) FSR   (b) System overview

Figure 4.1. Contact measurement system

Figure 4.2. Experimental scene

4.2.3 Experimental results

Fig.4.3 shows that representative FSR output of the subject A for two seconds during the rotating manipulation. The vertical axis indicates the FSR output and the horizontal axis indicates the time. The measured FSR activity increases as the applied force increases. It is interesting to investigate human's stability control during the rotating manipulation based on the measured applied force, but this is not the present concern. In this chapter, the contact pattern of each finger is focused.

When the fingertip applies the force on the object, the FSR can measure the pressure on the contact area. The contact condition between the fingertip and the object can be detected by analyzing the measured FSR information and binarizing at a certain threshold into "touch condition" and "release condition". Fig.4.3(a) is the measured FSR information of the subject A during the manipulation. The contact condition is also shown in Fig.4.3(b). The contact condition for the other subjects are also shown in Fig. 4.4(a)~(d). From these figures, we can observe the characteristic contact information depending on the subjects. To represent
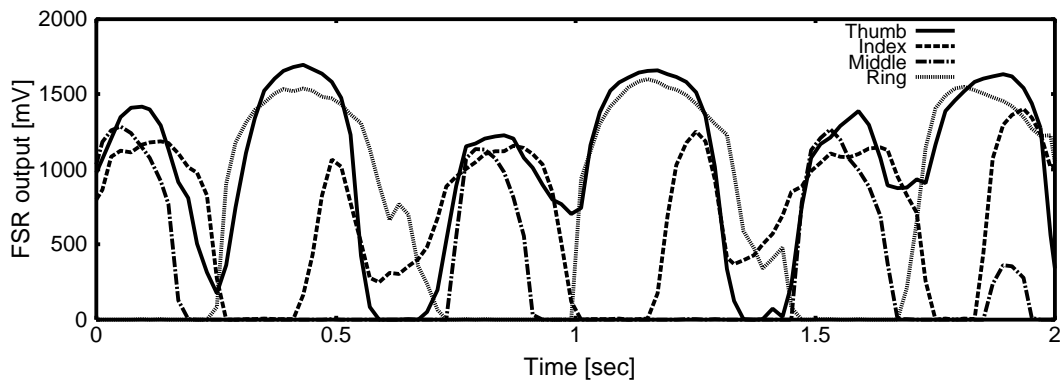
(a) FSR outputs
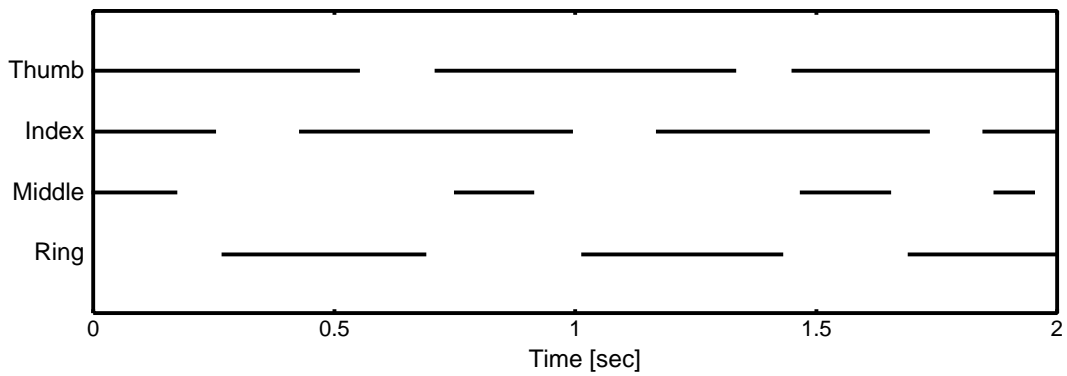
(b) Contact information

Figure 4.3. Contact condition during the rotating manipulation (Subject A)

47
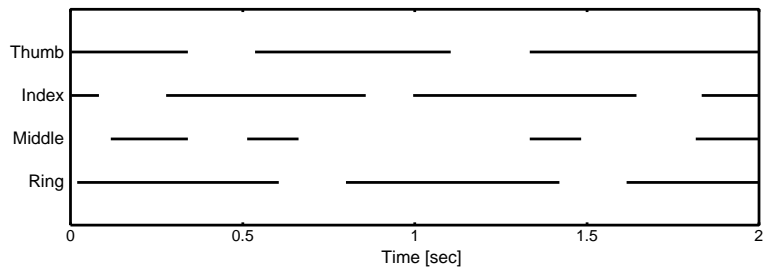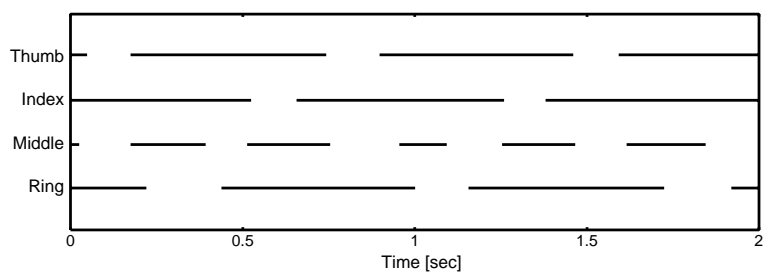
(a) Subject B

(b) Subject C
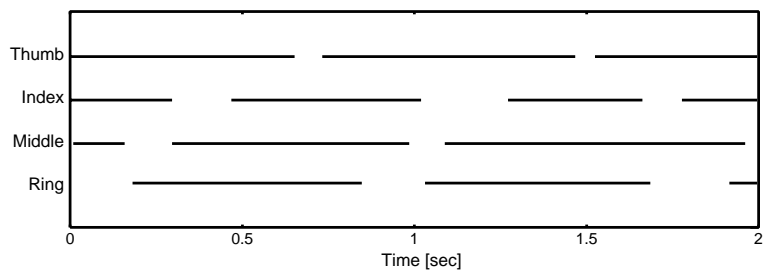
(c) Subject D
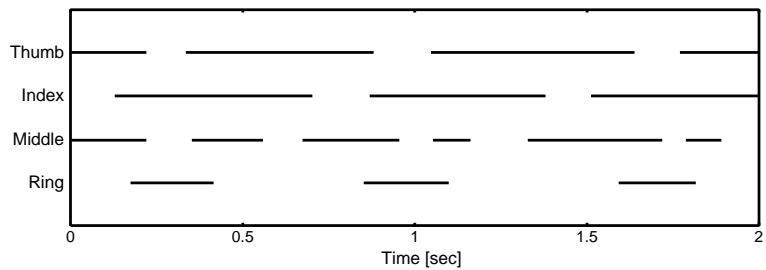
(d) Subject E

Figure 4.4. Contact condition during the rotating manipulation (Subject B $\sim$ E)

the individual characteristics clearly, the typical contact patterns are detected based on the measured information.

When the measured contact information is separated at the timing when the contact condition of the thumb becomes the touch condition from the release condition, most of the time period of the successful motion in one cycle is about $0.7 \sim 0.8$[sec] for all the subjects. Based on the analysis, the typical contact pattern is derived by the following procedures:

1. The measured contact information is separated at the timing when the contact condition of the thumb becomes the touch condition from the release condition and each separated data is supposed as the data of one cycle.

2. The data whose time period in one cycle is $0.7 \sim 0.8$[sec] is extracted.

3. The extracted data is interpolated linearly in order that the time period becomes 0.8[sec].

4. The average of the interpolated data at each time is calculated and the averaged data is binarized again.

The typical contact patterns can be represented by the time period of the touch condition in one cycle. The typical contact patterns for all the subjects are shown in Fig.4.5.

From the typical contact patterns, following characteristics can be observed:

1. When the thumb contacts, the ring finger is released.

2. When the ring finger contacts, the index finger is released.

3. When the index contacts, the thumb is released.

These results show that two fingers among the thumb, index, and ring fingers consistently touch on the object surface. Although the contact pattern of the middle finger varies widely depending on the subjects, it seems that the middle finger touches in synchronization with the thumb's movement and supports the stable grasp. For the subject E, the contact timing of the ring finger delays in comparison with the other subjects, but the middle finger supports the grasp by touching the object earlier.
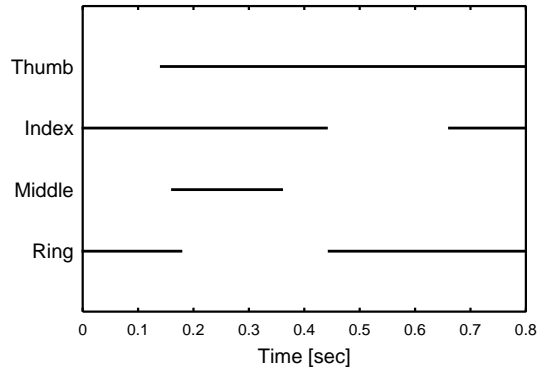
(a) Subject A
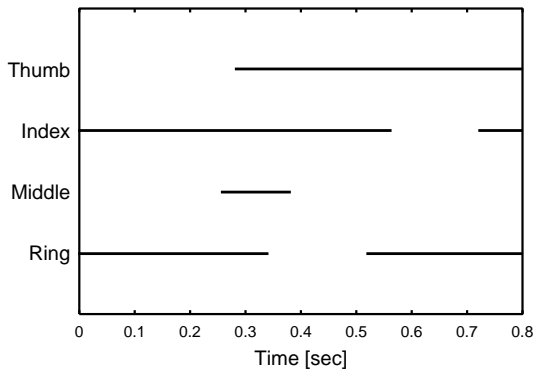
(b) Subject B
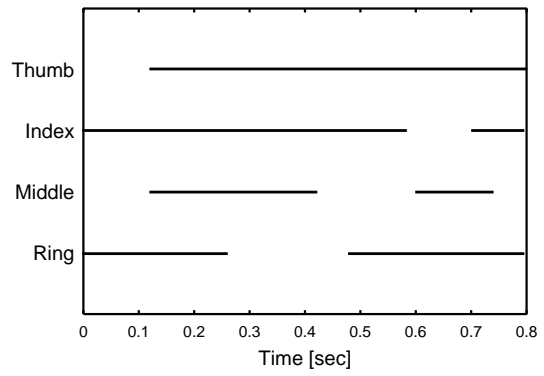
(c) Subject C
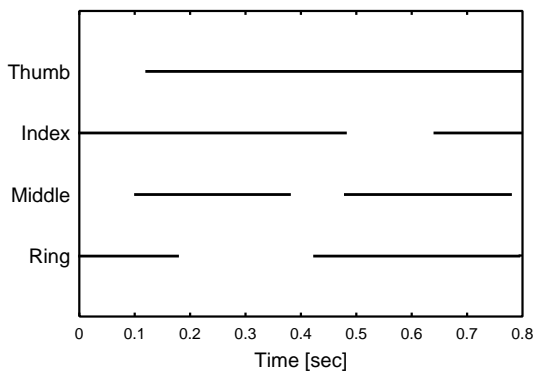
(d) Subject D
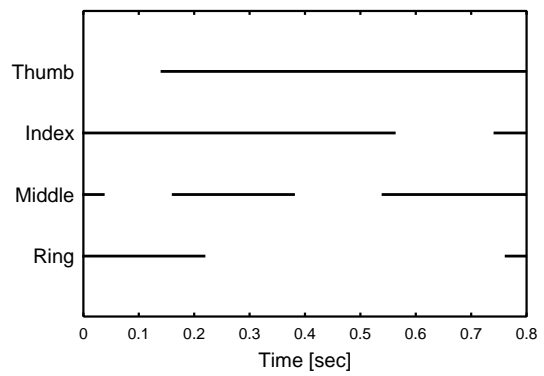
(e) Subject E

Figure 4.5. Typical contact patterns

50
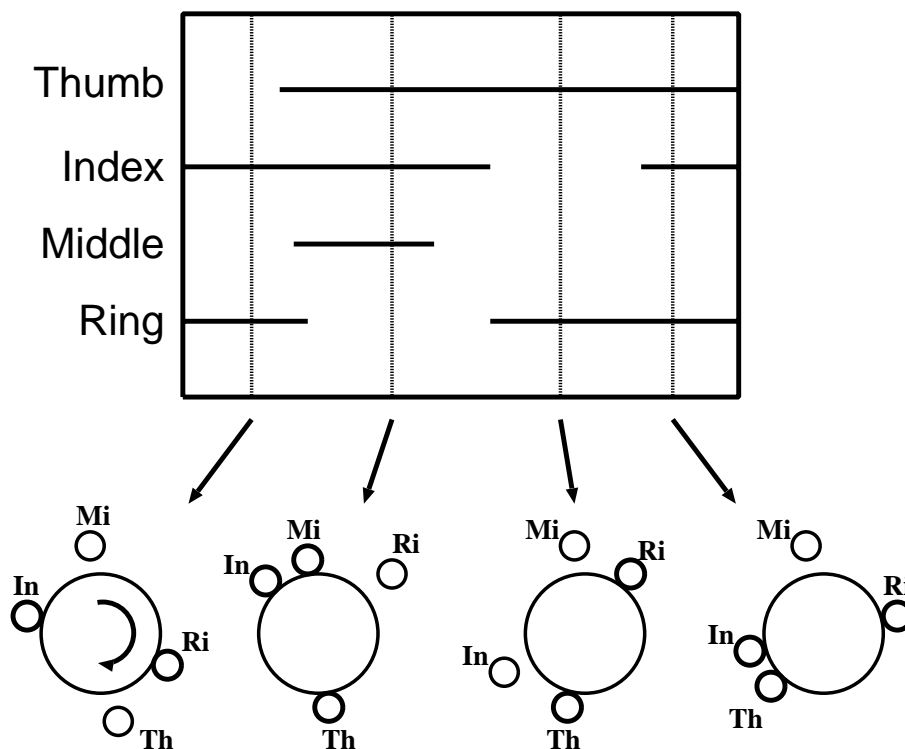
Figure 4.6. Switching patterns of the grasping fingers

These analyses suggest that the principal three fingers (thumb, index, and ring finger) mainly take a role for the stable grasp and the rotating manipulation; the middle finger supports those motions when the grasp and the manipulation can not be performed using only the principal three fingers.

We can investigate how the switching motions (relocating of the fingers) are performed based on the typical contact patterns. The switching motions during the rotating manipulation in the subject A are shown in Fig.4.6 that can be given by the measured contact pattern (shown in Fig.4.5(a)). During the manipulation, the frequent switches of the grasping configuration, from two fingers grasp to three fingers grasp and vice versa, can be observed.

The movable range of the fingers seems to affect the contact patterns. The rotating manipulation is performed by adductive/ abductive movements and flexion/ extension of the fingers. In such movements, the movable range of the thumb

is relatively wider than the movable range of the other fingers, especially in the adduction/abduction of the middle finger. These effects of the movable range may determine the contact patterns during manipulations.

4.3. Conclusion

This chapter concentrates on the rhythmic motions of humans and investigates contact patterns during rotating manipulations. When a person attains proficiency, the motions of the fingers during the rotating manipulations are controlled according to rhythmic patterns. By analyzing the contact pattern during the manipulation, the characteristics of the rhythmic manipulations can be investigated.

A measurement system has been developed and the contact condition of the fingers has been measured during the rotating manipulation. The contact condition has been measured by force sensing resistors (FSRs). A subject puts rubber fingercaps in that the FSRs are attached on the fingertips (thumb, index, middle, and ring fingers). He rotates a cylindrical object using these four fingers. In the rotating manipulation, switching motions (finger relocation) are consequently observed. The rhythmic movements of the fingers have been observed by the measured contact condition during the manipulation. Typical contact patterns have been detected based on the contact information. The typical contact patterns represent the touch condition in one cycle of the manipulation.

The measured typical contact patterns show the switching patterns of the grasping fingers. The role of each finger can be investigated from the typical contact pattern. The principal three fingers (thumb, index, and ring fingers) mainly take a role for the stable grasp and the rotating manipulation; the middle finger supports those motions when the grasp and the manipulation can not be performed using the principal three fingers. Movable range of the finger seems to affect the measured contact pattern. Few studies have investigated the rhythmic motion patterns based on the contact condition. The results in this chapter have presented a formalization method of manipulations using fingers.

In order to investigate the human's rhythmic manipulation skills, it is necessary to measure additional information during the manipulation. For example, the contact points between the object and the finger, the applied force and torque,

and the position and rotation of the manipulated object should be measured. Moreover, it is interesting to investigate the manipulation patterns when the object size and shape are changed. The measurement device that can measure such information will be required for the further investigation.

Chapter 5

CPG-based manipulation

5.1. Introduction

Neurophysiological studies have revealed that rhythmic motor patterns such as locomotion in animals and insects are coordinated by neural circuits referred to as central pattern generators (CPG) [69, 70, 71]. In walking of the animals, the musculo-skeletal system is driven by the rhythmic patterns generated from a rhythm generator in the vertebra and a reflex system based on the sensations from peripheral nerves. The animal's walking patterns adaptively change according to the walking velocity, for example, in walking, rattling, and rapid pace.

The rhythmic pattern that produces the locomotion has been constructed using neural oscillators[72, 52]. A CPG steadily generates oscillatory output unless external input is given. The CPG can generate various patterns based on the external input, such as sensory feedback. The measured typical contact patterns during a rotating manipulation addressed in the chapter 4 represents a model of the rhythmic motion pattern. If the pattern can be generated by a certain CPG, the CPG-based control method of walking for a multi-legged robot can be applied on the rhythmic manipulations for a multi-fingered hand.

This chapter addresses a neuron oscillator model and a CPG that is constructed by a mutual connection of the neurons. The constructed CPG generates a contact pattern of the fingers. Next, a control method of the fingers is described. The fingers are controlled by "motion-triggers" generated by the CPG. Then, the feedback of the external force into neurons by a force sensor on a fingertip is

proposed. The force feedback via the CPG can enhance the stability of the grasp when a disturbance is applied. Finally, a dynamic simulation system is developed and the effectiveness of the proposed CPG-based control is demonstrated by performing rotating manipulations using the contact pattern generated by the CPG.

5.2. CPG-based manipulation

5.2.1 Neural oscillator model

Various neural circuit models have been proposed that explain the mechanism of a rhythm generator[73, 74, 75]. In this study, the neural oscillator model that has been proposed by Matsuoka[72, 52] is adopted for a rhythm generator. Mathematical properties of Matsuoka's model and generating condition of the oscillatory output in a mutual inhibition network have been investigated.

The CPG-based control has been applied to an adaptive walking control of multi-legged robots and the effectiveness has been confirmed. Taga has proposed a walking control method that is robust against the changes of the terrain and the external force by connecting the neural model to the musculo-skeletal model of a bipedal walking robot[76, 51]. Kimura et al. have also developed a quadrant robot that can walk on smooth and rough terrain using the CPG-based control[77, 78].

The neural oscillator of the Matsuoka's model can be mathematically represented by the following equations:

$$\tau \dot{u}_i = -u_i - \beta v_i + \sum_{j=1}^{n} w_{ij} y_j + u_0 + S_i \tag{5.1}$$

$$\tau' \dot{v}_i = -v_i + y_i \tag{5.2}$$

$$y_i = f(u_i) \qquad (f(u_i) = \max(0, u_i)) \tag{5.3}$$

where u_i is the inner state of the i-th neuron; v_i is the variable representing the degree of adaptation or self-inhibition; y_i is the output of the neuron; u_0 is the external input with a constant rate; S_i is the feedback input; w_{ij} is the connecting weight between the i-th and the j-th neurons; β is the constant of adaptation; τ and τ' are the time constants of the inner state and the adaptation respectively.
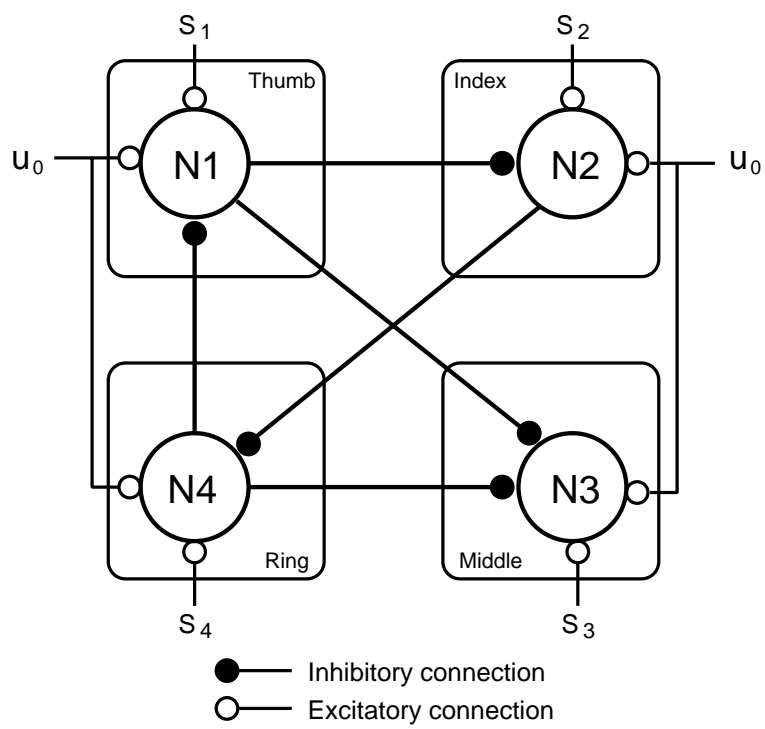
Figure 5.1. CPG model that generates a similar contact pattern to humans

A CPG can generate various patterns by connecting the neurons to each other. The measured typical contact pattern in the chapter 4 can be generated by the CPG. The constructed CPG is shown in Fig.5.1. $N_1 \sim N_4$ are the neurons that generate contact patterns of the thumb , index, middle, and ring fingers respectively. Fig.5.2(a) shows the output of each neuron where $S_i = 0$. The amplitude of each neural output is not important because the neurons generate the contact period of time. The generated contact pattern in one cycle from the constructed CPG is shown in Fig.5.2(b).

In the generated contact pattern, the thumb, index, and ring fingers touch on and release from the object alternately. Two fingers among those three fingers touch the object consistently during the manipulation. Additionally, the middle finger touches in order to support the role of the thumb and the index finger when the ring finger releases.

5.2.2 Generation of the motion-triggers by CPG

Fingers basically keep iterative motions on a constant trajectory during the rhythmic motions, therefore, it is not important to imitate the trajectories. Rotating manipulations can be conducted by classifying the motions into several categories and performing these motions.

Here, a rotating manipulation can be classified into the following four categories:

- Touching on an object (approach motion)

- Rotating the object (rotating motion)

- Releasing from the object (release motion)

- Moving back to an initial point (back motion)

The rotating motion is taken after the approach motion, and the back motion is taken after the release motion. The rhythmic rotating manipulations can be performed by issuing "motion-triggers" that starts these successive motions. The motion-triggers should be issued appropriately in order that the fingers cooperatively and synchronously move and manipulate the object. To generate such rhythmic motion-triggers, the CPG is exploited for issuing the commands.
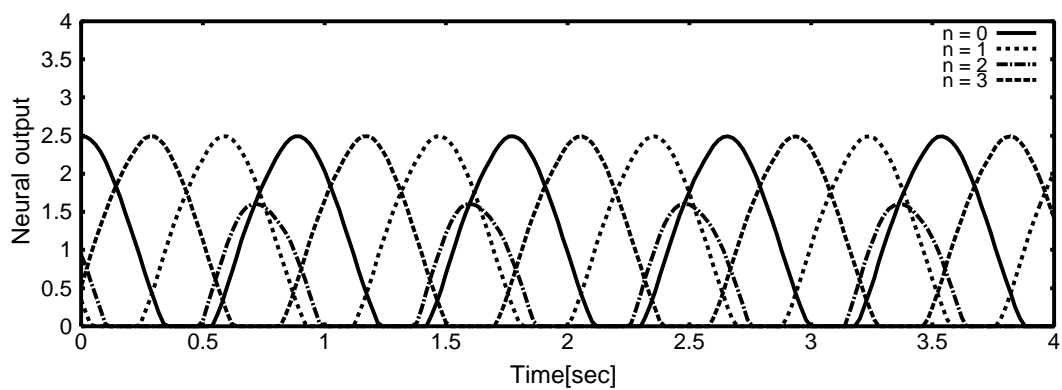
(a) Neural outputs
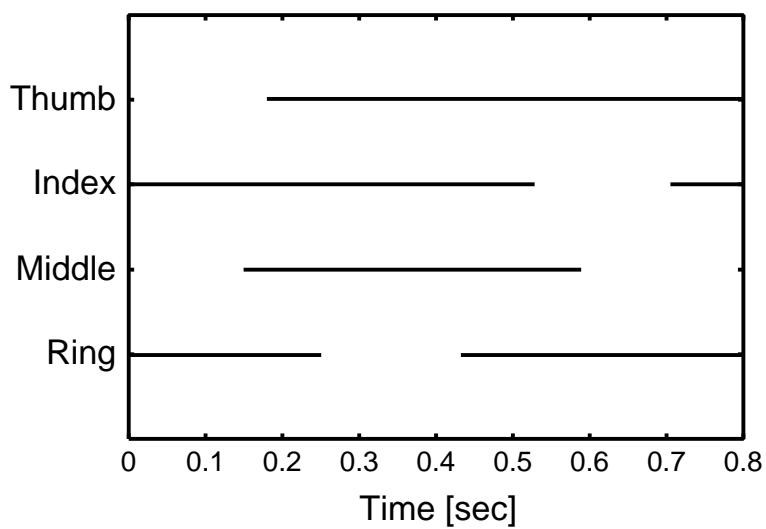
(b) Contact pattern in one cycle

Figure 5.2. Contact pattern generated by the constructed CPG ($\tau = 0.3, \tau' = 1.5, u_0 = 7.0, \beta = 3.0, w_{ij} = 2.2$)

In the rotating manipulations, the CPG generates two kinds of the motion-triggers:

- Command that starts the approach motion and the rotating motion (contact command).

- Command that starts the release motion and the back motion (return command).

The contact command is issued when the output of the i-th neuron becomes $y_i > 0$ from $y_i = 0$, and the return command is issued when the output becomes $y_i = 0$ from $y_i > 0$. By issuing these commands cooperatively on the fingers, the rhythmic manipulations can be performed that involve switching and relocating motions of the fingers.

5.2.3 Sensory feedback to the neurons

When large external force is applied on the grasped object during a manipulation, the object slips over the contact surface and may be dropped on the ground. Considering that the rotating manipulations are performed using the measured contact patterns in the section 5.2.1, frequent switches of the grasping configurations, from two fingers grasp to three fingers grasp and vice versa, have been observed. Assuming that the point contact holds between a rigid finger and a rigid object, when the object is grasped with two fingers, the action lines of the grip force should pass the two contact points and face each other in the equivalent force. Similarly, when the object is grasped with three fingers, the action lines of the force should be on the same plane that involves the three contact points and be parallel to each other, or the action lines have to pass on the center of the mass. If the fingers have elastic fingertips, soft-finger contact can be assumed and the described condition above has not to be strictly satisfied. However, it is apparent that the condition of the stable grasp with two fingers is less robust than with more fingers. The simple and effective way to deal with the problem is to enhance the grasp robustness by adding grasping fingers when external force is applied.

In order to add grasping fingers when a force sensor on a fingertip measures external force, the feedback term S_i in Eq.(5.1) is given by the following:

$$S_i = -k_s \max(0, s_{zi} + s_{\min}) \tag{5.4}$$

where s_{zi} is the sensor value of the i-th fingertip in the gravitational direction, $s_{\min}$ is the threshold that detects the external force, and $k_s > 0$ is the feedback gain.

When the external force is applied to the object in the opposite direction of the gravitational force, the feedback value S_i decreases as the measured force s_{zi} increases. Eq.(5.1) gives the variation of the inner state of the neuron. When the feedback value S_i decreases, the amplitude of the oscillatory output decreases and the output y_i keeps positive. Consequently, the neuron does not issue the return command to the finger and the finger keeps a contact state. Therefore, the fingers can keep grasping during the disturbance.

5.3. Rotating manipulation using the CPG

5.3.1 Condition of the simulation

The dynamic simulator shown in Fig.5.3 is developed using a dynamic simulation library (Open Dynamics Engine: ODE). The four-fingered hand model in the simulator consists of only fingertips without links. The mass of the object is 1.0[kg] and the gravity is set 0.1[m/s^2]; the weight of the object is 0.1[N]. The friction coefficient between the object and the fingertip is 1.0. The initial position of each fingertip is set 0[rad] (thumb), $2\pi/3$[rad] (index), π[rad] (middle), and $4\pi/3$[rad] (ring) based on the movable range of human's fingers.

5.3.2 Control of the fingers

Fig.5.4 shows the motions of each finger when the motion-triggers are issued to the finger. $\boldsymbol{f}_{appr}$ is the force applied on the object, $\boldsymbol{f}_{rot}$ is the force to grasp and rotate the object, $\boldsymbol{f}_{rele}$ is the force to release from the object, and $\boldsymbol{f}_{back}$ is the force to move back to the initial point. $\boldsymbol{f}_{rot}$ is the resultant force of the grasping force $\boldsymbol{f}_g$ and the rotating force $\boldsymbol{f}_w$.
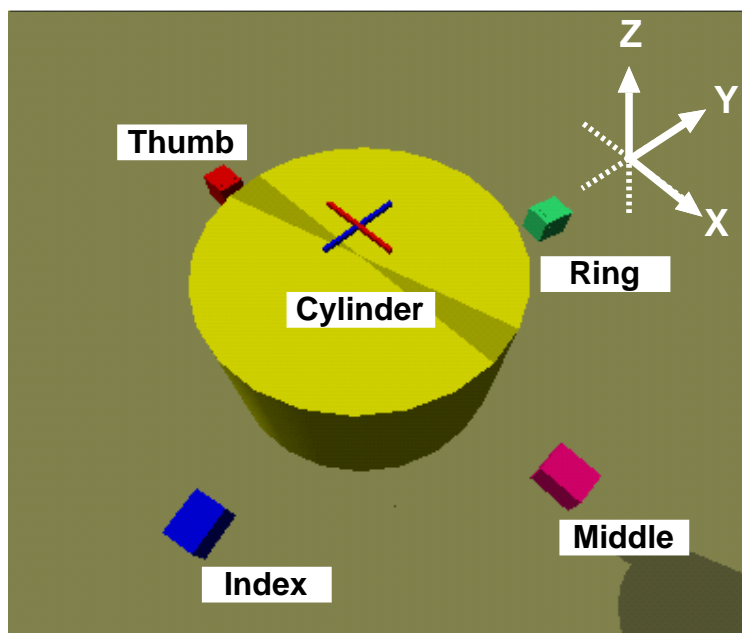
Figure 5.3. Developed dynamic simulator
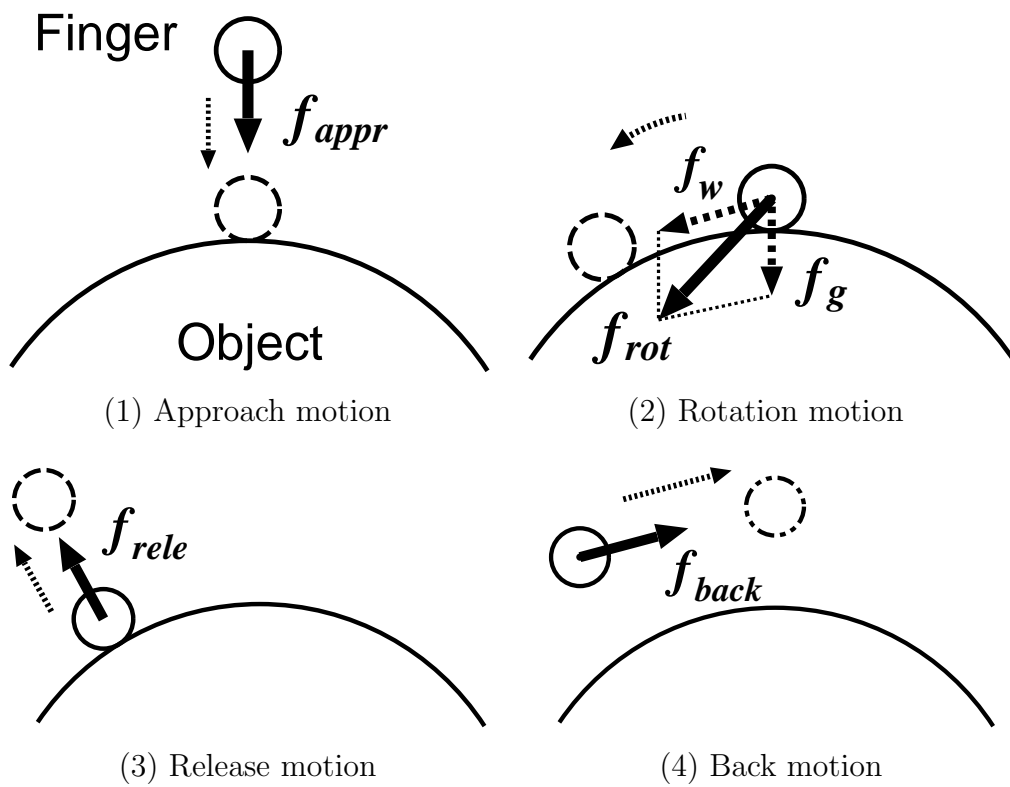
Figure 5.4. Finger motions during the rotating manipulation

In the rotation motion, the force $\boldsymbol{f}_{rot}$ is given by the following equation:

$$\boldsymbol{f}_{rot} = \boldsymbol{f}_w + \boldsymbol{f}_g \tag{5.5}$$

$$\boldsymbol{f}_w = k_{p1}(\boldsymbol{p}_d - \boldsymbol{p}) - k_v \dot{\boldsymbol{p}} \tag{5.6}$$

$$\boldsymbol{f}_g = \boldsymbol{f}_c \tag{5.7}$$

where $\boldsymbol{p}$ is the current position of the fingertip; $\boldsymbol{p}_d$ is the target position of the fingertip; $\dot{\boldsymbol{p}}$ is the velocity of the fingertip at the current point; k_{p1} and k_{v1} are the constants; $\boldsymbol{f}_c$ is the minimum grip force in order to grasp the object stably calculated by the object weight and the friction coefficient. The target position $\boldsymbol{p}_d$ is previously determined for each finger respectively. Furthermore, the compensation force is applied on each fingertip in order that the object position keeps the desired position by a PD control.

In the back motion, the force $\boldsymbol{f}_{back}$ is given by the following equation:

$$\boldsymbol{f}_{back} = k_{p2}(\boldsymbol{q}_d - \boldsymbol{p}) - k_{v2} \dot{\boldsymbol{p}} \tag{5.8}$$

where $\boldsymbol{q}_d$ is the target position of each finger; k_{p2} and k_{v2} are the constants. The target position $\boldsymbol{q}_d$ is previously determined for each finger respectively.

In the approach motion and the release motion, the force $\boldsymbol{f}_{appr}$ and $\boldsymbol{f}_{rele}$ are generated to each fingertip that are previously determined.

5.3.3 Simulation of a rotating manipulation

This section describes the evaluation of the CPG-based rotating manipulation using the developed dynamic simulator. The rotating manipulation is performed by issuing the contact/return commands to the fingers based on the output of the CPG in the section 5.2.1. In the simulation, the target position $\boldsymbol{p}_d$ is set in order that the thumb, index, and ring fingers rotate $\pi[\text{rad}]$, and the middle finger rotates $\pi/12[\text{rad}]$. The CPG parameters used in the simulation are shown in Table.5.1.

As is shown in Fig.5.5, the object rotates along z-axis (the opposite direction of the gravitational force) according to the contact patterns generated by the CPG model. The rotation angles of the object along x, y, and z-axes are shown in Fig.5.6(a) when the disturbance is not applied. The relative displacement from

Table 5.1. CPG parameters in the simulation

parameters	value
τ	0.9
τ'	12.0
u_0	7.0
β	3.0
w_{ij}	2.3

(1)   (2)   (3)

(4)   (5)   (6)
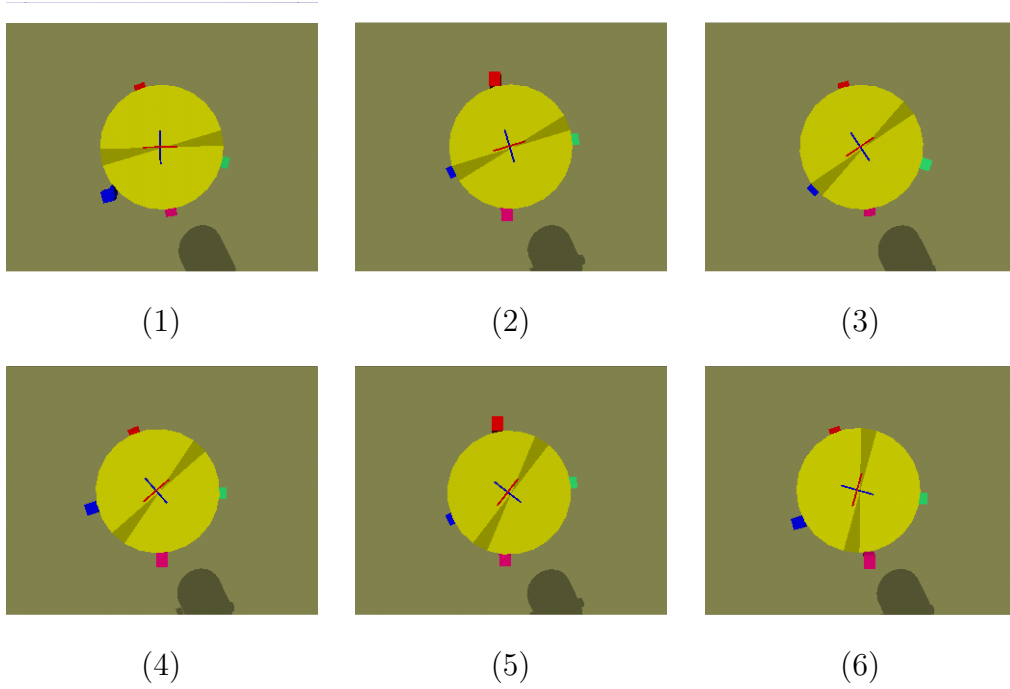
Figure 5.5. Rotating manipulation in the simulation
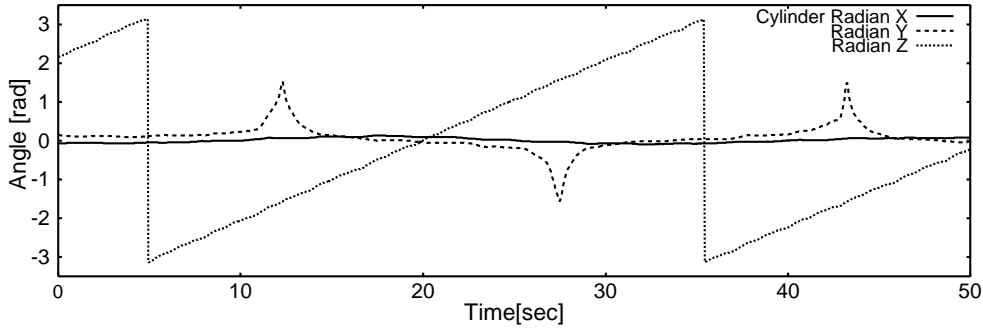
(a) Angle of the object
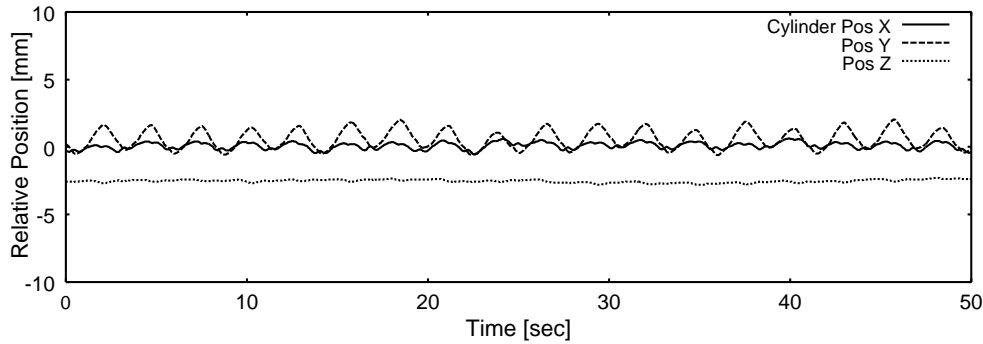
(b) Relative position of the object

Figure 5.6. Rotation and position of the object during the rotating manipulation (simulation, without disturbance)

the desired position of the object center $o_d = (0, 0, 30)$ is also shown in Fig.5.6(b). We can observe that the object consistently rotates along z-axis in the air.

The neural output and the measured sensory value along z-axis of each finger from 20[sec] to 40[sec] are shown in Fig.5.7(a)$\sim$(d). The sensory value responds when the finger touches on the object. From these figures, rhythmic contact with the object can be observed according to the rhythmic output of neurons. The results of the simulation indicate that the rotating manipulations of a cylindrical object can be performed using the output of the neurons.

Fig.5.8(a) and (b) show the rotation angles and the relative displacement of the object when the external force 3.0[N] along z-axis is applied on the object from 25.0[sec] to 26.5[sec]. Fig.5.9(a) $\sim$ (d) show the neural output and the
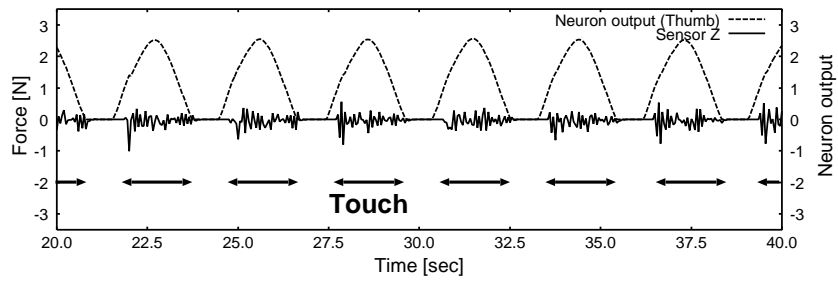
(a) Neuron and sensor outputs of the thumb
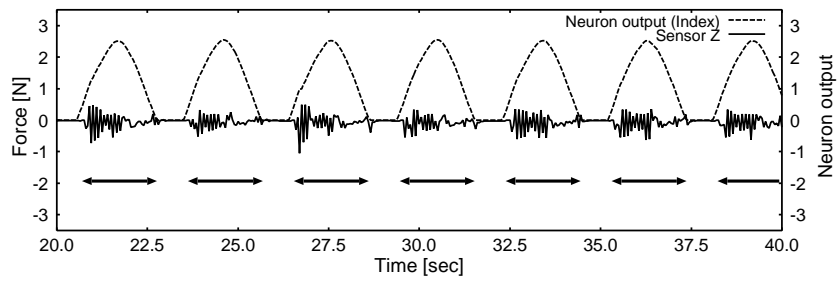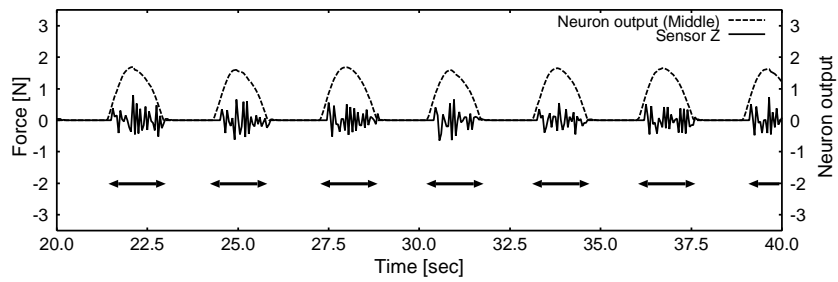
(b) Neuron and sensor outputs of the index finger

(c) Neuron and sensor outputs of the middle finger
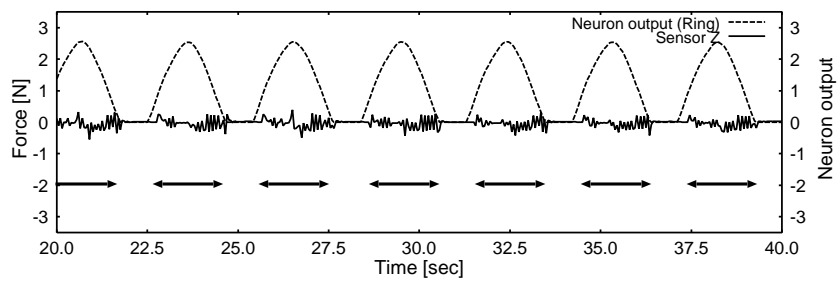
(d) Neuron and sensor outputs of the ring finger

Figure 5.7. Neural output and sensory value of each finger (simulation, without disturbance)
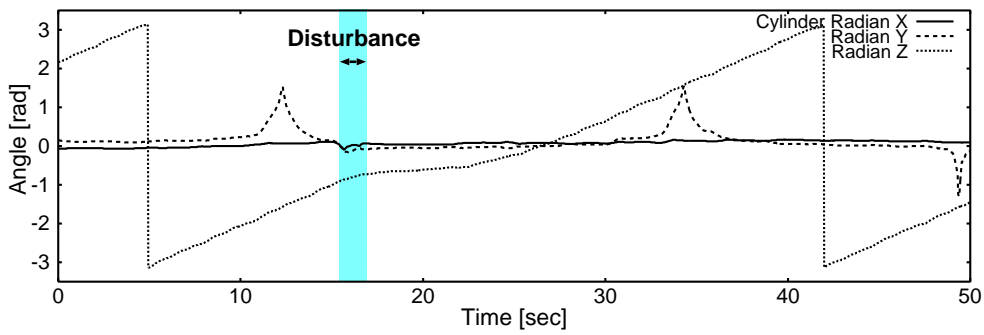
(a) Angle of the object
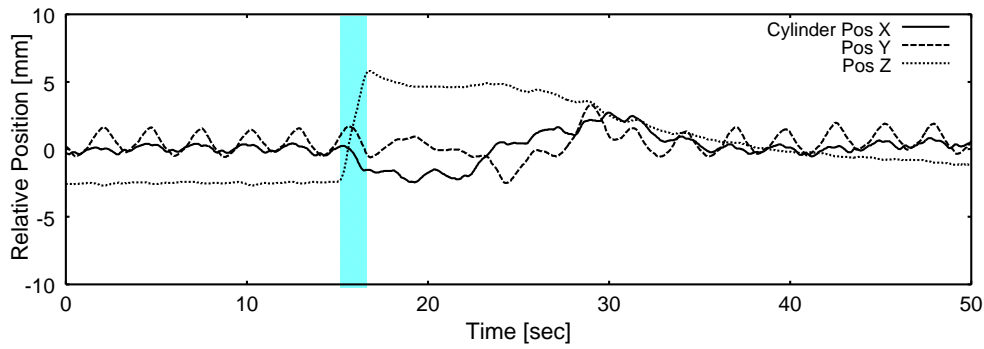
(b) Relative position of the object

Figure 5.8. Rotation and position of the object during the rotating manipulation (simulation, with disturbance)
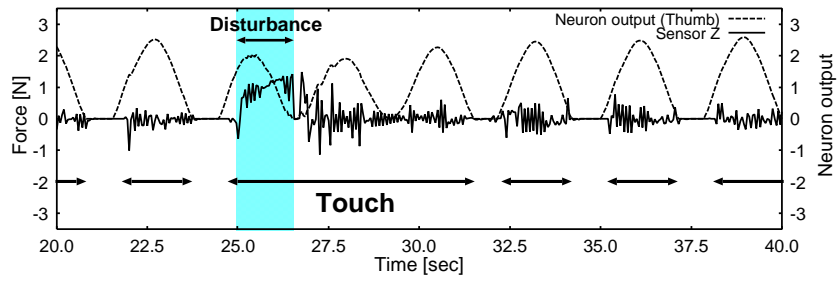
(a) Neuron and sensor outputs of the thumb
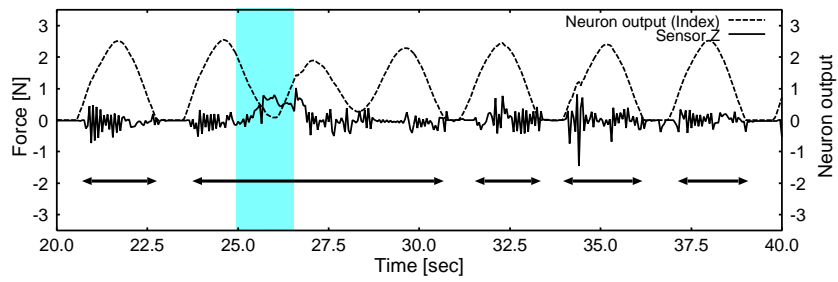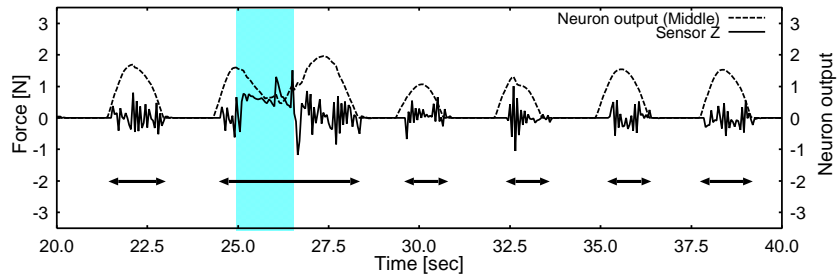
(b) Neuron and sensor outputs of the index finger

(c) Neuron and sensor outputs of the middle finger
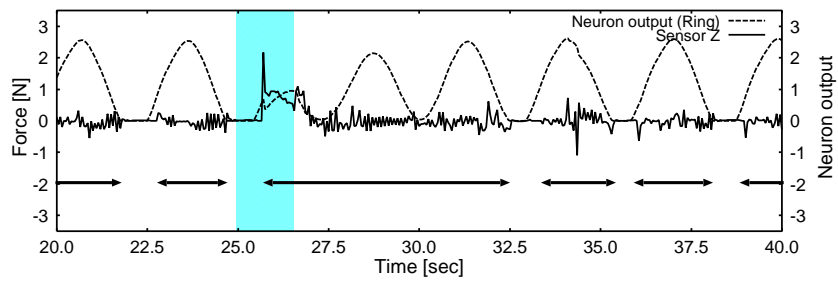
(d) Neuron and sensor outputs of the ring finger

Figure 5.9. Neural output and sensory value of each finger (simulation, with disturbance)

69

measured sensory value along z-axis from 20.0[sec] to 40.0[sec]. When the disturbance is applied, the sensory values of the fingers that contact on the object significantly respond in the positive direction along z-axis by the effect of the disturbance. The neurons of the contact fingers receive the inhibitory stimuli by the corresponding feedback input S_i and the output of the neuron keeps positive value. Consequently, the neuron keeps issuing the contact command. Since the fingers are controlled by the simple PD control described in Eq.(5.7), the fingers motions are stopped at the desired position. The rotating manipulation is halted if the contact command is extended and the release command is not issued. When the disturbance is terminated, each neuron begins to alternately issue the touch/release commands again and the rotating manipulation is resumed. We can observe from Fig.5.8(a) that the rotating manipulation is halted when the disturbance is applied, and resumed when the disturbance is terminated. The experimental results show that the rotating manipulations can be performed using the force feedback via the CPG if a disturbance is applied to the object.

5.4. Conclusion

This chapter has introduced a CPG that can generate a typical contact pattern of human that has been analyzed in the chapter 4 and demonstrated the CPG-based control method for a rotating manipulation using a dynamic simulator. In this study, the neural oscillator model that has been proposed by Matsuoka [72, 52] is adopted for a rhythm generator. The measured typical contact patterns during rotating manipulations addressed in the chapter 4 represent a model of rhythmic motion patterns.

At the first part, the CPG has been shown that can generate a typical contact pattern by a mutual inhibition network. In the generated contact pattern, the thumb, index, and ring fingers touch on and release from the object alternately. Two fingers among those three fingers touch the object consistently during the manipulation. Additionally, the middle finger touches in order to support the role of the thumb and the index fingers when the ring finger releases.

Fingers basically keep iterative motions on a constant trajectory during rhythmic motions and it is not important to imitate the trajectories. Rotating manip-

ulations can be conducted by classifying the motions into several categories and performing these motions in order. This study has classified the rotating manipulation into "approach motion", "rotating motion", "release motion", and "back motion". The rotating motion is taken after the approach motion, and the back motion is taken after the release motion. Rhythmic rotating manipulations can be performed by issuing "motion-triggers" that start these successive motions. The motion-triggers have to be issued appropriately in order that the fingers cooperatively and synchronously move and manipulate the object. To generate such rhythmic motion-triggers, the CPG can be exploited for issuing the commands.

When large external force is applied on the grasped object during a manipulation, the object slips on the contact surface and may be dropped on the ground. The simple and effective way to deal with the problem is to enhance the grasp robustness by adding grasping finger when the external force is applied. In order to add the grasping fingers when a force sensor of the fingertip measures the external force, the force feedback has given to the neurons. Consequently, the neuron does not issue the return command to the fingers and the fingers can keep grasping during the disturbance.

The last part of this chapter has addressed experimental results in a simulation using the proposed CPG-based control method. A dynamic simulation system has been developed and a four-fingered hand model has been built. The fingers have controlled by a simple PD control according to the motion-triggers generated by the constructed CPG model. The results of the simulation show that rotating manipulations of a cylindrical object in the air can be performed using the output of the neurons. Furthermore, robust rotating manipulations have been performed by keeping contact states using the force feedback via the CPG when a disturbance is applied on the object.

In all, the results in this chapter present that the CPG can generate a similar contact pattern to that of humans and rotating manipulations can be performed by the generated pattern. These results confirm the validity and the effectiveness of the CPG-based control on the measured contact patterns that analyzed in the previous chapter.

71

Chapter 6

Rhythmic manipulations using a multi-fingered hand by the CPG-based control

6.1. Introduction

In this chapter, the rhythmic manipulation is performed using a multi-fingered hand by the proposed CPG-based control. The period, phase and amplitude of the rhythmic output generated by the CPG are determined by the parameters of the neural oscillators. Moreover, the property of the oscillatory output can be changed by the appropriate feedback to the neurons. By using these characteristics of the CPG, a multi-fingered hand can perform rhythmic manipulations according to the state of the environment.

This chapter introduces a control method of the switching cycle of the grasping fingers by the joint margin feedback to the neurons. Since the switching cycle of the grasping fingers during rotating manipulations is affected by the movable range of the finger joints, the rotatable angle of the manipulated object in one cycle changes depending on the size of the object. However, it is difficult to precisely measure the size of the object without the object model. The CPG-based control is effective in such condition.

The first part of this chapter presents the CPG that consists of a simple mutual inhibition network. This chapter also describes a rotating manipulation

73

with the relocation of the fingers using the constructed CPG. Motion-triggers are used for the control of the fingers that are explained in the previous chapter.

At the next part, the effect of the movable range of the joints during the rotating manipulations is introduced. A control method is proposed that can change the switching cycle of the grasping fingers depending on the object size. The output of the CPG changes by the effect of the joint margin feedback and the issuing cycle of the motion-triggers is controlled depending on the object size.

Finally, a hardware system of a four-fingered hand is addressed and a control method of the fingers for the manipulation is introduced. The effectiveness of the proposed method is confirmed by performing the rotating and shifting manipulations of several sized objects using the hand system.

6.2. Switching cycle of the grasping fingers depending on the object size

6.2.1 Neural oscillator model

The mutual inhibition network that consists of the two neurons N_1 and N_2 is shown in Fig.6.1(a). The rhythmic output generated by each neuron is also shown in Fig.6.1(b). In this study, a rotating manipulation is demonstrated using the four-fingered hand system that is described in the section 6.3.1. The neurons N_1 and N_2 are assigned to each set of facing two fingers (a set of the first and the third fingers; a set of the second and the fourth fingers). The set of the facing fingers is synchronously controlled. Since the phases of the oscillatory output of the neurons have the difference of π[rad], the switching motions of the grasping fingers can be performed by issuing the motion-triggers to each set of the fingers.

The generated contact pattern from the CPG is shown in Fig.6.2. As is described in the section 5.2.2, the contact command is issued when the output of the i-th neuron becomes $y_i > 0$ from $y_i = 0$ and the return command is issued when the output becomes $y_i = 0$ from $y_i > 0$. The control diagram is shown in Fig.6.3. Consequently, rotating manipulations with the relocation of the fingers can be performed as shown in Fig.6.4.
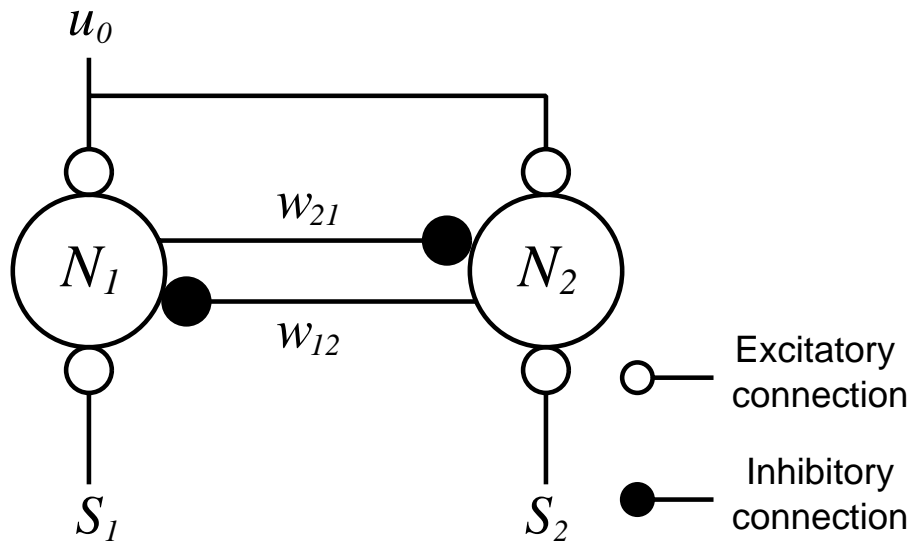
(a) Constructed CPG
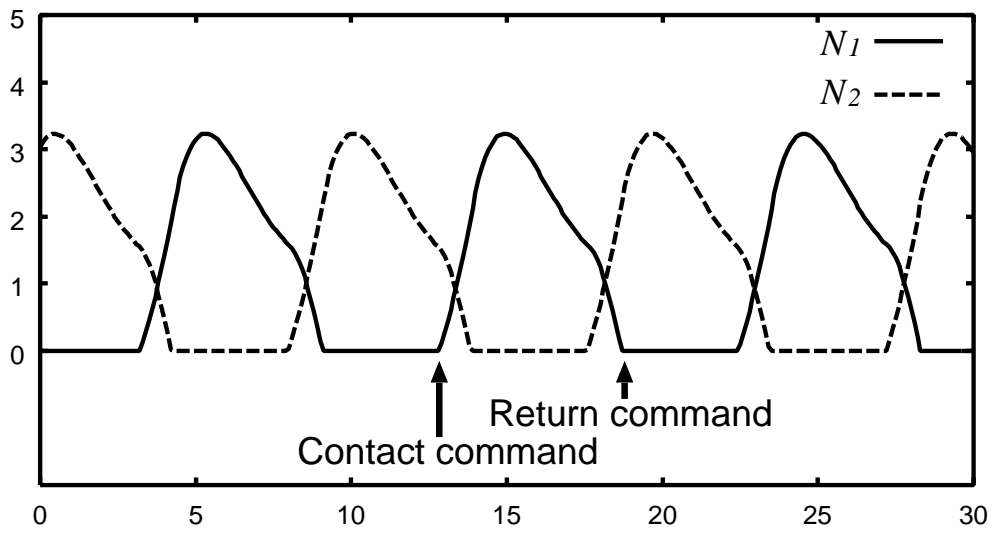
(b) Output of each neuron ($\tau = 1, \tau' = 9, u_0 = 10, \beta = 6, w_{ij} = 1.8, S_i = 0$)

Figure 6.1. Mutual inhibition network model by two neural oscillators
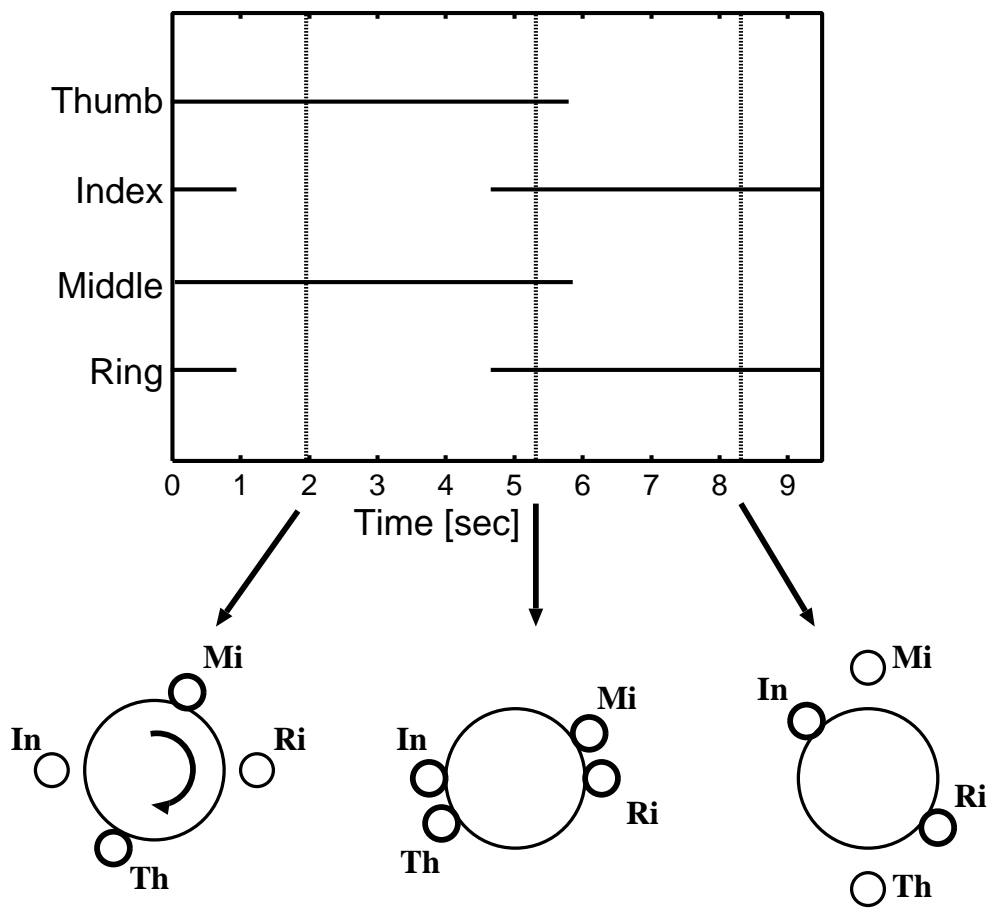
Figure 6.2. Contact pattern generated by the CPG
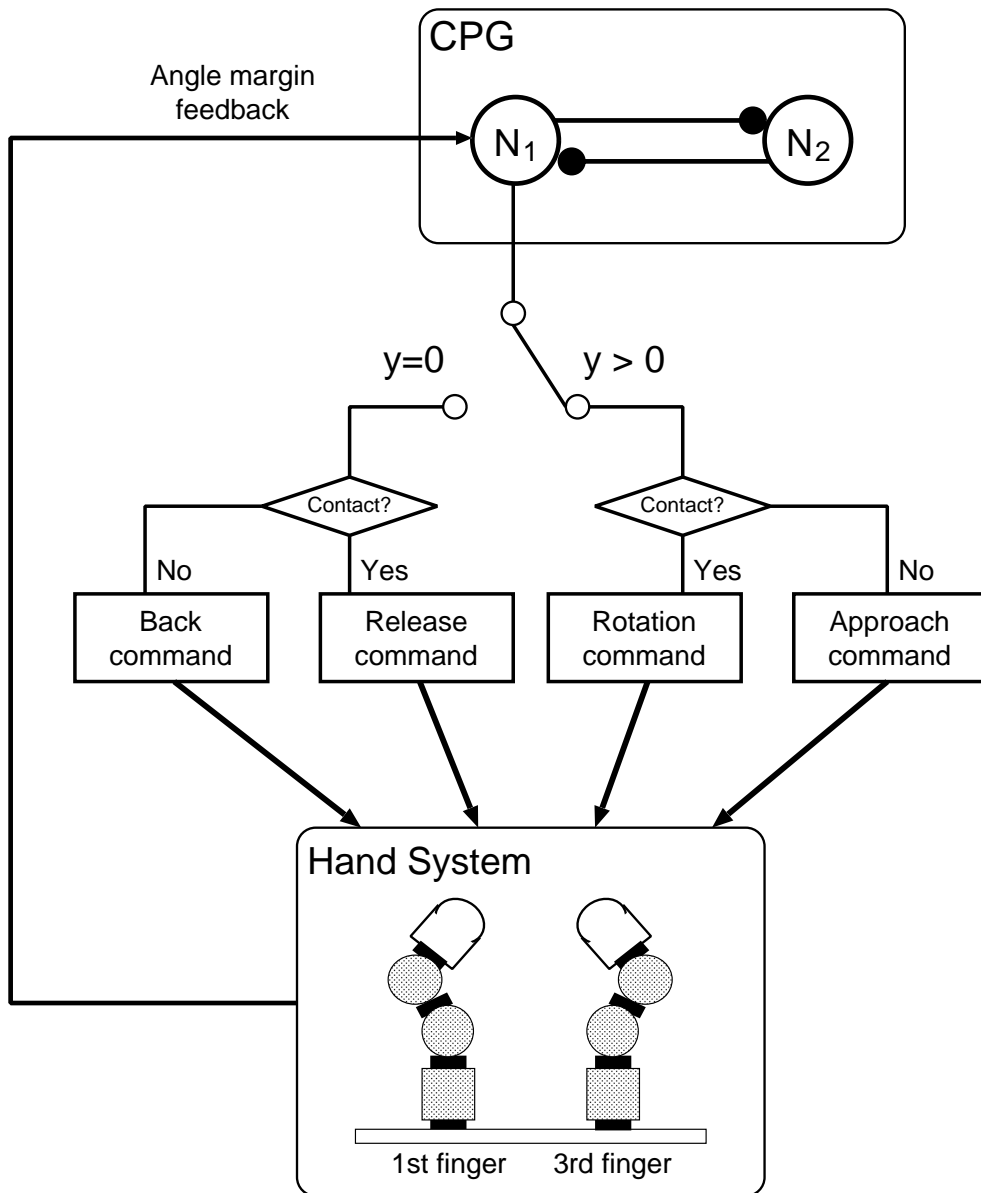
Figure 6.3. Control diagram of the rotating manipulation
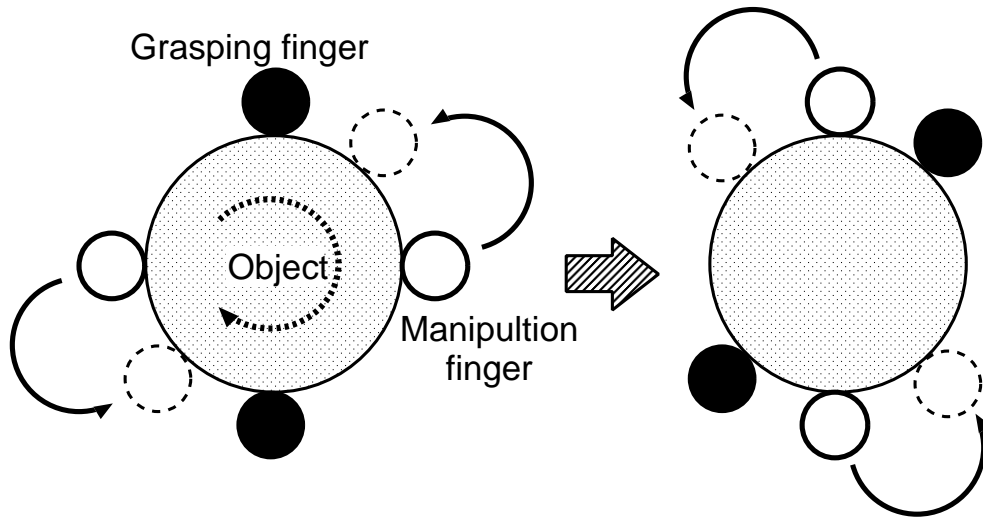
Figure 6.4. Rotating manipulation with the relocation of the grasping fingers

6.2.2 Joint margin feedback

The switching cycle of the fingers during the manipulation is affected by the movable range of the joints. The rotatable angle of an object in one cycle changes depending on the size of the object when the movable range of the joints is the same. For example, if the movable area of a finger from the upper view is given as the meshed area in Fig.6.5, the rotatable angle of a smaller object is larger than the angle of a larger object.

Because the switching motions of the fingers themselves do not make a contribution to the rotation of an object, too much relocation is not preferable from the point of the energy efficiency. Therefore, the grasping fingers should move up to the limit of the movable area. Considering the manipulation of a cylindrical object using a robot hand, the limit of the movable area can be calculated by the length of each link, the movable range of the joints, and the diameter of the grasped object. However, it is difficult to obtain the diameter of the object without the object model.

In order to deal with the problem, the joint margin feedback to the neurons is proposed, which can relocate the fingers when the fingers close to the limit.
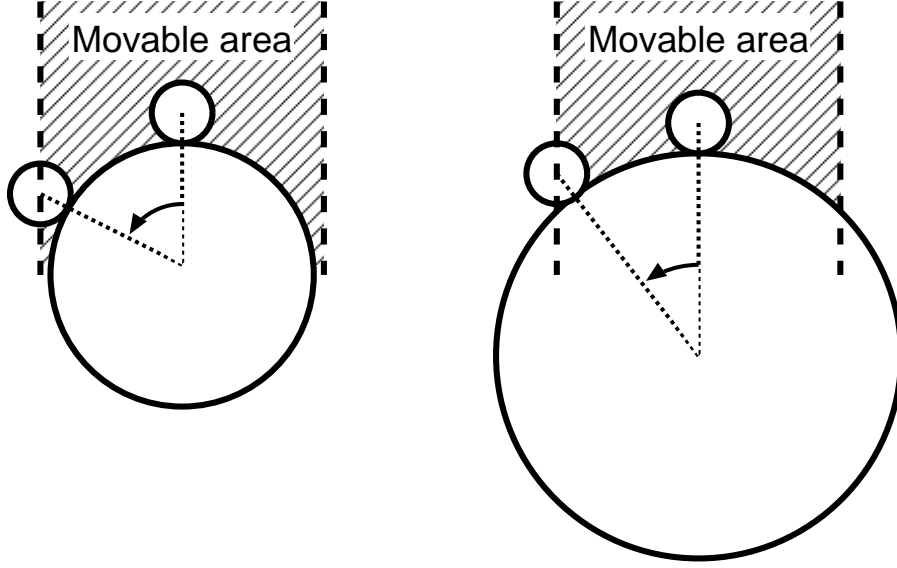
Figure 6.5. Movable area of the fingers during a rotating manipulation

Neural oscillators have the characteristics in that the output of the neurons are synchronized to the oscillatory input S_i in Eq.(5.1) when the frequency of the oscillatory input is sufficiently close to the frequency of the neural oscillator. The issuing cycle of the motion-triggers can be controlled by the joint margin feedback.

When the j-th joint angle of the i-th finger is denoted by θ_{ij}, the movable range of the joint can be given by $C_{ij\,\min} \leq \theta_{ij} \leq C_{ij\,\max}$, where $C_{ij\,\min}$ and $C_{ij\,\max}$ are the minimum and the maximum movable angles of the joint respectively. Now, the joint margin m_{ij} is defined as the following:

$$m_{ij} \triangleq \min\left(\left|C_{ij\,\min} - \theta_{ij}\right|, \left|C_{ij\,\max} - \theta_{ij}\right|\right) \tag{6.1}$$

The joint margin gets close to 0 as the j-th joint angle is close to the limit. Furthermore, the total joint margin of the i-th finger is defined as following:

$$n_i \triangleq \min\left(m_{i1}, \cdots, m_{ij}, \cdots, m_{iN_j}\right) \tag{6.2}$$

where N_j is the total number of the joints. The total joint margin n_i is the joint margin of the i-th finger that is the closest to 0 among all the joints.

Table 6.1. Specification of the joint actuator

Size	$29.5 \times 28.0 \times 46.0$ [mm]
Weight	100[g]
Power rating	0.47[W]
Torque rating	0.3[Nm]
Decelerator	Harmonic gear, Rg = 80

The feedback S_i in Eq.(5.1) is given by the following equations using the total joint margins:

$$S_1 = k_s \min \left(A_{11} n_1, \cdots, A_{1i} n_i \cdots, A_{1N_f} n_{N_f} \right) \tag{6.3}$$

$$S_2 = k_s \min \left(A_{21} n_1, \cdots, A_{2i} n_i \cdots, A_{2N_f} n_{N_f} \right) \tag{6.4}$$

where k_s is the feedback gain; A_{1i} is the variable that is 1 when the i-th finger corresponds with the N_1 neuron and 0 when the finger corresponds with the N_2 neuron in Fig. 6.1(a); A_{2i} is the variable that is 1 when the i-th finger corresponds with the N_2 neuron and 0 when the finger corresponds with the N_1 neuron.

6.3. Experiments using a multi-fingered hand by the CPG-based control

6.3.1 Multi-fingered hand system

The multi-fingered robot hand is exploited for the experiments, which has four fingers and mounts a 6-axis force-torque sensor on each fingertip [79]. Each finger has three degree-of-freedom and a joint actuator system. The specification of the actuator is shown in Table 6.1. The coordinate system is the right-handed coordinate system. The external view of the multi-fingered hand is shown in Fig.6.6. The construction of the finger and the hardware system are shown in Fig.6.7 and Fig.6.8 respectively.

The hand control system consists of a real-time layer and a non-real-time layer. The real-time layer is implemented on a real-time Linux (ART-Linux) and
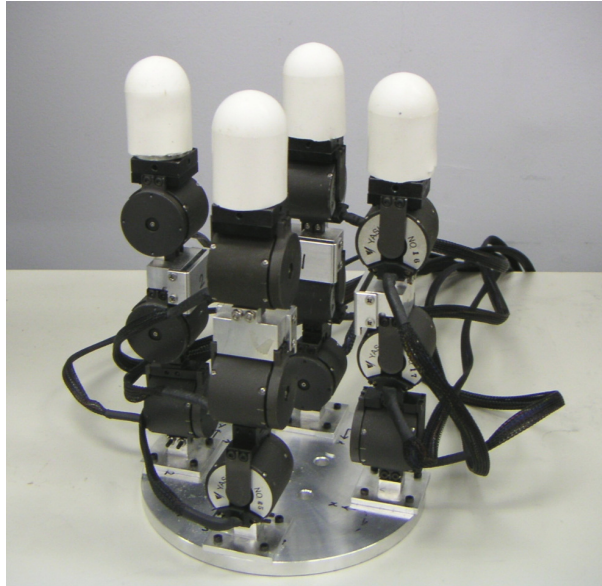
Figure 6.6. System overview of the four-fingered hand

takes the real-time control of the fingers. The control cycle of the object position and rotation is 60[ms]; the servo cycle of each finger is 3[ms]; the sampling time of the force sensors is 2[ms]. The non-real-time layer is implemented on a Linux system and displays various parameters of the system. The data communications between layers are made via Ethernet.

6.3.2 Control of the fingers

The fingers during the manipulations can be classified into grasping fingers and manipulation fingers from the viewpoint of the function on the manipulation. The grasping fingers apply the force to grasp and keep an object stable. The manipulation fingers are the fingers that actively move to manipulate the object and do not contact with the object surface in the switching motions.

If a soft finger contact is assumed between a fingertip and an object surface,
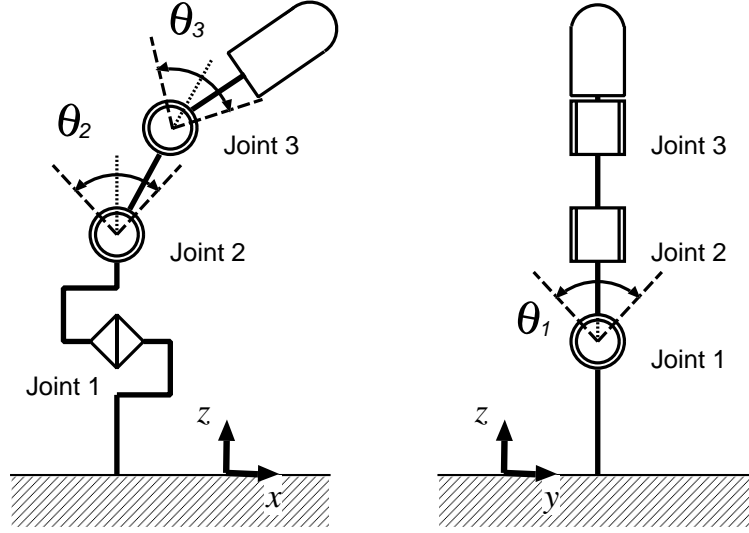
Figure 6.7. Degree-of-freedom of the robot finger

the applied force from the grasping fingers have to satisfy the following equations:

$$\sum_{i=1}^{N_f} B_{gi}\, \boldsymbol{f}_i \;=\; -\sum_{j=1}^{N_f} B_{mj}\, \boldsymbol{f}_j - \boldsymbol{f}_e \tag{6.5}$$

$$\sum_{i=1}^{N_f} B_{gi}\, \boldsymbol{r}_i \times \boldsymbol{f}_i \;=\; -\sum_{i=1}^{N_f} B_{gi} s_i\, \boldsymbol{n}_i - \sum_{j=1}^{N_f} B_{mj}\, \boldsymbol{r}_j \times \boldsymbol{f}_j$$

$$-\sum_{j=1}^{N_f} B_{mj} s_j\, \boldsymbol{n}_j - \boldsymbol{r}_e \times \boldsymbol{f}_e - \boldsymbol{m}_e \tag{6.6}$$

$$\boldsymbol{n}_i \cdot \boldsymbol{f}_i \;\geq\; \frac{1}{\sqrt{1+\mu^2}} \,\|\, \boldsymbol{f}_i \,\| \tag{6.7}$$

where $\boldsymbol{f}_i$ is the force from the i-th finger; $\boldsymbol{r}_i$ is the contact position; $\boldsymbol{n}_i$ is the normal vector of the contact; s_i is the amplitude of the moment; N_f is the number of fingers; μ is the friction coefficient between the fingertip and the object surface; B_{gi} is the variable that is 1 when the i-th finger is the grasping finger and 0 when the finger is the manipulation finger; B_{mi} is the variable that is 1 when the j-th finger is the manipulation finger and 0 when the finger is the grasping finger. $\boldsymbol{f}_e$, $\boldsymbol{m}_e$, and $\boldsymbol{r}_e$ are the external force (including the gravitational force),

82
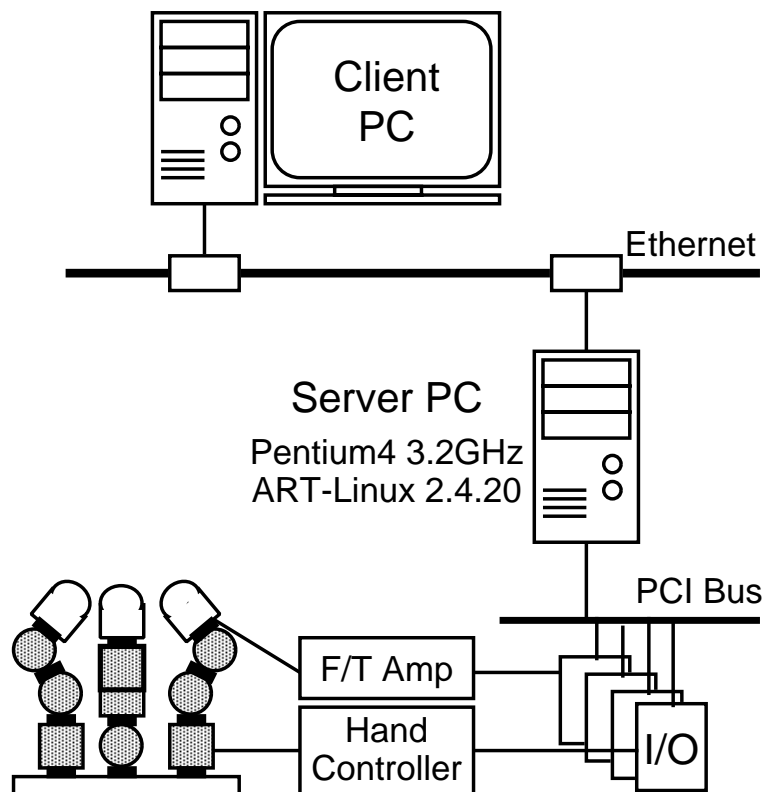
Figure 6.8. System configuration of the hand system

moment, and point of the application respectively. Eq.(6.5) and Eq.(6.6) indicate the equilibrium condition of the applied force by the fingers and the external force. Eq.(6.7) indicates the friction condition in order that the grasping fingers do not slip on the object surface. The contact position between the fingertip and the object can be detected by the force and torque information (see the appendix B).

The velocity of the i-th finger $\boldsymbol{v}_i$ in order to move the grasped object at the translation velocity $\boldsymbol{v}_o$ and the angular velocity $\boldsymbol{w}_o$ is given by:

$$
\begin{pmatrix}
\boldsymbol{v}_1 \\
\vdots \\
\boldsymbol{v}_i \\
\vdots \\
\boldsymbol{v}_{N_f}
\end{pmatrix}
=
\begin{pmatrix}
\boldsymbol{E}_{3\times3} & -\boldsymbol{r}_1 \\
\vdots & \vdots \\
\boldsymbol{E}_{3\times3} & -\boldsymbol{r}_i \\
\vdots & \vdots \\
\boldsymbol{E}_{3\times3} & -\boldsymbol{r}_{N_f}
\end{pmatrix}
\begin{pmatrix}
\boldsymbol{v}_o \\
\boldsymbol{w}_o
\end{pmatrix}
\tag{6.8}
$$

where $\boldsymbol{E}_{3\times3}$ is 3×3 unit matrix.

In the following experiment, the fingers rotate the object along z-axis. It is preferable that the change of the object velocity (acceleration) is smoothly given. For the smooth rotation of the object, it is necessary to determine the initial and the terminal position of the motion. However, if the diameter of the cylindrical object is not given, the terminal position can not be determined because the limit position of the movable area of the finger can not be calculated. Here, the desired angular velocity of the object w_{oz} is given by the output of the neuron:

$$
w_{oz} = k_w \, y_g
\tag{6.9}
$$

where y_g is the neural output of the grasping finger and k_w is the conversion coefficient from the neural output to the angular velocity.

By the nature, the neural output keeps the smooth increase and decrease as is shown in Fig.6.1(b). Although the output cycle of the neurons changes depending on the object size by the effect of the joint margin feedback, the nature of the neural output does not change. Therefore, the smooth rotating motions can be given by correlating neural output with the angular velocity.

Table 6.2. Parameters in the experiment (demonstration)

parameters	value	parameters	value
τ	1	$C_{1\,\mathrm{min}}$	$-\pi/9$ [rad]
τ'	9	$C_{1\,\mathrm{max}}$	$\pi/9$ [rad]
u_0	10	$C_{2\,\mathrm{min}}$	$-\pi/2$ [rad]
β	6	$C_{2\,\mathrm{max}}$	$4\pi/9$ [rad]
w_{ij}	1.8	$C_{3\,\mathrm{min}}$	0 [rad]
		$C_{3\,\mathrm{max}}$	$\pi/2$ [rad]

6.3.3 Experiments of the manipulations

Rotating motion

The effectiveness of the proposed method is demonstrated by the experiments using the four-fingered hand system. The robot hand is fixed downward and rotates the cylindrical object whose diameter is 50[mm], 60[mm], or 75[mm]. The approach, rotation, release, and back motion are performed by the motion-triggers (the contact and the release commands) from the constructed CPG shown in Fig.6.1(a). The parameters of the CPG and the preset movable range of the joint are shown in Table 6.2.

The experimental scenes of the manipulation are shown in Fig.6.9(1)∼(4). Fig.6.10(a) shows the output of the N_1 neuron y_1, the feedback value S_1, and the desired angular velocity w_{oz} for 30[sec] during the manipulation of the 50[mm] object. The joint angle of the first finger that is given by the calculation of the inverse-kinematics to move the desired position, and the movable limit of the first joint ($\pi/9$[rad]) are also shown in Fig.6.10(b). The experimental results in the manipulations of the 60[mm] and 75[mm] objects are shown in Fig.6.11 and Fig.6.12 respectively.

When the output of the neuron y_1 exceeds 0 (**A** and **C**), the contact command is issued to the corresponding set of the facing two fingers (the first and the third fingers) and the fingers begin to rotate the object after the approach motion.

(1)   (2)

(3)   (4)

Figure 6.9. Experimental scenes during the rotating motion
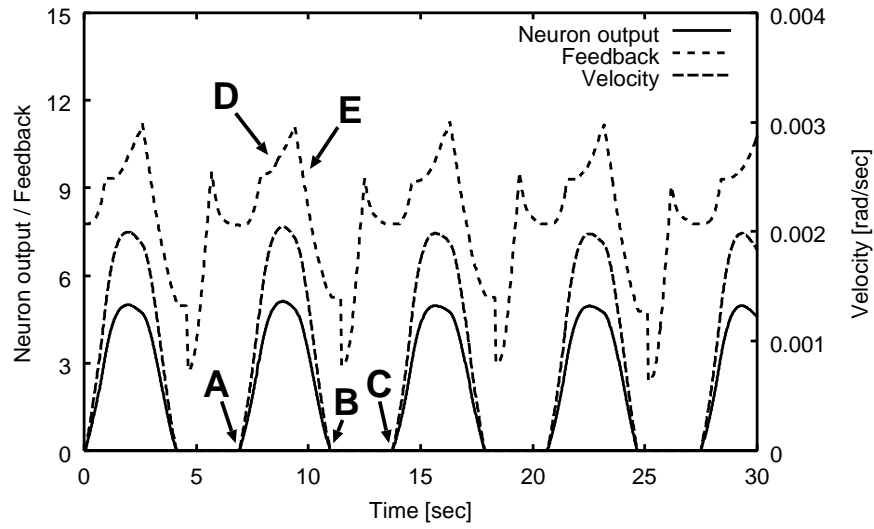
(a) Neural output, feedback value and object's velocity
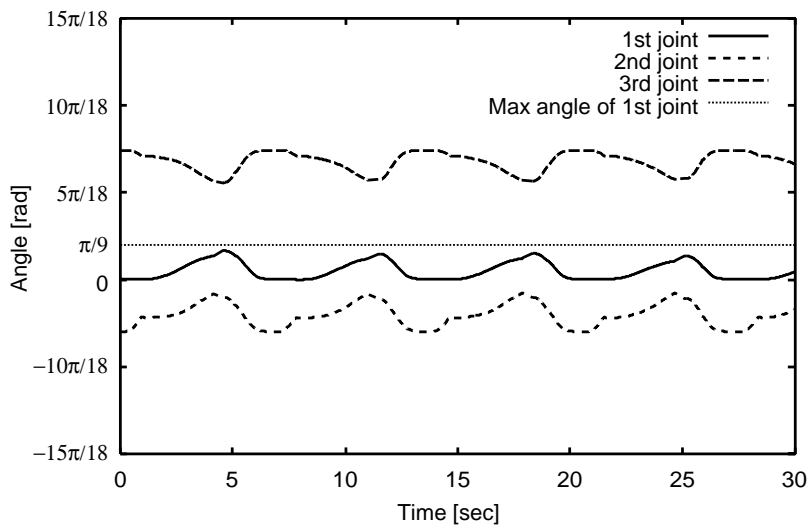
(b) Joint angle

Figure 6.10. Experimental result (size:50[mm], rotation)
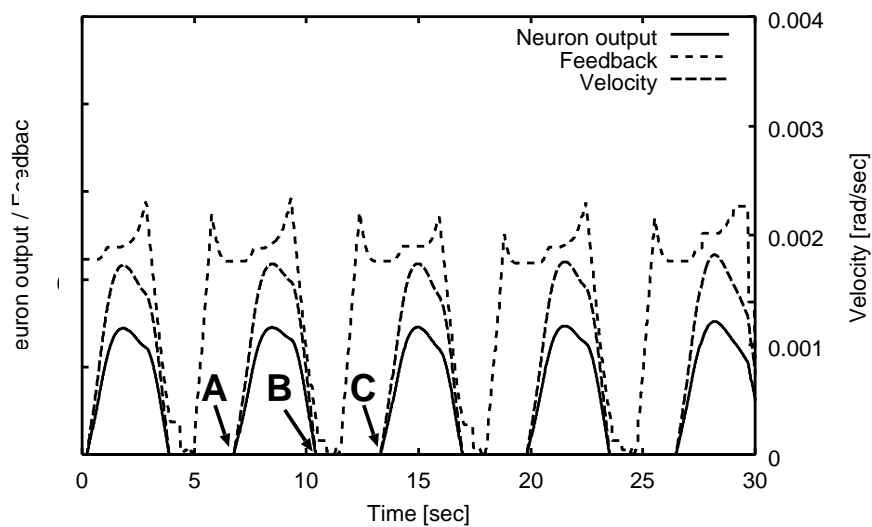
(a) Neural output, feedback value and object's velocity
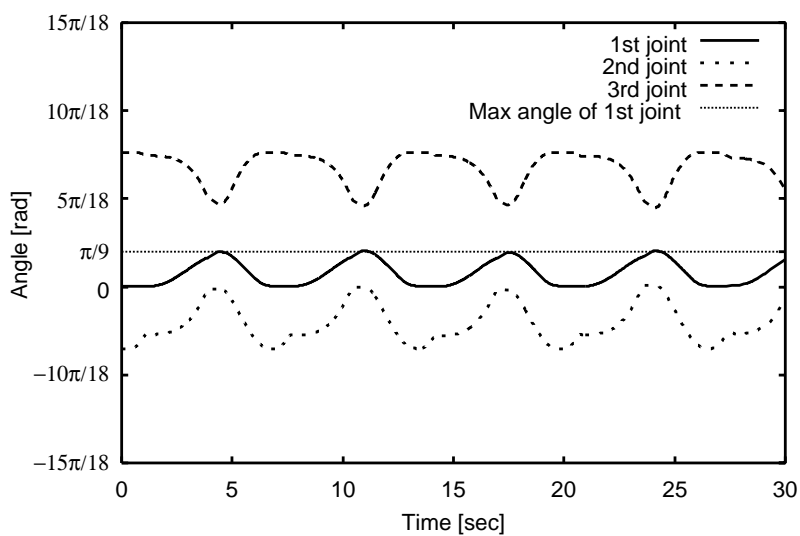
(b) Joint angle

Figure 6.11. Experimental result (size:60[mm], rotation)
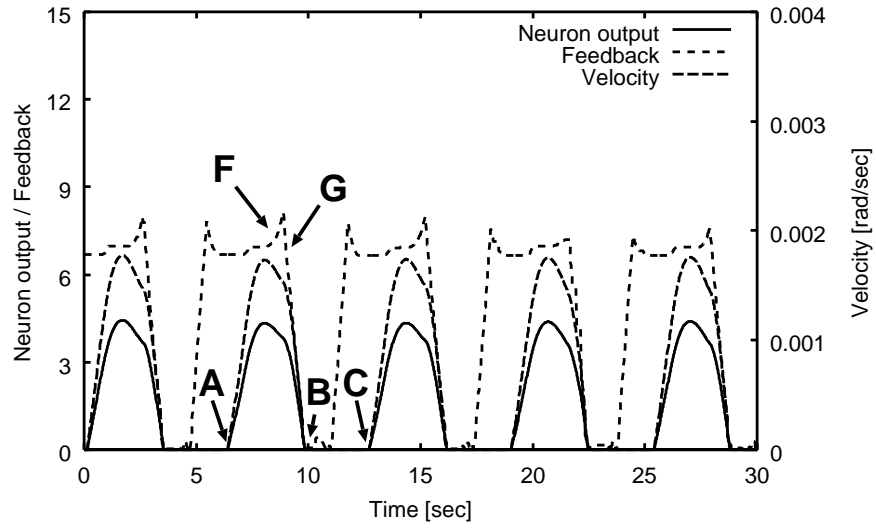
(a) Neural output, feedback value and object's velocity
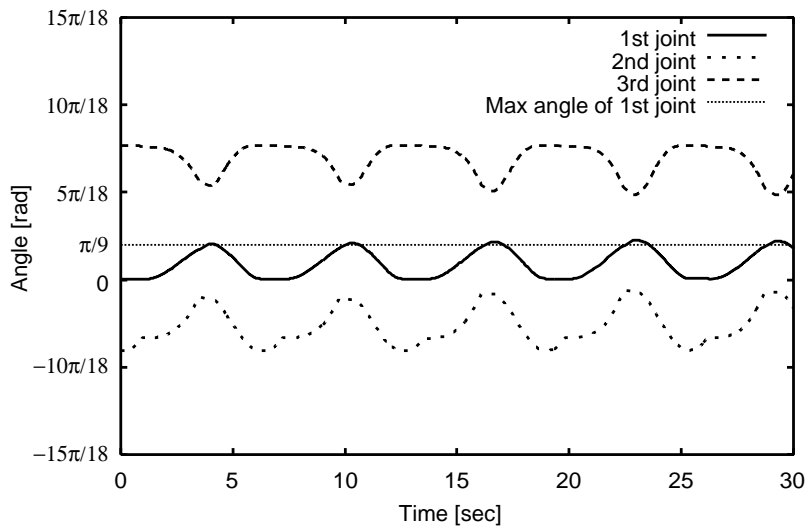
(b) Joint angle

Figure 6.12. Experimental result (size:75[mm], demonstration)

89

When the output of the neuron y_1 becomes 0 (**B**), the return command is issued to the fingers and the fingers begin to move back to the initial position after the release motion. The desired angular velocity during the rotation motion (from **A** to **B**) is given by Eq.(6.9). In the experiment, the conversion coefficient is set $k_w = 0.0004$.

The joint angle increases or decreases by the rotation motion. Since the finger moves back to the preset initial position by the back motion, we can observe the oscillatory output of the joint angles. In the experiment, the angle of the first joint at the initial position in the back motion is 0[rad] and the angle increases in the rotation motion. Because the first joint has the smallest movable range, the angle of the first joint has the dominant effect on the feedback value S_i.

When the object whose diameter is 50[mm] is manipulated, the feedback value increases by the rotation motion (**D** in Fig.6.10(a)) because the joint margin after the start of the rotating motion is larger than the margin at the start position. However, the feedback value decreases as the joint moves close to the movable limit (**E**). When the object whose diameter is 75[mm] is manipulated, although the feedback value similarly increases by the rotation motion (**F** in Fig.6.12(a)), the value decreases quickly (**G**). The angle of the first joint reaches the movable limit $\pi/9$[rad] because the joint angle largely changes by the effect of the object size.

It can also be observed that the output cycle of the neuron changes depending on the size of the object. The rotation angle and the time period in one cycle of each object are shown in Fig.6.13. The boxes in the figure indicate the rotation angle and the lines indicate the time period. When the object size is 50[mm], it is about 6.8[sec] in one cycle (the period from **A** to **C** in the figures); about 6.6[sec] when the size is 60[mm]; about 6.3[sec] when the size is 75[mm].

If the object size is different, the feedback value during the non-contact period (the period from **B** to **C**) is not so changed because the release motion and the back motion during the non-contact period are not changed. Accordingly, the time period during the non-contact period is almost the same (about 2.8[sec] when the object size is 50[mm]; about 2.9[sec] when the size is 60[mm]; about 2.9[sec] when the size is 75[mm]). The difference of the cycle is mainly affected by the difference of the time period during the contact period (about 4.0[sec] when
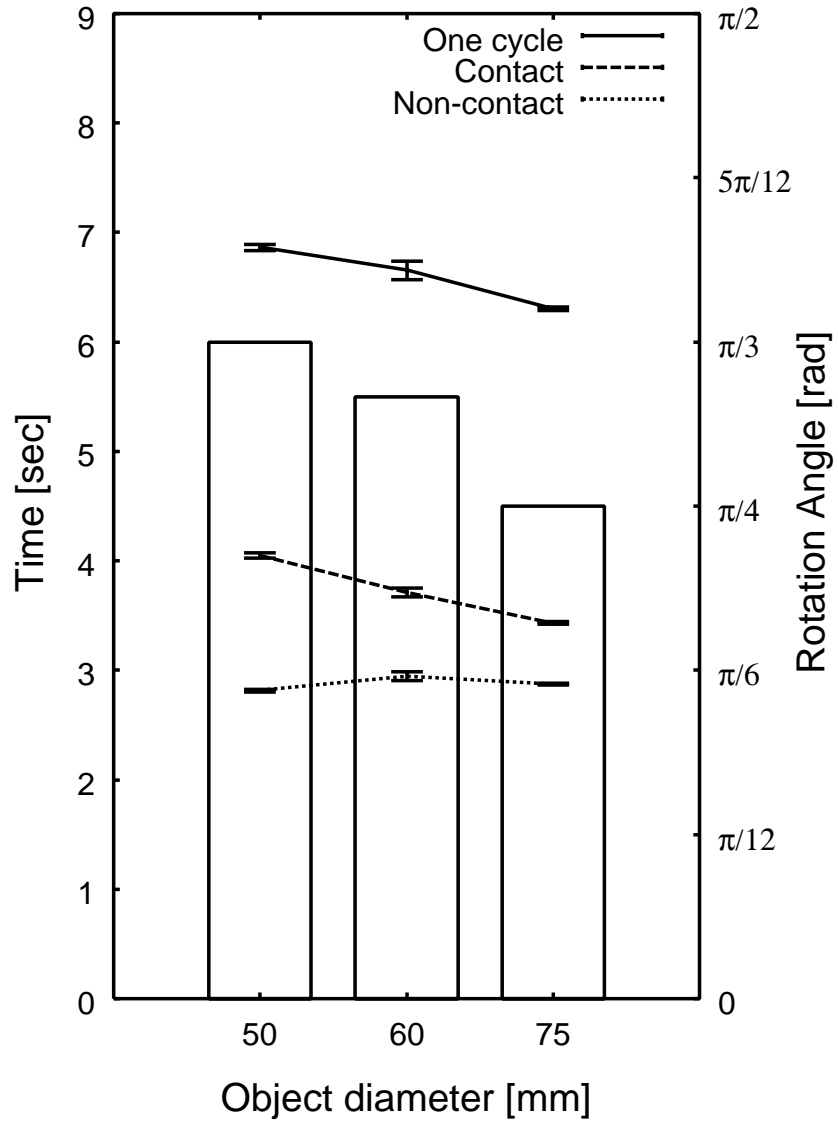
Figure 6.13. Rotation angle and time period for each size of the object

the object size is 50[mm]; about 3.7[sec] when the size is 60[mm]; about 3.4[sec] when the size is 75[mm] in the period between **A** and **B**). The difference of the cycle affects the rotation angle of the object in one cycle. The rotation angle in one cycle is about $\pi/3$[rad] when the object size is 50[mm], about $11\pi/36$[rad] when the size is 60[mm], and about $\pi/4$[rad] when the size is 75[mm].

These experimental results suggest that the issuing cycle of the motion-triggers is changed by the feedback of the joint margin and the object rotates for the appropriate angle according to the object size. Furthermore, we can observe that the neural output keeps the smooth increase and decrease if the output cycle is changed. The smooth change of the desired velocity can be given by correlating the neural output with the object's velocity.

Lifting motion

Rhythmic shifting (translational) motions can also be performed by giving $\boldsymbol{v}_o$ in Eq.6.8. In order to perform the shifting motion in the z direction (lifting motion), the translational velocity of the object v_{oz} is given by the following equation:

$$v_{oz} = k_v \, y_g \tag{6.10}$$

where k_v is the conversion coefficient from the neural output to the translational velocity. The smooth lifting motions can also be given by correlating the neural output with the translational velocity.

The experimental scenes of the lifting manipulation are shown in Fig.6.14. At first, the object is lifted using the facing two fingers of the robot hand. When the fingers reach the movable limit, the object is temporarily grasped using four fingers, and the another facing two fingers are used for the manipulation. The continuous lifting manipulation can be performed by the rhythmic regrasping motions.

The issuing cycle of the motion-triggers can also be changed according to the object size by the joint margin feedback. The experimental results in the manipulations of the 50[mm] and 80[mm] objects are shown in Fig.6.15 and Fig.6.16. It can be observed that the output cycle of the neuron is obviously different between the objects. In the lifting motion, the angle of the third joint is dominant on the feedback value. Since the third joint angle reaches the limit (0[rad]) earlier as the
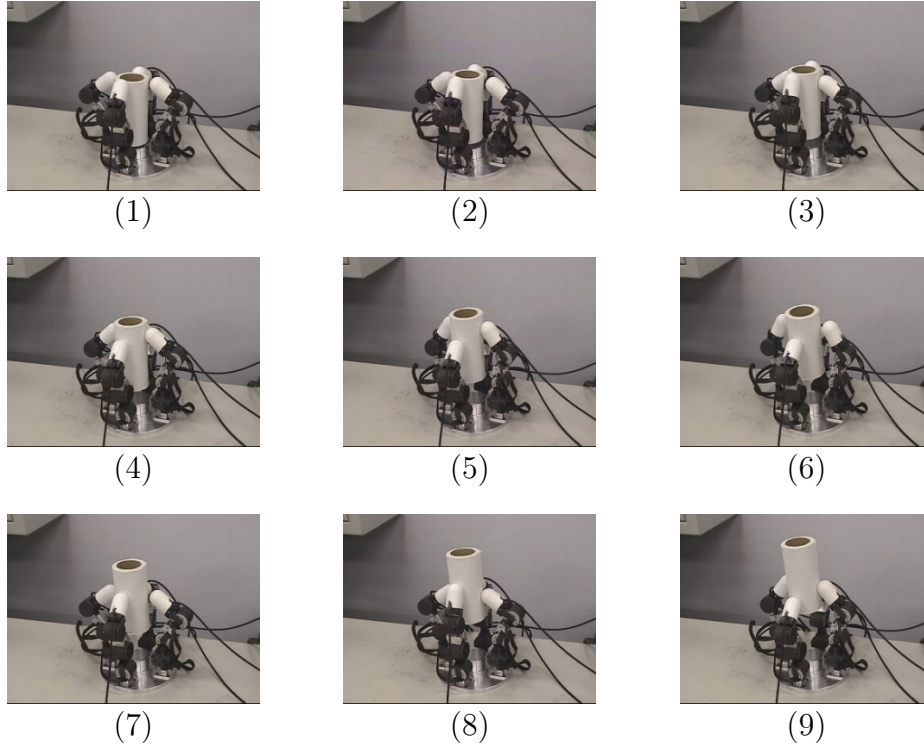
Figure 6.14. Experimental scenes during the lifting motion

size of the object is smaller, the switching cycle of the grasping fingers when the object size is 50[mm] is earlier than the cycle when the size is 80[mm].

sliding motion

Different contact patterns can be generated by the constructed CPG shown in Fig.6.1 by changing the correlation of the fingers with the neurons. For example, the contact pattern shown in Fig.6.17 can be generated by correlating the adjacent two fingers (the first and the second fingers, and the third and the forth fingers). In order to perform the shifting motion in the x direction (sliding motion), the translational velocity of the object v_{ox} is given by the following equation:

$$v_{ox} = k_v \, y_g \tag{6.11}$$

The experimental scenes in the sliding manipulation are shown in Fig.6.18.
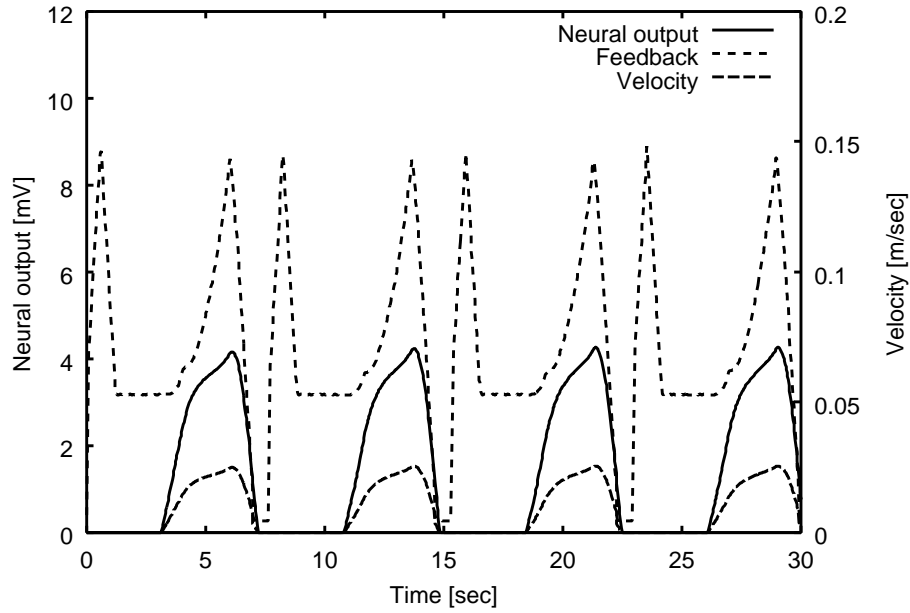
(a) Neural output, feedback value and object's velocity
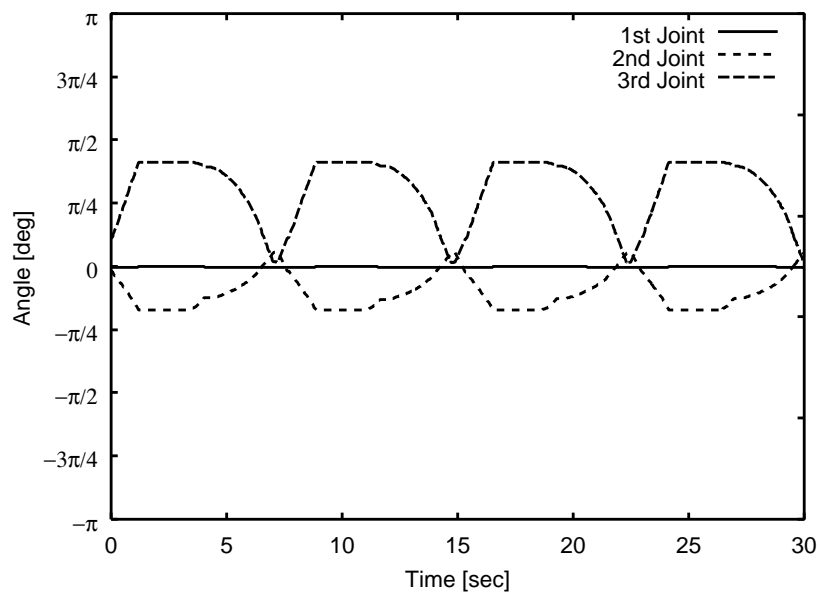
(b) Joint angle

Figure 6.15. Experimental result (size:50[mm], lifting)
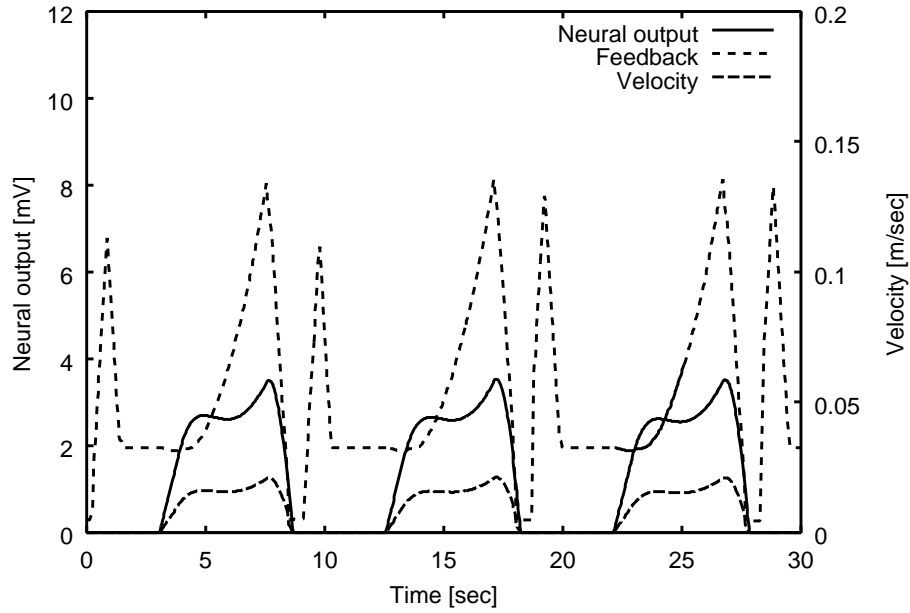
(a) Neural output, feedback value and object's velocity
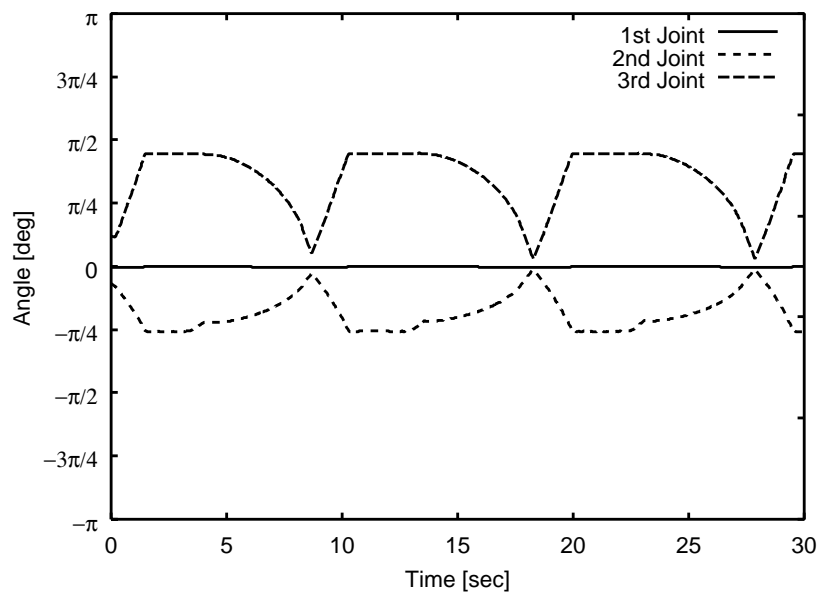
(b) Joint angle

Figure 6.16. Experimental result (size:80[mm], lifting)
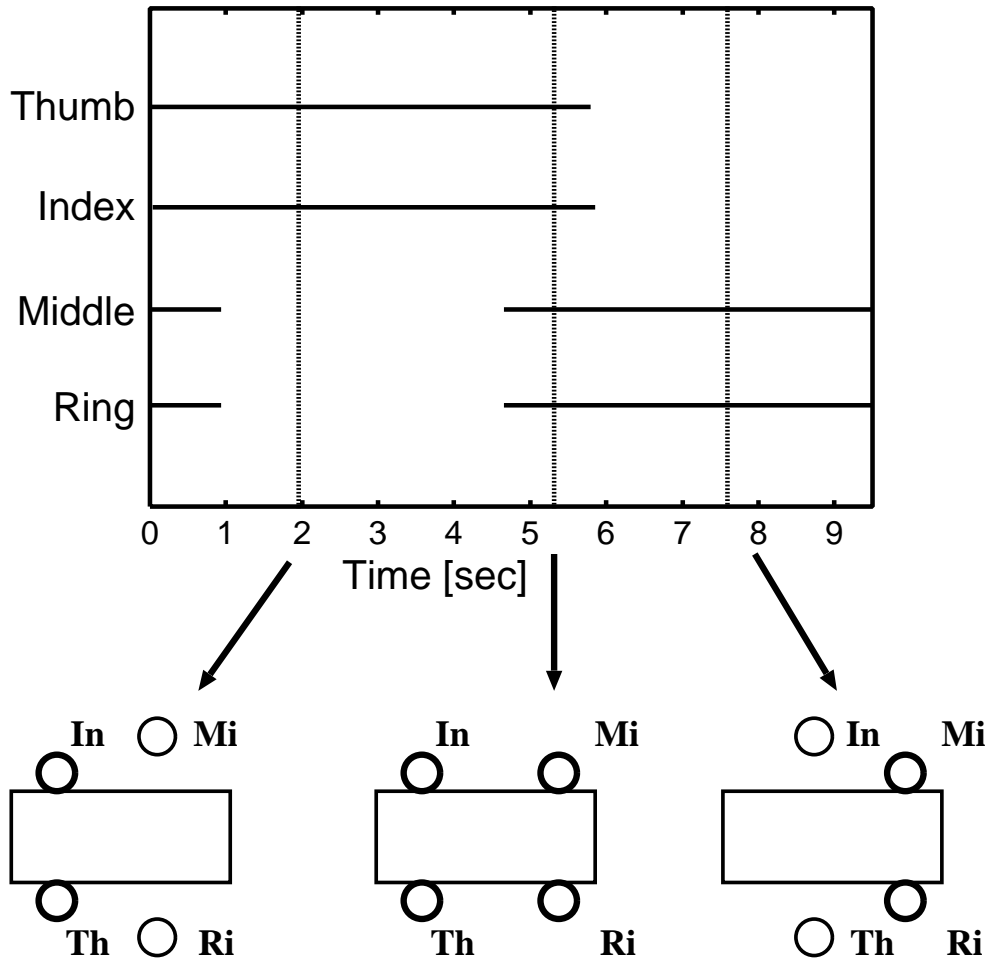
Figure 6.17. Contact pattern for the sliding motion
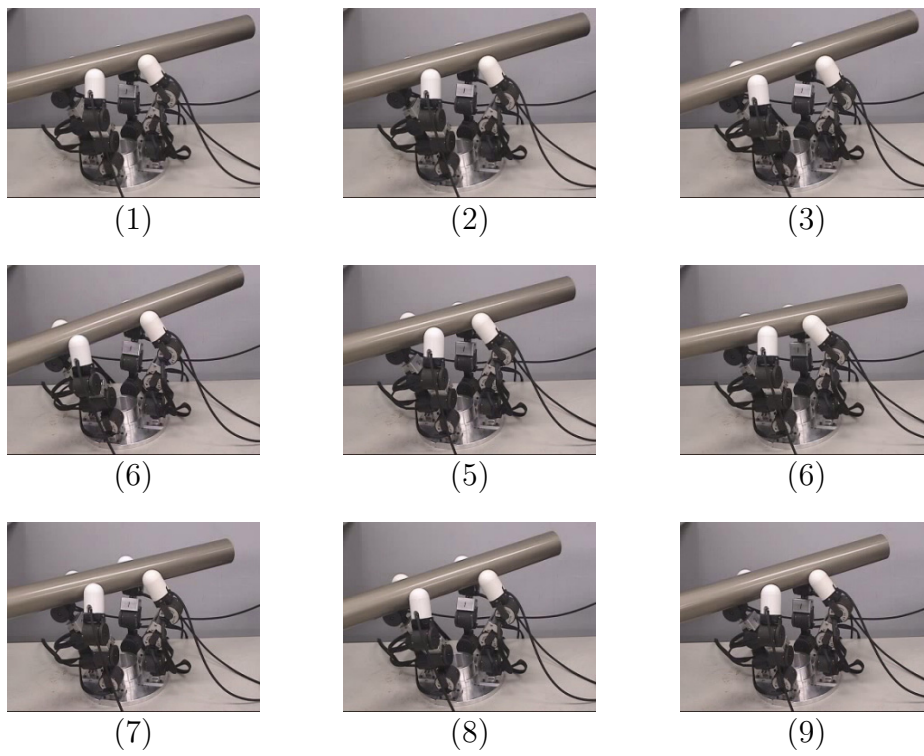
Figure 6.18. Experimental scenes during the sliding motion

6.4. Conclusion

This chapter has demonstrated the rhythmic manipulation using a four-fingered hand system by the CPG-based control. The proposed control method can change the switching cycle of the grasping fingers by the joint margin feedback to the neurons of the CPG depending on the object size. The smooth change of the desired velocity has been given by correlating the neural output with the desired velocity.

A CPG has been built by a simple mutual inhibition network that consists of two neurons. Since the phases of the oscillatory neural output have the difference of $\pi[\mathrm{rad}]$, the switching motions of the grasping fingers can be performed by issuing the motion-triggers to the set of the fingers during the manipulation using a four-fingered hand system.

The switching cycle of the fingers during the manipulation is affected by the movable range of the finger joints. For example, in the rotating manipulation, the rotatable angle of an object in one cycle changes depending on the size of the object when the movable range of the joints is the same. Although the limit of the movable area can be calculated by the length of each link, the movable range of joints, and the diameter of the object, it is difficult to obtain the diameter of the object without the object model. In order to deal with the problem, the joint margin feedback to the neurons that constitute the CPG has been proposed that can adaptively relocate the fingers when the fingers close to the limit. Additionally, for the smooth manipulation, it is necessary to determine the initial and the terminal position of the motion. However, if the diameter of the cylindrical object is not given, the terminal position can not be determined because the limit position of the movable area of the finger can not be calculated. By correlating the neural output with the desired velocity, the smooth changes of the velocity can be given.

The effectiveness of the proposed method has been demonstrated by the experiments using a multi-fingered hand system. The multi-fingered robot hand system has four fingers and mounts a 6-axis force-torque sensor on each fingertip. The rotating, lifting, and sliding manipulations of an object have been performed by the proposed method. The experimental results suggest that the issuing cycle of the motion-triggers can be changed by the feedback of the joint margin and

the object is manipulated according to the object size. Furthermore, the smooth change of the desired velocity can be given by correlating the neural output with the object's velocity.

The results in this chapter suggest that the proposed CPG-based method can rhythmically manipulate objects whose models are not given.

Chapter 7

Conclusion

7.1. Summary

Many of traditional methods for multi-fingered manipulations have been based on the precise model of the grasped object. To make the unpractical assumption easy, a number of researchers have proposed various sensing methods of the grasped objects. However, because sensors are consistently affected by noises in the real environment, it is very difficult to even build a precise model of one object, much less all the objects in the environments. In recent years, the biologically inspired control has been proposed. Motions of animals that can adapt to a variety of environments are controlled by a nervous system covering all the body. Rhythmic patterns take an important role in the rhythmic activities, such as breathing and walking, that generated by the central pattern generators (CPG). In studies of the walking control for multi-legged robots, the CPG-based adaptive control has been proposed and the effectiveness of the adaptive walking in real environments has been confirmed. However, few approaches based on the analyses of human's rhythmic motions have been proposed for multi-fingered manipulations. Humans can dextrously manipulate various objects using their fingers cooperatively. To achieve dextrous capabilities like humans by a robot hand, it is important to analyze the human skills and applying the findings to the robot hand manipulations. Recently, it has been observed that rhythmic motions appear in rotating manipulations when a person attains proficiency. The CPG-based control of the fingers can achieve the dextrous manipulations like human.

This thesis proposes a CPG-based control for rhythmic manipulations by a multi-fingered hand based on human's rhythmic manipulations. The results in each chapter are shown as follows.

Chapter 3: Investigation of feedforward control in human grasping motions

This chapter has investigated the rhythmic effects and the feedforward control of grasping motions by measuring the grip/load force and the finger surface EMG of AbPB/AdP muscles simultaneously.

The simultaneous measurement system has developed that consists of a measurement device of the applied force and a surface EMG measurement system. Since the grip and load force can be measured after the contact between the object and the fingertips, the measured force is used for the detection of the contact.

Adductor Pollicis (AdP) and Abductor Pollicis Brevis (AbPB) muscles have been measured by the EMG measurement system. The AdP muscle controls the adduction motions of the thumb and the AbPB muscle controls the abduction motions. Since these intrinsic muscles are easy to measure by a surface EMG measurement method and not significantly affected by the motions of the arm, these muscles are suitable for the measurement. The measured EMG activities have been exploited for analyzing the force programming before the correction by the tactile sensations.

A pilot experiment has been conducted to determine the analysis method for the measured surface EMG. The intensive activities of the AbPB muscle have been measured in the range of 0.4[sec] before the contact. The range has been defined as "pre-contact period".

The experiments have been conducted using the simultaneous measurement system. Six subjects have grasped the measurement device whose weight is 300[g], 600[g], or 900[g]. In the experiment, two conditions are set up. In the rhythm condition, the subjects have been required to perform the tasks rhythmically keeping the timing with the bell. In the free condition, they have not been required the rhythmical actions. The difference of the measured EMG activities in the pre-contact period have been statistically analyzed by the Bonferroni's significance

test. The experimental results suggest that the object weight affects the AbPB EMG activity. The weight-related activities in the AbPB EMG have not been reported yet. These analyses indicate the importance of the feedforward control in the grasping motions and the rhythmic motions in the human's manipulations.

Chapter 4: Rhythmic motion patterns in human's manipulations

This chapter concentrates on the rhythmic motions of humans and investigates contact patterns during rotating manipulations. When a person attains proficiency, the motions of the fingers during the rotating manipulations are controlled according to rhythmic patterns. By analyzing the contact pattern during the manipulation, the characteristics of the rhythmic manipulations can be investigated.

A measurement system has been developed and the contact condition of the fingers has been measured during the rotating manipulation. The contact condition has been measured by force sensing resistors (FSRs). A subject puts rubber fingercaps in that the FSRs are attached on the fingertips (thumb, index, middle, and ring fingers). He rotates a cylindrical object using these four fingers. In the rotating manipulation, switching motions (finger relocation) are consequently observed. The rhythmic movements of the fingers have been observed by the measured contact condition during the manipulation. Typical contact patterns have been detected based on the contact information. The typical contact patterns represent the touch condition in one cycle of the manipulation.

The measured typical contact patterns show the switching patterns of the grasping fingers. The role of each finger can be investigated from the typical contact pattern. The principal three fingers (thumb, index, and ring fingers) mainly take a role for the stable grasp and the rotating manipulation; the middle finger supports those motions when the grasp and the manipulation can not be performed using the principal three fingers. Movable range of the finger seems to affect the measured contact pattern. Few studies have investigated the rhythmic motion patterns based on the contact condition. The results in this chapter have presented a formalization method of manipulations using fingers.

In order to investigate the human's rhythmic manipulation skills, it is neces-

sary to measure additional information during the manipulation. For example, the contact points between the object and the finger, the applied force and torque, and the position and rotation of the manipulated object should be measured. Moreover, it is interesting to investigate the manipulation patterns when the object size and shape are changed. The measurement device that can measure such information will be required for the further investigation.

Chapter 5: CPG-based manipulation

This chapter has introduced a CPG that can generate a typical contact pattern of human that has been analyzed in the chapter 4 and demonstrated the CPG-based control method for a rotating manipulation using a dynamic simulator. In this study, the neural oscillator model that has been proposed by Matsuoka [72, 52] is adopted for a rhythm generator. The measured typical contact patterns during rotating manipulations addressed in the chapter 4 represent a model of rhythmic motion patterns.

At the first part, the CPG has been shown that can generate a typical contact pattern by a mutual inhibition network. In the generated contact pattern, the thumb, index, and ring fingers touch on and release from the object alternately. Two fingers among those three fingers touch the object consistently during the manipulation. Additionally, the middle finger touches in order to support the role of the thumb and the index fingers when the ring finger releases.

Fingers basically keep iterative motions on a constant trajectory during rhythmic motions and it is not important to imitate the trajectories. Rotating manipulations can be conducted by classifying the motions into several categories and performing these motions in order. This study has classified the rotating manipulation into "approach motion", "rotating motion", "release motion", and "back motion". The rotating motion is taken after the approach motion, and the back motion is taken after the release motion. Rhythmic rotating manipulations can be performed by issuing "motion-triggers" that start these successive motions. The motion-triggers have to be issued appropriately in order that the fingers cooperatively and synchronously move and manipulate the object. To generate such rhythmic motion-triggers, the CPG can be exploited for issuing the commands.

When large external force is applied on the grasped object during a manipu-

lation, the object slips on the contact surface and may be dropped on the ground. The simple and effective way to deal with the problem is to enhance the grasp robustness by adding grasping finger when the external force is applied. In order to add the grasping fingers when a force sensor of the fingertip measures the external force, the force feedback has given to the neurons. Consequently, the neuron does not issue the return command to the fingers and the fingers can keep grasping during the disturbance.

The last part of this chapter has addressed experimental results in a simulation using the proposed CPG-based control method. A dynamic simulation system has been developed and a four-fingered hand model has been built. The fingers have controlled by a simple PD control according to the motion-triggers generated by the constructed CPG model. The results of the simulation show that rotating manipulations of a cylindrical object in the air can be performed using the output of the neurons. Furthermore, robust rotating manipulations have been performed by keeping contact states using the force feedback via the CPG when a disturbance is applied on the object.

In all, the results in this chapter present that the CPG can generate a similar contact pattern to that of humans and rotating manipulations can be performed by the generated pattern. These results confirm the validity and the effectiveness of the CPG-based control on the measured contact patterns that analyzed in the previous chapter.

Chapter 6: Rhythmic manipulations using a multi-fingered hand by the CPG-based control

This chapter has demonstrated the rhythmic manipulation using a four-fingered hand system by the CPG-based control. The proposed control method can change the switching cycle of the grasping fingers by the joint margin feedback to the neurons of the CPG depending on the object size. The smooth change of the desired velocity has been given by correlating the neural output with the desired velocity.

A CPG has been built by a simple mutual inhibition network that consists of two neurons. Since the phases of the oscillatory neural output have the difference

of π[rad], the switching motions of the grasping fingers can be performed by issuing the motion-triggers to the set of the fingers during the manipulation using a four-fingered hand system.

The switching cycle of the fingers during the manipulation is affected by the movable range of the finger joints. For example, in the rotating manipulation, the rotatable angle of an object in one cycle changes depending on the size of the object when the movable range of the joints is the same. Although the limit of the movable area can be calculated by the length of each link, the movable range of joints, and the diameter of the object, it is difficult to obtain the diameter of the object without the object model. In order to deal with the problem, the joint margin feedback to the neurons that constitute the CPG has been proposed that can adaptively relocate the fingers when the fingers close to the limit. Additionally, for the smooth manipulation, it is necessary to determine the initial and the terminal position of the motion. However, if the diameter of the cylindrical object is not given, the terminal position can not be determined because the limit position of the movable area of the finger can not be calculated. By correlating the neural output with the desired velocity, the smooth changes of the velocity can be given.

The effectiveness of the proposed method has been demonstrated by the experiments using a multi-fingered hand system. The multi-fingered robot hand system has four fingers and mounts a 6-axis force-torque sensor on each fingertip. The rotating, lifting, and sliding manipulations of an object have been performed by the proposed method. The experimental results suggest that the issuing cycle of the motion-triggers can be changed by the feedback of the joint margin and the object is manipulated according to the object size. Furthermore, the smooth change of the desired velocity can be given by correlating the neural output with the object's velocity.

The results in this chapter suggest that the proposed CPG-based method can rhythmically manipulate objects whose models are not given.

7.2. Future work and vision

When the CPG-based control is exploited, how to determine the parameters of the CPG is a considerable problem. The parameters give the period, phase, and amplitude of the oscillatory output. Various determination methods of the appropriate parameters have been proposed, for example, the determination of the parameters by a genetic algorithm[80] and the determination from a viewpoint of the energy efficiency[81]. In this thesis, the CPG parameters are manually determined. The determination method of the parameters should be considered depending on the object properties and the objective of the manipulation.

In addition, the generated patterns from the CPG in animals and insects adaptively change according to a variety of environments. The CPG steadily generates oscillatory output unless external input is given. Besides, the CPG is largely affected by the external input, such as somatic sensations and signals from central nerves. The CPG can generate various patterns based on the external input. In the studies of legged robots, a reflex system via the CPG has been exploited for the generation of the adaptive walking patterns, for example, the vestibulo-spinal reflex, the stretch/flexion reflex, and the tonic labyrinthine reflex[78]. Although the joint margin feedback that is exploited in this study approximately corresponds to the tonic stretch reflex, the effect of the reflex systems on the manipulations has limitations because the CPG has been exploited only to generate the contact patterns so far. The model that reflects biological reflex systems can be constructed by connecting the neurons to the musculo-skeletal systems of the robot hand, such as joint actuators.

Furthermore, quadrupeds like horses change walking patterns depending on the walking velocity, such as walk, trot, and gallop. However, few researches have investigated the rhythmic nature of human's manipulations because the dexterity and the complexity of the manipulation using the fingers have been strongly emphasized. There are many topics arising from the manipulation patterns. They include the classification of the manipulation patterns, the selection criterion, the mechanical validity and the significance of the grasping patterns.

These works would give us further understandings of human manipulation skills and guidelines for the achievement of dextrous manipulations by a robot hand.

107

References

[1] T.Okada. Object-handling system for manual industry. *IEEE Transactions on Systems, Man and Cybernetics*, 9(2):79–89, 1979.

[2] J.K.Salisbury and J.J.Craig. Articulated hands: force control and kinematic issues. *International Journal of Robotics Research*, 1(1):4–17, 1982.

[3] S.C.Jacobson, J.E.Wood, D. F. Knutti, and K. B. Biggers. The utah/m.i.t dextrous hand : work in progress. *International Journal of Robotics Research*, 3(4):21–50, 1984.

[4] I.Kato and K.Sadamoto. *Mechanical hands illustrated*. Springer-Verlag, 1987.

[5] K.Rao, G.Medioni, H.Liu, and G.A.Bekey. Robot hand-eye coordination: shape description and grasping. In *Proceedings of IEEE International Conference on Robotics and Automation*, pages 407–411, 1988.

[6] C.Melchiorri and G.Vassura. Mechanical and control features of the university of bologna hand version 2. In *Proceedings of IEEE/RSJ International Conference on Intelligent Robotics and Systems*, pages 187–193, 1992.

[7] J.Butterfass, M.Grebenstein, H.Liu, and G.Hirzinger. Dlr-hand ii: Next generation of a dextrous robot hand. In *Proceedings of IEEE International Conference on Robotics and Automation*, pages 109–114, 2001.

[8] K.Machida, Y.Toda, Y.Murase, and S.Komada. Precise space telerobotic system using 3-finger multisensory hand. In *Proceedings of IEEE International Conference on Robotics and Automation*, pages 32–38, 1995.

[9] M.Buss and K.P.Kleinmann. Multi-fingered grasping experiments using real-time grasping force optimization. In *Proceedings of IEEE International Conference on Robotics and Automation*, pages 1807–1812, 1996.

[10] M.Ebner and R.S.Wallce. A direct-drive hand: design, modeling, and control. In *Proceedings of IEEE International Conference on Robotics and Automation*, pages 1668–1674, 1995.

[11] M.R.Cutkosky. On grasp choice, grasp models, and the design of hands for manufacturing tasks. *IEEE Transactions on Robotics and Automation*, 5(3):269–279, 1989.

[12] J.A.Coelho and R.A.Grupen. Online grasp synthesis. In *Proceedings of IEEE International Conference on Robotics and Automation*, pages 2137–2142, 1996.

[13] R.A.Grupen. Planning grasp strategies for multi-fingered robot hands. In *Proceedings of IEEE International Conference on Robotics and Automation*, pages 646–651, 1991.

[14] H.Zhang, K.Tanie, and H.Maekawa. Dextrous manipulation planning by grasp transformation. In *Proceedings of IEEE International Conference on Robotics and Automation*, pages 3055–3060, 1996.

[15] R.Fearing. Simplified grasping and manipulation with dextrous robot hands. In *Proceedings of IEEE International Conference on Robotics and Automation*, pages 188–195, 1986.

[16] J.Kerr and B.Roth. Analysis of multifingered hand. *International Journal of Robotics Research*, 4(4):3–17, 1986.

[17] Z.Li and S.Sastry. Task-oriented optimal grasping by multi-fingered robotic hands. *IEEE Journal of Robotics and Automation*, 4(1):32–44, 1987.

[18] M.Teichmann. A grasp metric invariant under right motions. In *Proceedings of IEEE International Conference on Robotics and Automation*, pages 2143–2148, 1996.

[19] M.A.Diftler and I.D.Walker. Experiments in mating threaded parts using a dextrous robotic hand. In *Proceedings of IEEE-SMC Symposium on Robotics and Cybernetics*, pages 459–464, 1996.

[20] G.P.Starr. An experimental investigation of object stiffness control using a multifingered hand. *Robotics and Autonomous Systems*, 10:33–42, 1992.

[21] V.Nguyen. Constructing force-closure grasps. *International Journal of Robotics Research*, 7(3):3–16, 1988.

[22] E.Rimon and J.Burdick. New bounds on the number of frictionless fingers required to immobilize 2d objects. In *Proceedings of IEEE International Conference on Robotics and Automation*, pages 751–757, 1995.

[23] A.Bicchi. On the closure properties of robotic grasping. *International Journal of Robotics Research*, 14(4):319–334, 1995.

[24] T.Yoshikawa. Passive and active closure by constraining mechanisms. In *Proceedings of IEEE International Conference on Robotics and Automation*, pages 1477–1484, 1996.

[25] A.Bicchi. Hands for dextrous manipulation and powerful grasping: a difficult road towards simplicity. In *Proceedings of IEEE International Conference on Robotics and Automation*, pages 1–13, 1996.

[26] D.Brock and S.Chin. Environment perception of an articulated robot hand using contact sensors. *ASME Robotics and Manufacturing Automation*, 15:89–96, 1985.

[27] H.Shinoda, K.Matsumoto, and S.Ando. Acoustic resonant tensor cell for tactile sensing. In *Proceedings of IEEE International Conference on Robotics and Automation*, pages 3087–3092, 1997.

[28] T.Maeno, T.Kawamura, and S.Cheng. Friction estimation by pressing an elastic finger-shaped sensor against a surface. *IEEE Transactions on Robotics and Automation*, 20(2):222–228, 2004.

111

[29] Y.Yamada, H.Morita, and Y.Umetani. Vibrotactile sensor generation impulsive signals for distinguishing only slipping state. In *Proceedings of IEEE/RSJ International Conference on Intelligent Robotics and Systems*, pages 844–850, 1999.

[30] M.R.tremblay and M.R.Cutkosky. Estimating friction using incipient slip sensing during a manipulation task. In *Proceedings of IEEE International Conference on Robotics and Automation*, pages 258–265, 2000.

[31] N.J.Ferrier and R.W.Brockett. Reconstructing the shape of a deformable membrane from image data. *International Journal of Robotics Research*, 19(9):795–816, 2000.

[32] M.Tada, T.Shibata, and T.Ogasawara. Investigation of the touch processing model in human grasping based on the stick ratio within a fingertip contact interface. In *Proceedings of IEEE International Conference on Systems, Man and Cybernetics*, page tp1n4, 2002.

[33] M.A.Farooqi, T.Tanaka, Y.Ikezawa, T.Omata, , and K.nagata. Sensor based control the execution of regrasping primitives on a multifingered robot hand. In *Proceedings of IEEE International Conference on Robotics and Automation*, pages 3217–3223, 1999.

[34] M.Huber and R.A.Gruppen. Robust finger gaits from closed-loop controllers. In *Proceedings of IEEE/RSJ International Conference on Intelligent Robots and Systems*, pages 1578–1584, 2002.

[35] R.S.Johansson and G.Westling. Roles of glabrous skin receptors and sensorimotor memory in automatic control of precision grip when lifting rougher or more slippery objects. *Experimental Brain Research*, 56:550–564, 1984.

[36] R.S.Johansson and G.Westling. Signals in tactile afferents from the fingers eliciting adaptive motor responses during precision grip. *Experimental Brain Research*, 66:141–154, 1987.

[37] R.S.Johansson and G.Westling. Coordinated isometric muscle commands adequately and erroneously programmed for the weight during lifting task with precision grip. *Experimental Brain Research*, 71:59–71, 1988.

[38] A.M.Gordon, H.Forssberg, R.S.Johansson, and G.Westling. Visual size cues in the programming of manipulative forces during precision grip. *Experimental Brain Research*, 83(1991):477–482, 1991.

[39] A.M.Gordon, H.Forssberg, R.S.Johansson, and G.Westling. The integration of haptically acquired size information in the programming of precision grip. *Experimental Brain Research*, 83(1991):483–488, 1991.

[40] A.M.Gordon, H.Forssberg, R.S.Johansson, and G.Westling. Integration of sensory information during the programming of precision grip: comments on the contributions of size cues. *Experimental Brain Research*, 85(1991):226–229, 1991.

[41] A. Dutta and G. Obinata. Variation of initial grasping force with length of an object. In *IEEE International Workshop on Robot and Human Interactive Communication*, pages 224–228, 2000.

[42] J.R.Flanagan and M.A.Beltzer. Independence of perceptual and sensorimotor predictions in the size-weight illusion. *Nature Neuroscience*, 3(7):737–741, 2000.

[43] M.Gentilucci, S.Chieffi, E.Daprati, M.C.Saetti, and I.Toni. Visual illusion and action. *Neuropsychologia*, 34(5):369–376, 1996.

[44] E.Brenner and J.B.J.Smeets. Size illusion influences how we lift but not how we grasp an object. *Experimental Brain Research*, 111:473–476, 1996.

[45] E.Daprati and M.Gentilucci. Grasping an illusion. *Neuropsychologia*, 35(12):1577–1582, 1997.

[46] J.R.Flanagan and A.M.Wing. Modulation of grip force with load force during point-to-point arm movements. *Experimental Brain Research*, 95:131–143, 1993.

[47] J.R.Flanagan and A.M.Wing. The stability of precision grip forces during cyclic arm movements with a hand-held load. *Experimental Brain Research*, 105:455–464, 1995.

[48] J.R.Flanagan and A.M.Wing. The role of internal models in motion planning and control: evidence from grip force adjustments during movements of hand-held loads. *The Journal of Neuroscience*, 17(4):1519–1528, 1997.

[49] M.L.Shik and G.N.Orlovsky. Neurophysiology of locomotor automation. *Physiol Review*, 56:465–501, 1976.

[50] S.Grillner. Neurobiological bases of rhythmic motor acts in vertebrates. *Science*, 228:143–149, 1985.

[51] G.Taga. A model of the neuro-musculo-skeletal system for human locomotion ii. real-time adaptability under various constraints. *Biological Cybernetics*, 73:113–121, 1995.

[52] K.Matsuoka. Mechanisms of frequency and pattern control in neural rhythm generators. *Biological Cybernetics*, 56:345–353, 1987.

[53] J.R.Napier. The prehensile movements of the human hand. *The Journal of Bone and Joint Surgery*, 38-B:902–913, 1956.

[54] G.Westling and R.S.Johansson. Factors influencing the force control during precision grip. *Experimental Brain Research*, 53:277–284, 1984.

[55] M.A.Arbib, T.Iberall, and D.Lyons. Coordinated control programs for control of the hands. *Experimental Brain Research*, 10:111–129, 1985.

[56] M.Jeannerod, M.A.Arbib, G.Rizzolatti, and H.Sakata. Grasping objects: The cortical mechanisms of visuomotor transformation. *Trends in Neurosciences*, 18:314–320, 1995.

[57] M.R.Cutkosky and R.D.Howe. Human grasp choice and robotic grasp analysis. In *Dextrous Robot Hands*, pages 5–31. Springer-Verlag, 1990.

[58] S.B.Kang and K.Ikeuchi. Toward automatic robot instruction from perception-mapping human grasps to manipulator grasps. *IEEE Transactions on Robotics and Automation*, 13(1):81–95, 1997.

114

[59] C.Exner. In-hand manipulation. In J.Case-Smith and C.Pehoski, editors, *Development of hand skills in the child*, pages 35–46. American Occupational Therapy Association, 1992.

[60] H. Taguchi, K. Hase, and T. Maeno. Analysis of the motion pattern and the learning mechanism for manipulation objects by human fingers (in japanese). *Transactions of the Japan Society of Mechanical Engineers*, 68(670):1647–1654, 2002.

[61] H.Fukuda, N.Fukumura, M.Katayama, and Y.Uno. Relation between object recognition and formation of hand shape: A computational approach to human grasping movements. *Systems and Computers in Japan*, 31(12):1315–1326, 2000.

[62] M.Hepp-Reymond, E.J.Huesler, and M.A.Maier. Precision grip in humans -temporal and spatial synergies-. In *Hand and Brain*, chapter 3, pages 37–68. Academic Press, 1996.

[63] A.M.Wing. Anticipatory control of grip force in rapid arm movement. In *Hand and Brain*, chapter 15, pages 301–324. Academic Press, 1996.

[64] E.Muybridge. *Animals in motion*. Dover Pub., 1957.

[65] P.P.Gambaryan. *How mammals run*. John Wiley & Sons, 1974.

[66] T. Massie. A tangible goal for 3d modeling. *IEEE Computer Graphics and Applications*, pages 62–65, 1995.

[67] C.Maggioni and B.Kammerer. Gesture computer – history,design, and applications. In *Computer Vision for Human-Machine Interface*. Cambridge University Press, 1998.

[68] K.Nagata, F.Saitou, and T.Suehiro. Development of the master hand for grasping information capturing. In *Proceedings of IEEE/RSJ International Conference on Intelligent Robots and Systems*, pages 1757–1762, 2001.

[69] G.S.Stent, W.B.Jr.Kristan, W.D.Friesen, C.A.A.Ort, M.Poon, and R.L.Carabrese. Neural generation of the leech swimming movement. *Science*, 200:1348–1357, 1978.

[70] J.T.Bachanam and S.Grillner. Newly identified glutamate interneurons and their role in locomotion in lamprey spinal cord. *Science*, 236:312–314, 1987.

[71] J.J.Collins and I.Stewart. Coupled nonlinear oscillators and the symmetries of animal gaits. *Nonlinear Science*, 3:349–392, 1993.

[72] K.Matsuoka. Sustained oscillations generated by logical. *Biological Cybernetics*, 52:367–376, 1985.

[73] K.Tsutsumi and H.Matsumoto. Ring neural network que a generator of rhythmic oscillation with period control mechanism. *Biological Cybernetics*, 51:181–194, 1984.

[74] J.S.Bay and H.Hemami. Modeling of a neural pattern generator with coupled nonlinear oscillators. *IEEE Transactions on Biomedical Engineering*, 34(4):297–306, 1987.

[75] H.Yuasa and M.Ito. Coordination of many oscillators and generation of locomotory patterns. *Biological Cybernetics*, 63:177–184, 1990.

[76] G.Taga, Y.Yamaguchi, and H.Shimizu. Self-organized control of bipedal locomotion by neural oscillators. *Biological Cybernetics*, 65:147–159, 1991.

[77] H.Kimura, K.Sakurama, and S.Akiyama. Dynamic walking and running of the quadruped using neural oscillators. In *Proceedings of IEEE/RSJ International Conference on Intelligent Robots and Systems*, pages 50–57, 2000.

[78] Hiroshi Kimura Yasuhiro Fukuoka and Avis H. Cohen. Adaptive dynamic walking of a quadruped robot on irregular terrain based on biological concepts. *International Journal of Robotics Research*, 22(3-4):187–202, 2003.

[79] K.Nagata, T.Keino, and T.Omata. Multifingered hand system which can acquire the object model by manipulation with a multifingered hand. In *Proceedings of IEEE/SICE/RSJ International Conference on Multisensor Fusion and Integration for Intelligent Systems*, pages 100–107, 1996.

[80] K.Hase and N.Yamazaki. Computational evolution of human bipedal walking by a neuro-musculo-skeletal model. *Artificial Life and Robotics*, 3:133–138, 1999.

[81] H.Takemura, J.Ueda, Y.Matsumoto, and T.Ogasawara. A study of a gait generation of a quadruped robot based on rhythmic control - optimization of cpg parameters by a fast dynamics simulation environment. In *Proceedings of the Fifth International Conference on Climbing and Walking Robots*, pages 759–766, 2002.

Published papers

Journals

1. Yuichi Kurita, Jun Ueda, Yoshio Matsumoto, and Tsukasa Ogasawara, "CPG Based Manipulation: Measurement of Human's Rhythmic Finger Gaits," Journal of the Japan Society of Mechanical Engineers, Vol.70, No.699, pp.3220–3226, 2004.

2. Yuichi Kurita, Atsutoshi Ikeda, Jun Ueda, and Tsukasa Ogasawara, "Fingerprint Pointing Device Utilizing the Deformation of the Fingertip during the Incipient Slip," IEEE Transactions on Robotics, 2005.

3. Atsutoshi Ikeda, Yuichi Kurita, Jun Ueda, Yoshio Matsumoto, and Tsukasa Ogasawara, "Grip force control of the elastic body based on contact surface eccentricity during the incipient slip," The Journal of the Robotics Society of Japan, Vol.23, No.3, 2005.

4. Atsutoshi Ikeda, Yuichi Kurita, Jun Ueda, and Tsukasa Ogasawara, "Development of a compact pointing device utilizing the fingerprint deformation during the incipient slip," Journal of Information Processing Society of Japan, Vol.45, No.7, pp.1769-1778, 2004.

International Conferences

1. Yuichi Kurita, Jun Ueda, Yoshio Matsumoto, and Tsukasa Ogasawara, "CPG-Based Manipulation : Generation of Rhythmic Finger Gaits from Human Observation," In Proceedings of the 2004 IEEE International Conference on Robotics and Automation, pp.1209-1214, New Orleans, USA,

April 2004.

2. Yuichi Kurita, Mitsunori Tada, Yoshio Matsumoto, and Tsukasa Ogasawara, "Simultaneous Measurement of the Grip/Load Force and the Finger EMG : Effects of the Object Weight," In Proceedings of 2002 IEEE International Conference on Systems, Man and Cybernetics, TP1B6, Hammamet, Tunisia, October 2002.

3. Yuichi Kurita, Mitsunori Tada, Yoshio Matsumoto, and Tsukasa Ogasawara, "Simultaneous Measurement of the Grip/Load Force and the Finger EMG : Effects of the Grasping Condition," In Proceedings of the 2002 IEEE International Workshop on Robot and Human Interactive Communication, pp.217-222, Berlin, Germany, September 2002.

4. Atsutoshi Ikeda, Yuichi Kurita, Jun Ueda, Yoshio Matsumoto, and Tsukasa Ogasawara, "Grip Force Control for an Elastic Finger using Vision-based Incipient Slip Feedback," In Proceedings of the 2004 IEEE/RSJ International Conference on Intelligent Robots and Systems, pp.100-105, Sendai, Japan, September 2004.

5. Yuichi Kurita, Atsutoshi Ikeda, Jun Ueda, Yoshio Matsumoto, and Tsukasa Ogasawara, "A Novel Pointing Device Utilizing the Deformation of the Fingertip," In Proceedings of the 2003 IEEE/RSJ International Conference on Intelligent Robots and Systems, pp.13-18, Las Vegas, USA, October 2003.

Domestic Conferences

1. Yuichi Kurita, Kazuyuki Nagata, Jun Ueda, and Tsukasa Ogasawara, "Rhythmic manipulation using neuron oscillators," Technical report of IEICE, Vol.104, No.348, pp.13–18, 2004.

2. Yuichi Kurita, Kazuyuki Nagata, Jun Ueda, and Tsukasa Ogasawara, "Rotating manipulation using the neural oscillators," In Proceedings of JSME Annual Conference on Robotics and Mechatronics, p.2P1-L1-5, 2004.

3. Yuichi Kurita, Jun Ueda, and Tsukasa Ogasawara, "CPG representation for finger touch pattern in rotating a cylindrical object," In Proceedings of the 21th Annual Conference of the Robotics Society of Japan, p.3C14, 2003.

4. Yuichi Kurita, Mitsunori Tada, Yoshio Matsumoto, and Tsukasa Ogasawara, "Simultaneous Measurement of the Grip/Load Force and the Finger EMG: Effects of the Movement Condition," In Proceedings of the the 17th Symposium on Biological and Physiological Engineering, pp.255-256, 2002.

5. Yuichi Kurita, Mitsunori Tada, Yoshio Matsumoto, and Tsukasa Ogasawara, "Simultaneous Measurement of Grip/Load Force and Finger EMG to Analyse Human's Preliminary Force Programming - Effects of the Object Weight on Human Grasping -," In Proceedings of JSME Annual Conference on Robotics and Mechatronics, p.1P1-J05, 2002.

6. Yuichi Kurita, Mitsunori Tada, and Tsukasa Ogasawara, "Simultaneous Measurement of Finger EMG and Grip/Load Force to Analyse Human's Preliminary Force Programming," In Proceedings of SICE Symposium on Systems and Information, pp.313-318, 2001.

7. Atsutoshi Ikeda, Yuichi Kurita, Jun Ueda, Yoshio Matsumoto, and Tsukasa Ogasawara, "Grip force control of an elastic body based on contact surface eccentricity during the incipient slip," In Proceedings of JSME Annual Conference on Robotics and Mechatronics, p.1A1-H-35, 2004.

8. Atsutoshi Ikeda, Yuichi Kurita, Jun Ueda, Yoshio Matsumoto, and Tsukasa Ogasawara, "Grip force control of the elastic body utilizing the incipient slip sensor," In Proceedings of SICE System Integration Division Annual Conference, pp.424-425, 2003.

9. Jun Ueda, Atsutoshi Ikeda, Yuichi Kurita, and Tsukasa Ogasawara, "Development of a novel pointing device utilizing the fingertip deformation," In Proceedings of 2003 Human Interface Symposium, pp.251-254, 2003.

10. Atsutoshi Ikeda, Yuichi Kurita, Jun Ueda, and Tsukasa Ogasawara, "Development of a novel pointing device using the fingertip deformation - Analysis

of the fingertip deformation in the sliding motion -," In Proceedings of the 21th Annual Conference of the Robotics Society of Japan, p.3F18, 2003.

11. Atsutoshi Ikeda, Yuichi Kurita, Jun Ueda, Yoshio Matsumoto, and Tsukasa Ogasawara, "Development of a new pointing device utilizing deformation of fingerprint images," In Proceedings of JSME Annual Conference on Robotics and Mechatronics, p.1A1-3F-B4, 2003.

12. Yuichi Kurita, Mitsunori Tada, Yoshikazu Imai, and Tsukasa Ogasawara, "Measurement of incipient slip while grasping motion using fingerprint pattern," In Proceedings of JSME Annual Conference on Robotics and Mechatronics, p.1P1-H3, 2001.

Appendix

A. Bonferroni significance test

The simple significance test between two factors is shown as the following equations:

$$t = \frac{\sum\limits_{j}^{m} w_j \overline{X_j}}{\sqrt{MS_e \sum\limits_{j}^{m} \dfrac{w_j^2}{ND_j}}} \tag{A.1}$$

where $\overline{X_j}$, m, MS_e, ND_j, and w_j indicate as follows:

$\overline{X_j}$	:	the average of the j-th factor.
m	:	the number of factors.
MS_e	:	the mean square of errors in the test of the factors (unbiased estimation value of errors).
ND_j	:	the number of data that are used for the calculation of $\overline{X_j}$.
w_j	:	the weight coefficient for the mean of factors in each comparison.

Given one factor is j and the other is j', we have $w_j = 1$ and $w_{j'} = -1$ in the paired comparison. Since the other weight coefficients are 0, Eq.(A.1) can be shown in the following equation:

$$t = \frac{\overline{X_j} - \overline{X_{j'}}}{\sqrt{MS_e \left(\dfrac{1}{ND_j} + \dfrac{1}{ND_{j'}} \right)}} \tag{A.2}$$

t in Eq.(A.2) follows the Student's t distribution, provided that the null hypothesis: "Population mean of each factor in the comparison is the same". In order

to compare the j-th factor with the j'-th, the critical value of t is calculated from the preset significant level (α level: 5% or 1%). Then, the significance is detected by comparing the calculated t from Eq.(A.2) with the critical value.

When performing n multiple independent significance tests each at the α level, the probability of making at least one error (rejecting the null hypothesis inappropriately) is $1 - (1 - \alpha)n$. For example, with $n = 10$ and $\alpha = 0.05$, there is a 40% chance of at least one of the ten tests 0% being declared significant under the 0% null hypothesis.

The Bonferroni adjustment works by making it more difficult for any one test to be statistically significant. The Bonferroni's significance test works by dividing the α level by the number of tests:

$$\alpha' \;=\; \alpha/n \tag{A.3}$$

For example, suppose ten tests on the same database are performed. The Bonferroni adjusted level of significance (α') is $0.05/10 = 0.005$. Any test that results in a probability value of less than 0.005 would be statistically significant. Any test statistic with a probability value greater than 0.005 would be deemed non-significant.

B. Detection of the contact position in the soft finger contact

A fingertip can apply torque along the normal of the contact surface in the soft finger contact. Now, the torque is denoted as $\boldsymbol{p}$, we have:

$$\boldsymbol{p} = T \, \boldsymbol{n} \tag{B.1}$$

where T is the constant and $\| \, \boldsymbol{n} \, \| = 1$ is the outward unit normal vector of the contact surface.

Here, let $\boldsymbol{S}(r) = 0$ be the equation that represents the fingertip surface, we have:

$$\boldsymbol{n} = \frac{\nabla \, \boldsymbol{S}(r)}{\| \, \nabla \, \boldsymbol{S}(r) \, \|} \tag{B.2}$$

Then, the measured moment $\boldsymbol{m}$ by the sensor on the fingertip can be derived by:

$$\boldsymbol{m} = T \frac{\nabla \, \boldsymbol{S}(r)}{\| \, \nabla \, \boldsymbol{S}(r) \, \|} + \boldsymbol{r} \times \boldsymbol{f}_c \tag{B.3}$$

where $\boldsymbol{r}$ is the contact point and $\boldsymbol{f}_c$ is the applied force on the fingertip.

Considering a cylindrical fingertip whose radius is R and the center axis is along z-axis, the surface of the fingertip can be given by:

$$x^2 + y^2 = R^2 \tag{B.4}$$

Since the fingertip surface can be also given by $\boldsymbol{S}(r) = 0$, we have:

$$\frac{\nabla \, \boldsymbol{S}(r)}{\| \, \nabla \, \boldsymbol{S}(r) \, \|} = \frac{\boldsymbol{r}'}{R} \tag{B.5}$$

where $\boldsymbol{r}' = (x, y, 0)^T$.

Given that $T/R = K$, Eq.(B.3) takes:

$$
\begin{aligned}
\boldsymbol{m} &= \frac{T}{R} \boldsymbol{r}' + \boldsymbol{r} \times \boldsymbol{f}_c \\
&= K \, \boldsymbol{r}' + \boldsymbol{r} \times \boldsymbol{f}_c \\
&= \boldsymbol{\Gamma} \, \boldsymbol{r}
\end{aligned} \tag{B.6}
$$

where

$$\mathbf{\Gamma} = \begin{bmatrix} K & f_z & -f_y \\ -f_z & K & f_x \\ f_y & -f_x & 0 \end{bmatrix} \tag{B.7}$$

Therefore, when $K \neq 0$, we have:

$$\boldsymbol{r} = \mathbf{\Gamma}^{-1}\, \boldsymbol{m} \tag{B.8}$$

Here,

$$\begin{aligned}\texttt{det}(\,\mathbf{\Gamma}) &= K(f_x^2 + f_y^2) \\ &= K\, \boldsymbol{f}'^T\, \boldsymbol{f}'\end{aligned} \tag{B.9}$$

$$\begin{aligned}\mathbf{\Gamma}^{-1} &= \frac{1}{\texttt{det}(\,\mathbf{\Gamma})} \begin{bmatrix} f_x^2 & f_x f_y & K f_y + f_x f_z \\ f_x f_y & f_y^2 & -K f_x + f_y f_z \\ -K f_y + f_x f_z & K f_x + f_y f_z & K^2 + f_z^2 \end{bmatrix} \\ &= \frac{1}{\texttt{det}(\,\mathbf{\Gamma})} \left[K^2\, \boldsymbol{E}_z + K\, \mathrm{Skew}(\,\boldsymbol{f}') + \boldsymbol{f}\, \boldsymbol{f}^T \right]\end{aligned} \tag{B.10}$$

where

$$\boldsymbol{E}_z = \begin{bmatrix} 0 & 0 & 0 \\ 0 & 0 & 0 \\ 0 & 0 & 1 \end{bmatrix} \tag{B.11}$$

Eq.(B.6) gives:
$$\boldsymbol{r}^T\, \boldsymbol{m} = KR^2 \tag{B.12}$$

Putting Eq.(B.8) into Eq.(B.12) gives:

$$\boldsymbol{m}^T\, \mathbf{\Gamma}^{-1T}\, \boldsymbol{m} = KR^2 \tag{B.13}$$

It follows:

$$K^2 = \frac{(\, \boldsymbol{f}^T\, \boldsymbol{m})^2}{R^2\, \boldsymbol{f}'^T\, \boldsymbol{f}' - \boldsymbol{m}^T\, \boldsymbol{E}_z\, \boldsymbol{m}} \tag{B.14}$$

Here, the sign of K is the inverse of the sign of $\boldsymbol{f}^T \boldsymbol{m}$ because $\boldsymbol{f}^T \boldsymbol{r}' \leq 0$. Therefore,

$$T = RK \tag{B.15}$$

Consequently, the contact position $\boldsymbol{r}$ is given by Eq.(B.8) $\sim$ Eq.(B.10):

$$\boldsymbol{r} = \frac{K^2 \, \boldsymbol{E}_z \, \boldsymbol{m} + K \, \boldsymbol{f}' \times \, \boldsymbol{m} + (\, \boldsymbol{f}^T \, \boldsymbol{m}) \, \boldsymbol{f}}{K \, \| \, \boldsymbol{f}' \, \|^2} \tag{B.16}$$